NILU OR : 65/85
REFERENCE: O-8510
DATE : DECEMBER 1985

SPECIAL MEASUREMENTS AT NY ÅLESUND: PHYSICAL AND CHEMICAL PROPERTIES OF THE ARCTIC AEROSOL

by

Val Vitols and Jozef M. Pacyna

NILU

NORWEGIAN INSTITUTE FOR AIR RESEARCH

ROYAL NORWEGIAN COUNCIL FOR SCIENTIFIC AND INDUSTRIAL RESEARCH

NILU OR : 65/85
REFERENCE: O-8510
DATE : DECEMBER 1985

SPECIAL MEASUREMENTS AT NY ÅLESUND: PHYSICAL AND CHEMICAL PROPERTIES OF THE ARCTIC AEROSOL

by

Val Vitols and Jozef M. Pacyna

NORWEGIAN INSTITUTE FOR AIR RESEARCH
P.O. BOX 130, N-2001 LILLESTRØM
NORWAY

ISBN 82-7247-636-3

ABSTRACT

Physical and chemical properties of the arctic aerosol at Ny Ålesund, Spitsbergen, have been studied during the arctic winter and summer seasons. Size-differentiated chemical composition of aerosols is used to assess the origin(s) of the winter and summer aerosol. Concurrently observed physical properties of the aerosol imply both natural production and long-range transport in summertime.

TABLE OF CONTENTS

SPECIAL MEASUREMENTS AT NY ÅLESUND: PHYSICAL AND CHEMICAL PROPERTIES OF THE ARCTIC AEROSOL

1 INTRODUCTION

The bulk of this report presents the results of special measurements of aerosol physical and chemical properties at the Ny Ålesund (NYA) reference stations, NILU I and NILU II, during all BP Project campaigns. These measurement data then form the basis for a preliminary discussion of the possible source(s) of aerosols at NYA.

Summaries of wind direction measurements at the NYA stations and aerosol light scattering at the Bjørnøya (BJO) ground station are also included.

The special instrumentation at NYA measured
(a) in near real-time:
- condensation nuclei (CN) concentration;
- aerosol light scattering coefficient, σ_{sp} ; and
- aerosol particle number-size distribution;

(b) by two different methods over various averaging times (1 day or more):
- size-differentiated trace element mass distributions in aerosols.

2 EXPERIMENTAL

2.1 MEASUREMENT METHODS AND DEVICES

Physical properties and size-differentiated chemical composition of aerosols at the Ny Ålesund reference station were measured during five BP Project campaigns.

The two NY Ålesund (NYA) stations NILU I and NILU II, the BJO station, and the special instrumentation for aerosol physical and chemical property determinations, have been described by Vitols and Wasseng (1985).

For convenience, the locations of NYA and BJO are shown in Figure 1, and the main features of the Ny Ålesund area in Figure 2. The measuring devices and their functions are listed below.

The NYA stations had:

- continuous flow condensation nuclei counter (CNC) for continuous display and recording of CN concentrations;

- high-sensitivity, custom-made integrating nephelometer (A-IN) for continuous display and recording of aerosol particle light scattering coefficient, σ_{sp};

- near-forward scattering optical particle counter (OPC) for continuous aerosol particle number-size classification in five equivalent scattering diameter (ESD) ranges, and printout at 10-min. and 60-min. intervals;

- low-volume cascade impactor (BTL C.I.) for aerosol mass fractionation in seven equivalent aerodynamic diameter (EAD) ranges, and subsequent trace element analyses by PIXE*;

- parallel-branch fractionation system (P.-B.F.) for aerosol mass separation in six equivalent aerodynamic/diffusion diameter (EDD) ranges, and subsequent trace element analyses by PIXE;

Supporting wind data for the two NYA stations came from:

- wind "sector meter" for wind direction frequency classification in eight 45^0 sectors at NILU I (and "MISU 1981");

- mechanical "wind station" (W.STA.) for continuous recording of wind speed and direction at NILU II.

---

* PIXE = particle induced X-ray emission.

Figure 1: Locations of Ny Ålesund (NYA) and Bjørnøya (BJO) ground stations.

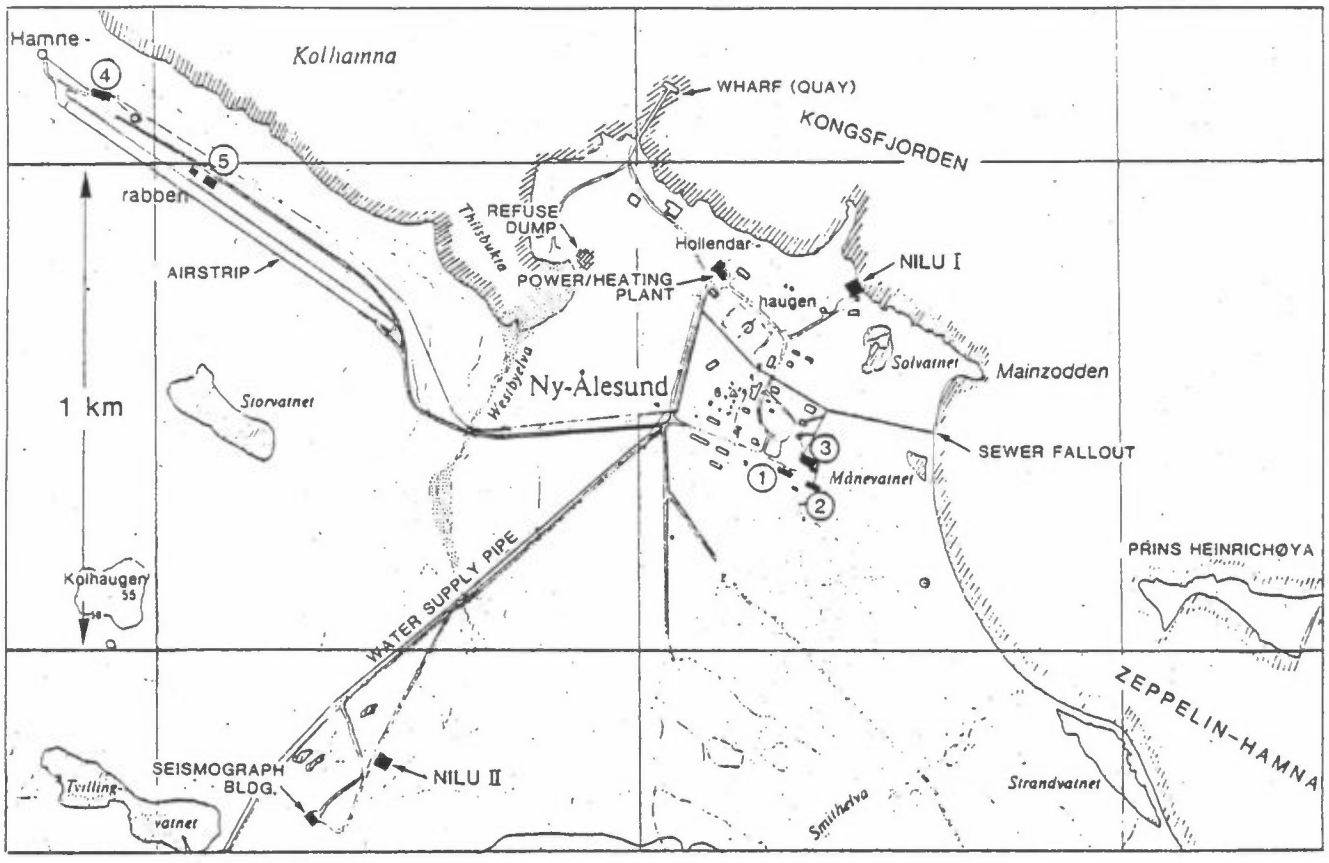

Figure 2: Main features of the Ny Ålesund settlement.

1: NPI research station
2: bachelors' quarters
3: mess/recreation building
4: MISU station in 1981
5: plane hangar and windsock

At the Bjørnøya ground station (BJO), a medium-sensitivity integrating nephelometer (IN) for continuous measurement, display and recording of aerosol scattering coefficient, σ_{sp}, was operated during part of the BP Project.

2.2 DATA REDUCTION AND SAMPLE ANALYSIS

The continuous recordings of near real-time CN concentrations and σ_{sp} were first reduced by hand to hourly medians, from which approximately 12-hour medians were obtained.

The printouts of 60-min particle counts in five size ranges from OPC measurements were computer-processed at NILU as number, surface area, and volume versus particle size distribution spectra.

The size-differentiated aerosol fractions, collected by BTL C.I. and the P.-B.F. system, were analysed by PIXE at the Departement of Nuclear Physics, Lund Institute of Technology, Lund, Sweden. The detailed procedures (as well as the accuracy and precission) of the PIXE method for impactor substrate and NP filter analysis have been described by Carlsson et al. (1981).

3 *MEASUREMENT RESULTS*

The special measurement results are for the most part shown graphically in the figures under the various measurement heading.

Note that most of the BP Project campaign periods "straddled" the conventional season boundaries*, with the result, that some of the season "labels" on the figures do not strictly adhere to these designations, e.g., "winter" may stand for "winter/spring", and "fall" for "summer/fall".

3.1 PHYSICAL PROPERTIES OF AEROSOLS

The physical parameters of the arctic aerosol were measured in situ and in near real-time by CNC, A-IN and the OPC during the intensive BP Project campaigns. These measurements at NYA usually began and ended a few days before and after the "official" periods for Hi-Vol and PUR sampling.

The near real-time IN measurements at BJO were continuous from 1982-11-28 to 1983-08-30 (except for a two week period in March 1983).

3.1.1 CNC and σ_{sp}

The approximately 12-hour median values of CN concentrations (CNC) and (when available) aerosol light scattering coefficient (σ_{sp}) are shown as time series graphs for NYA in Figures 3 through 8. The time series of 12-hour σ_{sp}

* Winter: Dec. - Feb.; spring: Mar. - May; summer: June - Aug.; fall: Sep. - Nov.

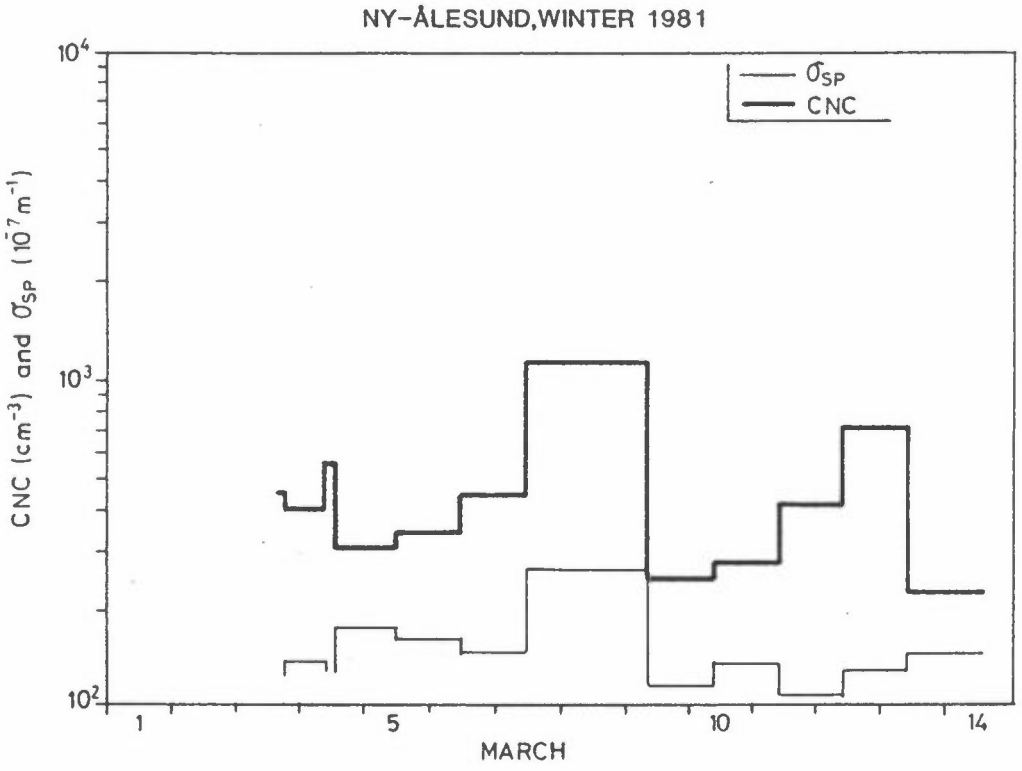

Figure 3: CN concentrations (CNC) and aerosol light scattering coefficients (σ_{sp}) averages over various time intervals, measured at "MISU 1981" site in Ny Ålesund (Heintzenberg et al., 1983)

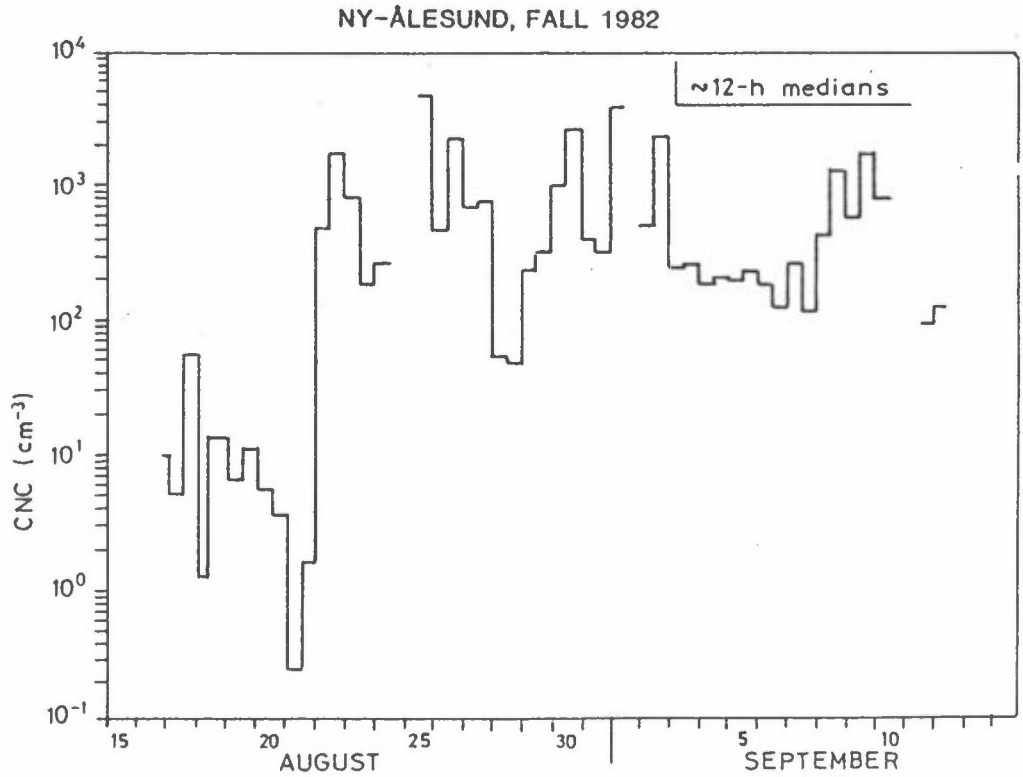

Figure 4: 12-hour CN concentration (CNC) medians, measured at NILU I during the Fall 1982 campaign (Heintzenberg et al., 1983). (The missing data are due to prolonged local emission disturbances.)

medians for BJO are plotted in Figures 9 through 11.

Figure 3 shows results of CNC and σ_{sp} measurements by personnel of the Department of Meteorology, University of Stockholm (MISU) at the "MISU 1981" site in Ny Ålesund (see Figure 2), during the first two weeks in March, 1981 (Heintzenberg et al., 1983). During the BP Project Summer/Fall 1982 campaign, the MISU-operated IN at NILU I site (see Figure 2) was malfunctioning, so that only CNC medians are shown in Figure 4.

The CNC and σ_{sp} medians in Figure 5 were supplied by MISU*, who operated their CNC instrument and NILU's A-IN integrating nephelometer at NILU I during the Winter/Spring 1983 campaign.

For the remaining BP Project campaigns at NILU II (see Figure 2), the CNC and σ_{sp} medians are presented in Figures 6 through 8.

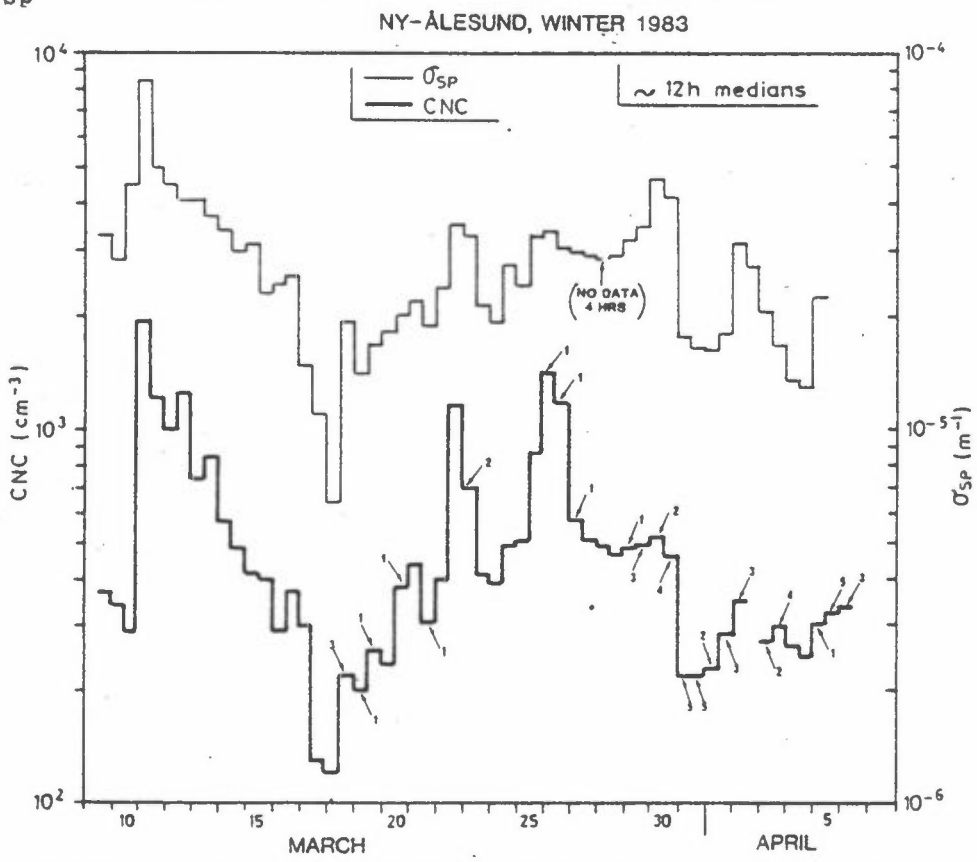

Figure 5: 12-hour CN concentration (CNC) and aerosol light scattering coefficient (σ_{sp}) medians at NILU I during the Winter/Spring 1983 BP Project campaign (data courtesy of MISU).
The numbers on the CNC graph indicate hours with local emission disturbances during each 12-h period.

* Unpublished data, courtesy of Dr. Jost Heintzenberg, MISU.

The number of hours, indicated on the CNC plots in these figures, show the sampling time lost during each 12-h period due to direct local emission influence, as exemplified by strongly fluctuating CNC recording traces. These period were excluded from the 12-h median determination. In most cases, the A-IN did not respond in a similar manner to such local pollutant interference, due to its relative insensitivity to very fine, mostly combustion-generated Aitken particles, and no exclusions from the σ_{sp} medians were necessary. The calibration procedure for the A-IH, however, required ca. 2 hour sampling interruptions from time to time.

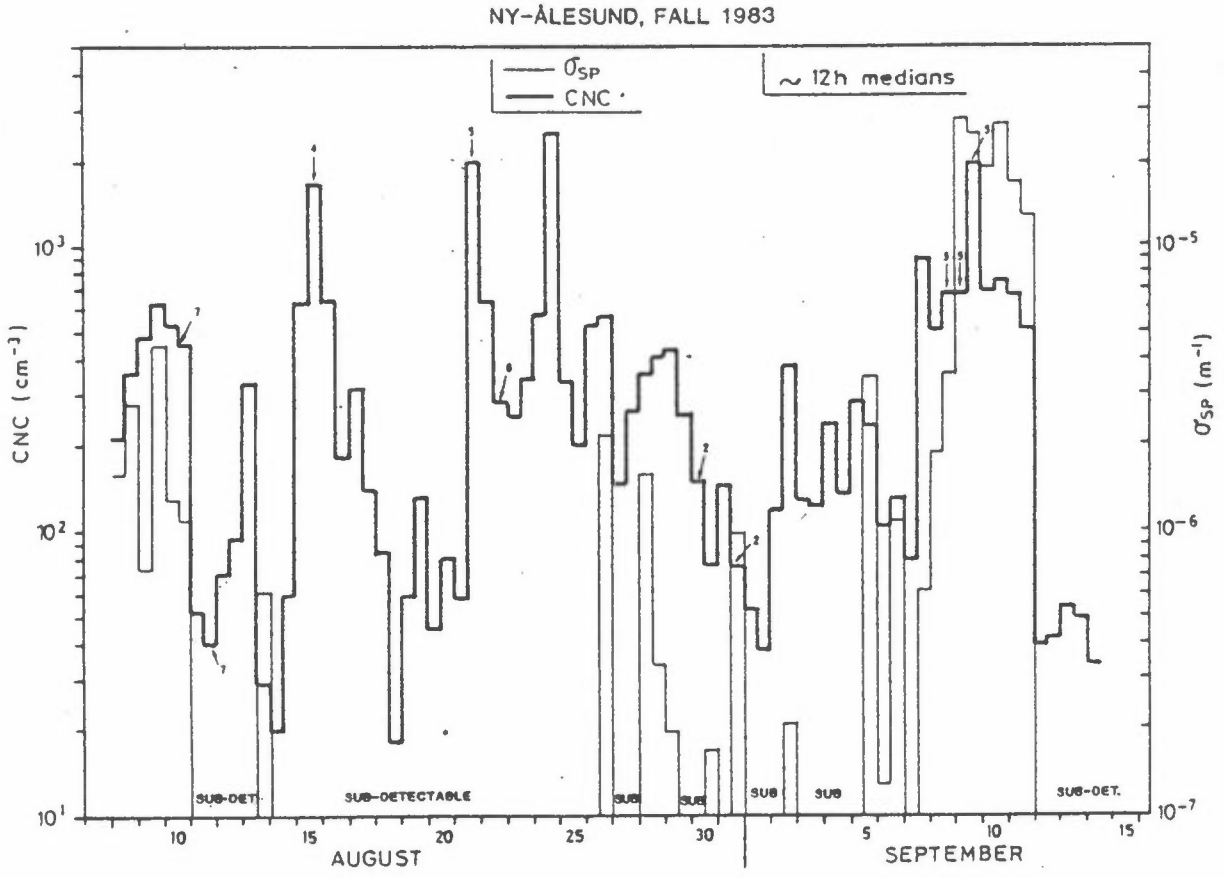

Figure 6: 12-hour CN concentration (CNC) and aerosol light scattering coefficient (σ_{sp}) medians at NILU II during the Summer/Fall 1983 BP Project campaign.

The numbers on the CNC graph indicate hours with local emission disturbances during each 12-h period; "sub-detectable" for the σ_{sp} graph means below detection limit of the A-IN.

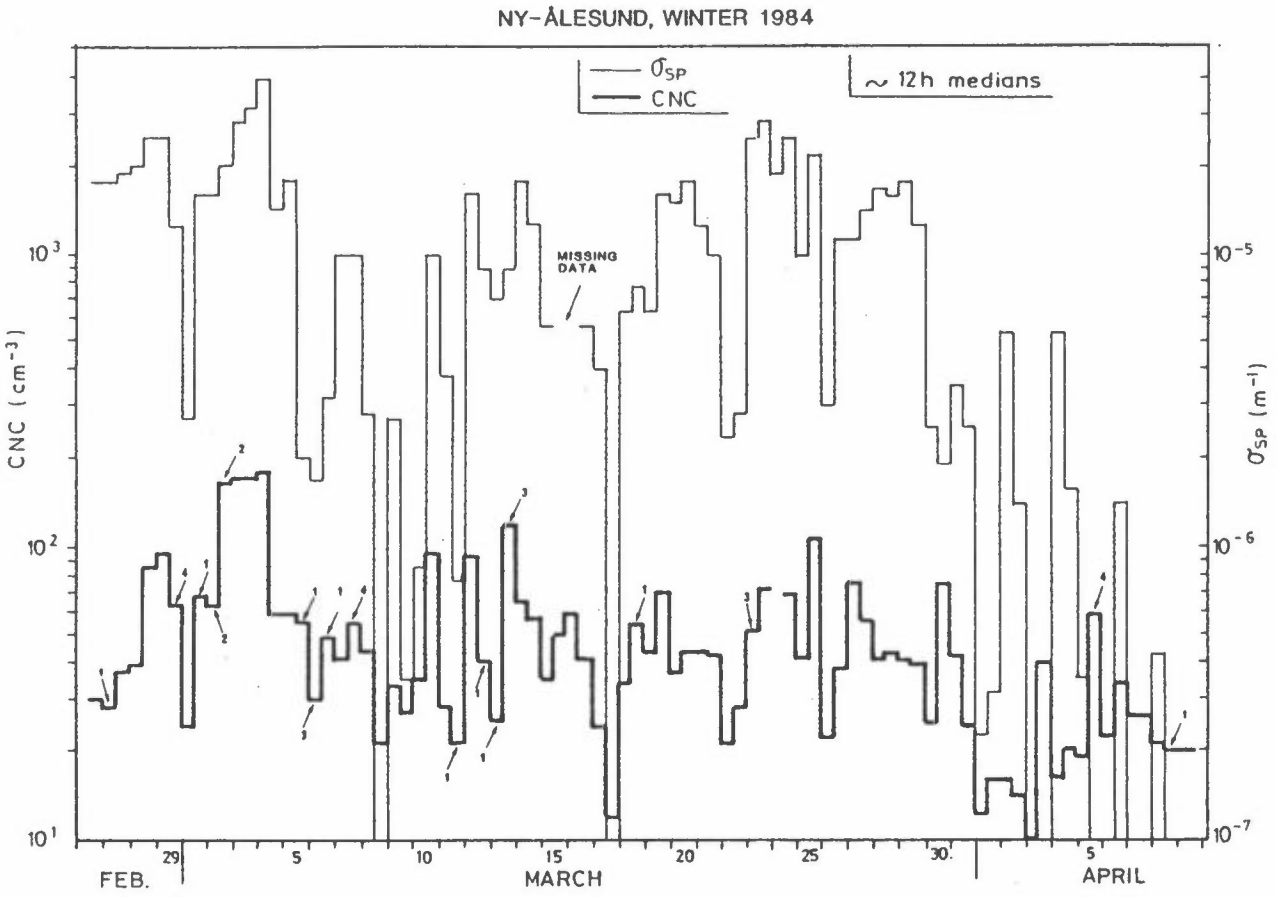

Figure 7: 12-hour CN concentration (CNC) and aerosol light scattering coefficient (σ_{sp}) medians at NILU II during the Winter/Spring 1984 BP Project campaign.

The numbers on the CNC graph indicate hours with local emission disturbances during each 12-h period.

The ca. 1-day long missing data period for σ_{sp} was due to A-IN power supply breakdown.

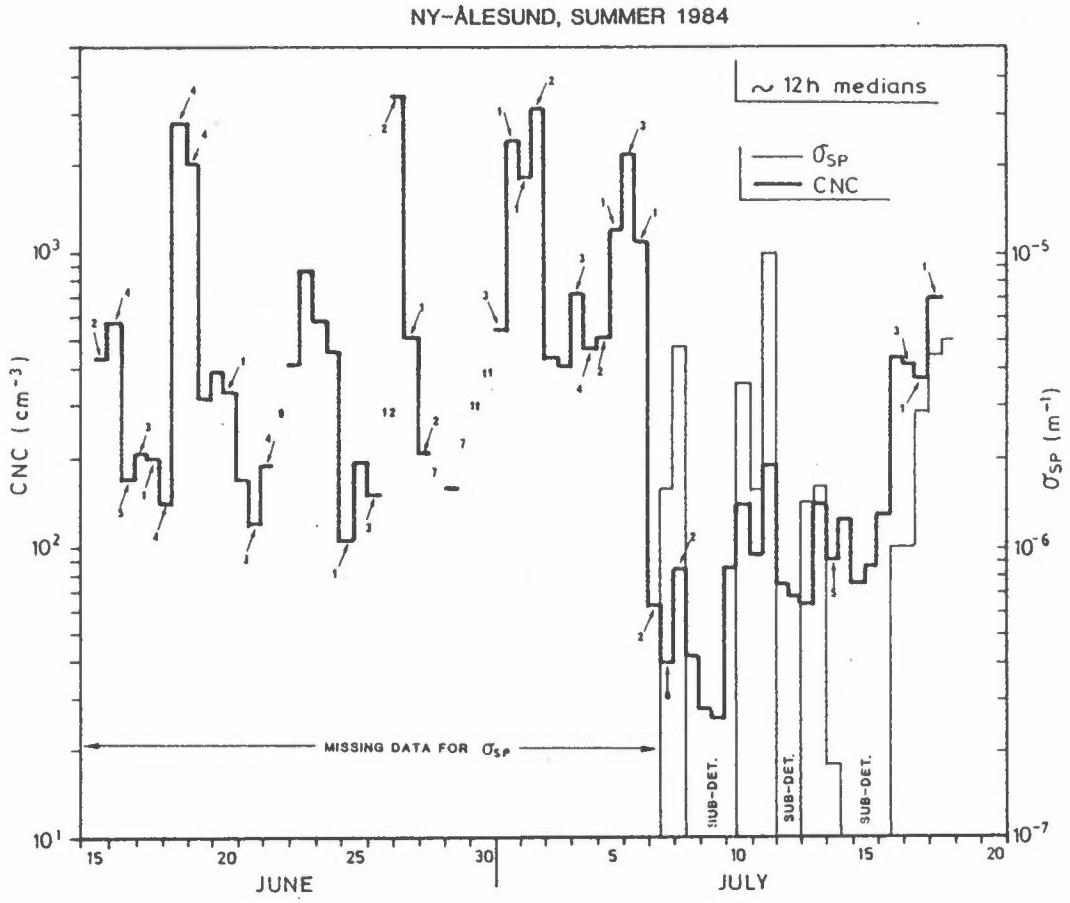

Figure 8: 12-h CN concentration (CNC) and aerosol light scattering coefficient (σ_{sp}) medians at NILU II during the Summer 1984 BP Project campaign.

The numbers on the CNC graph indicate hours with local emission disturbances during each 12-h period; "sub-det." for the σ_{sp} graph means below detection limit of the A-IH.

The 3-week long period of missing σ_{sp} data in Figure 8 was the result of A-IN malfunctioning, later discovered to be due to shipping damage. Subsequent emergency repair at Longyearbyen allowed the resumption of σ_{sp} measurements on 1984-07-07.

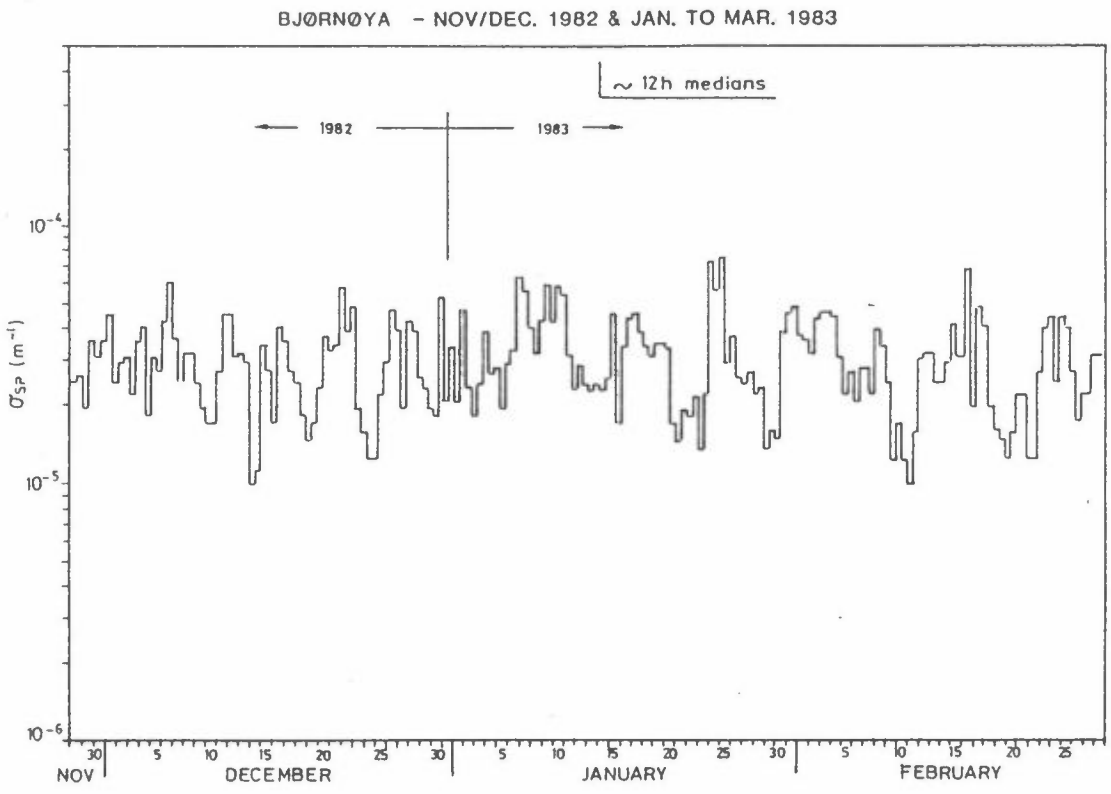

Figure 9: 12-h medians of aerosol light scattering coefficient (σ_{sp}) at Bjørnøya, 1982-11-28 to 1983-02-28.

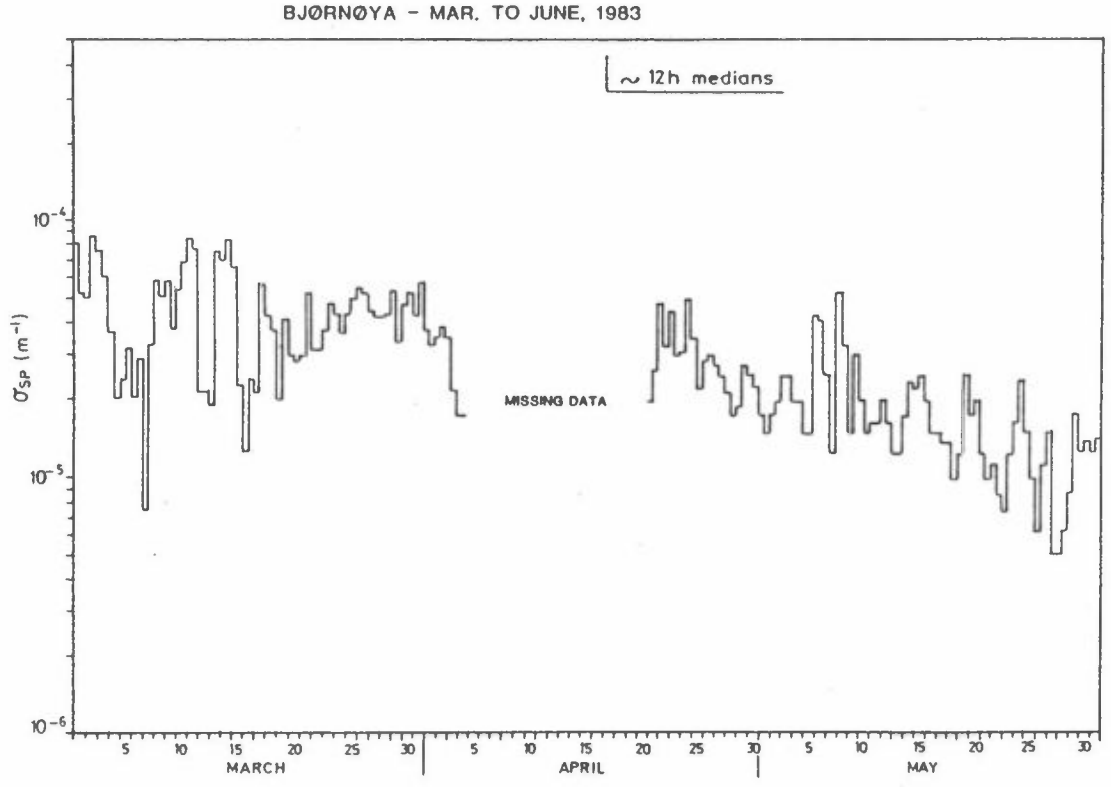

Figure 10: 12-hour medians of aerosol light scattering coefficient (σ_{sp}) at Bjørnøya, 1983-03-01 to 1983-04-03 and 1983-04-21 to 1983-05-31.

The missing σ_{sp} data period at BJO from 1983-04-04 to 1983-04-20 was due to needed instrument maintainence and repairs.

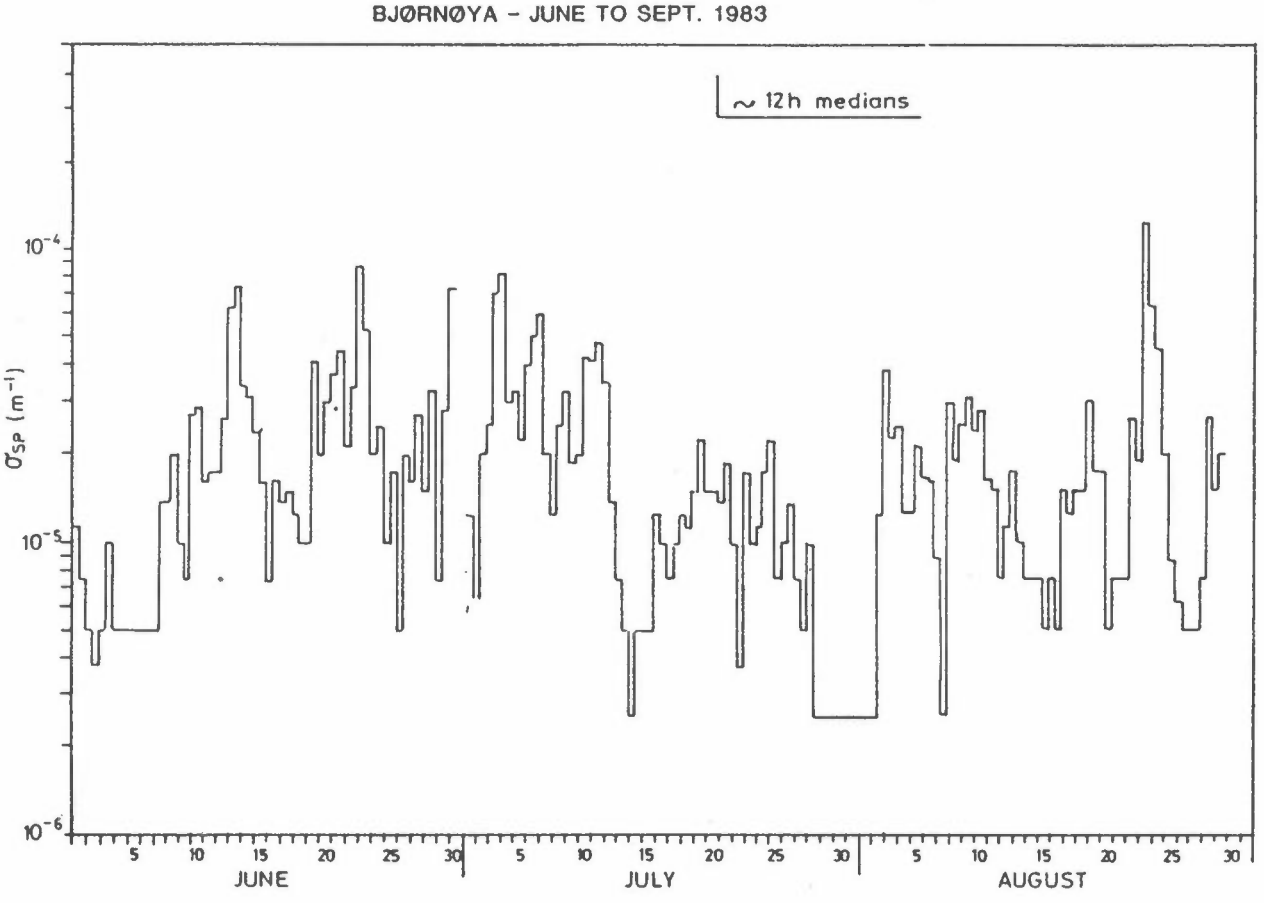

Figure 11: 12-hour medians of aerosol light scattering coefficient (σ_{sp}) at Bjørnøya, 1983-06-01 to 1983-08-30.

3.1.2 Aerosol size distributions

The Royco Model 225 optical particle counter (OPC), used at NILU I and NILU II during four BP Project campaigns (see Vitols and Wasseng, 1985), counted and classified aerosol particles in five equivalent scattering diameter (ESD) ranges: ~0.3-0.5, 0.5-1.4, 1.4-3.0, 3.0-5.0, and >5.0 μm. The particle counts in each of the five size ranges were printed out at 10-min. and 60-min. intervals. Subsequently, these were converted to aerosol particle number concentrations (particles cm^{-3}), and then reduced to the 12-hour averages* shown in Figures 12, 13, 14 and 15 for the four campaigns.

Because the OPC printer is programmed to centre the hourly counts on the full hour, the 12-h averages lag the 12-hour CN concentration and σ_{sp} medians in Section 3.1.1 by 30 minutes. With one exception, the averages were only computed and shown for periods during which all twelve hourly counts were available. The missing data are mainly due to OPC printer malfunctioning (because of sensitivity to low voltages), but, in the case of the last half of the Winter/Spring 1984 campaign, due to OPC transformer burn-out.

Following the conventional practice of OPC data presentation, the 12-h average concentrations were further computer-processed in terms of aerosol particle number ($\Delta N/\Delta \log D_p$), surface area ($\Delta A/\Delta \log D_p$), and volume ($\Delta V/\Delta \log D_p$) spectra. For this, all particles in a given ESD range were assumed to be spherical and to have one size only, which here is taken as the arithmetic mean of the five OPC range limit diameters. For computing and plotting purposes, 10 μm ESD was arbitrarily assigned as the upper size limit of sampled particles. Thus , for the >5 μm ESD particles, the slopes of the distributions depend on this choice of the upper size limit for the interval.

Despite the use of the 12-h averages, the data set of these spectra for all four campaigns is too voluminous to be presented here in its entirety, but is available by special request from NILU**. Thus, only selected distribution spectra are plotted in Figures 16 through 25, chosen for the purpose of illustrating various aerosol distribution features and/or for comparison with the patterns of the CNC and σ_{sp} 12-h medians in Section 3.1.1.

---

* OPC counts showed no extreme values.

** Contact Forsker Einar Joranger, NILU, P.b. 130, N-2001 Lillestrøm, Norway.

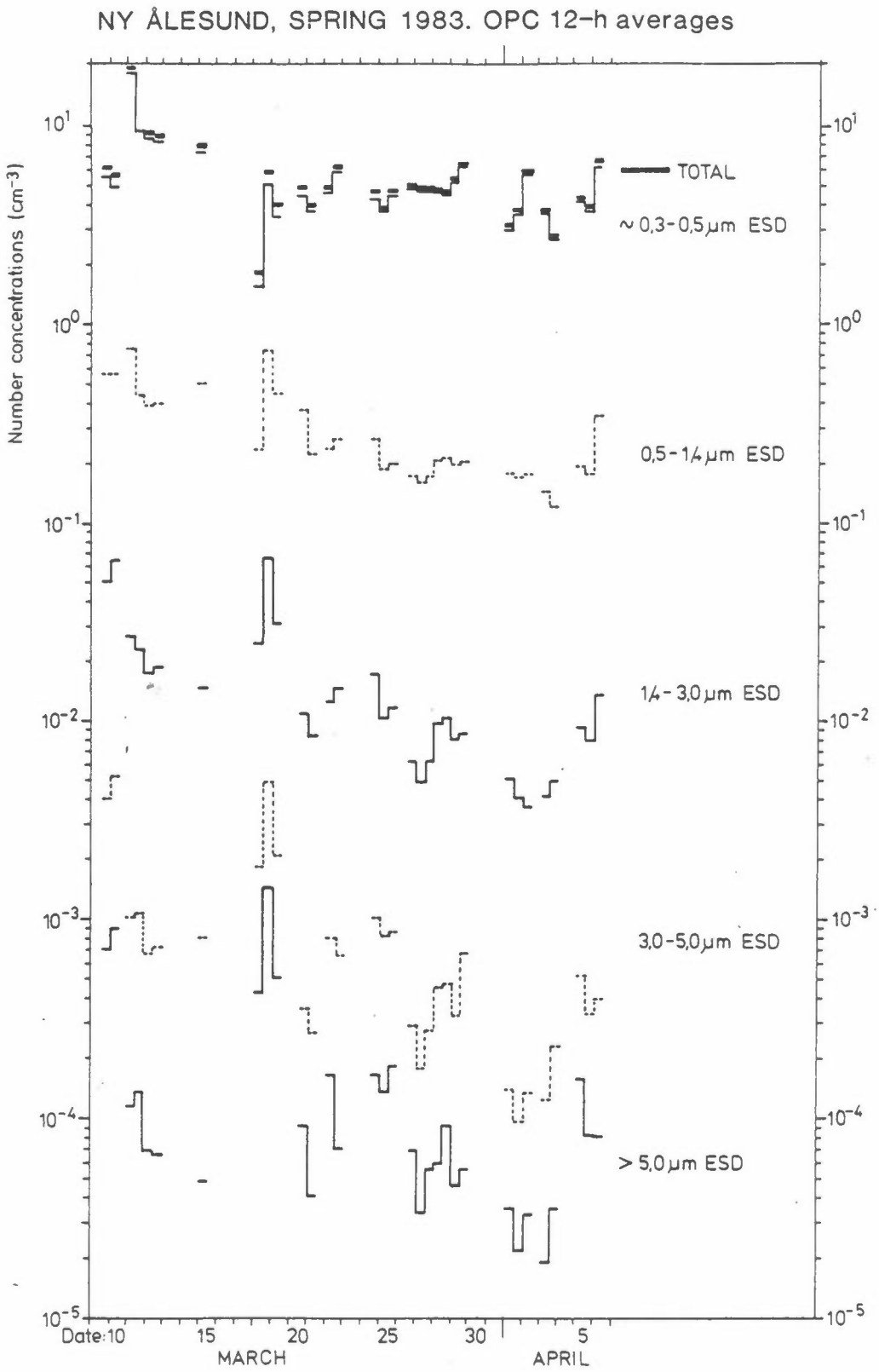

Figure 12: Aerosol particle number concentrations (cm^{-3}) in the 5 size ranges of the Royco 225 OPC measured during the Spring 1983 campaign at NILU I in Ny Ålesund.

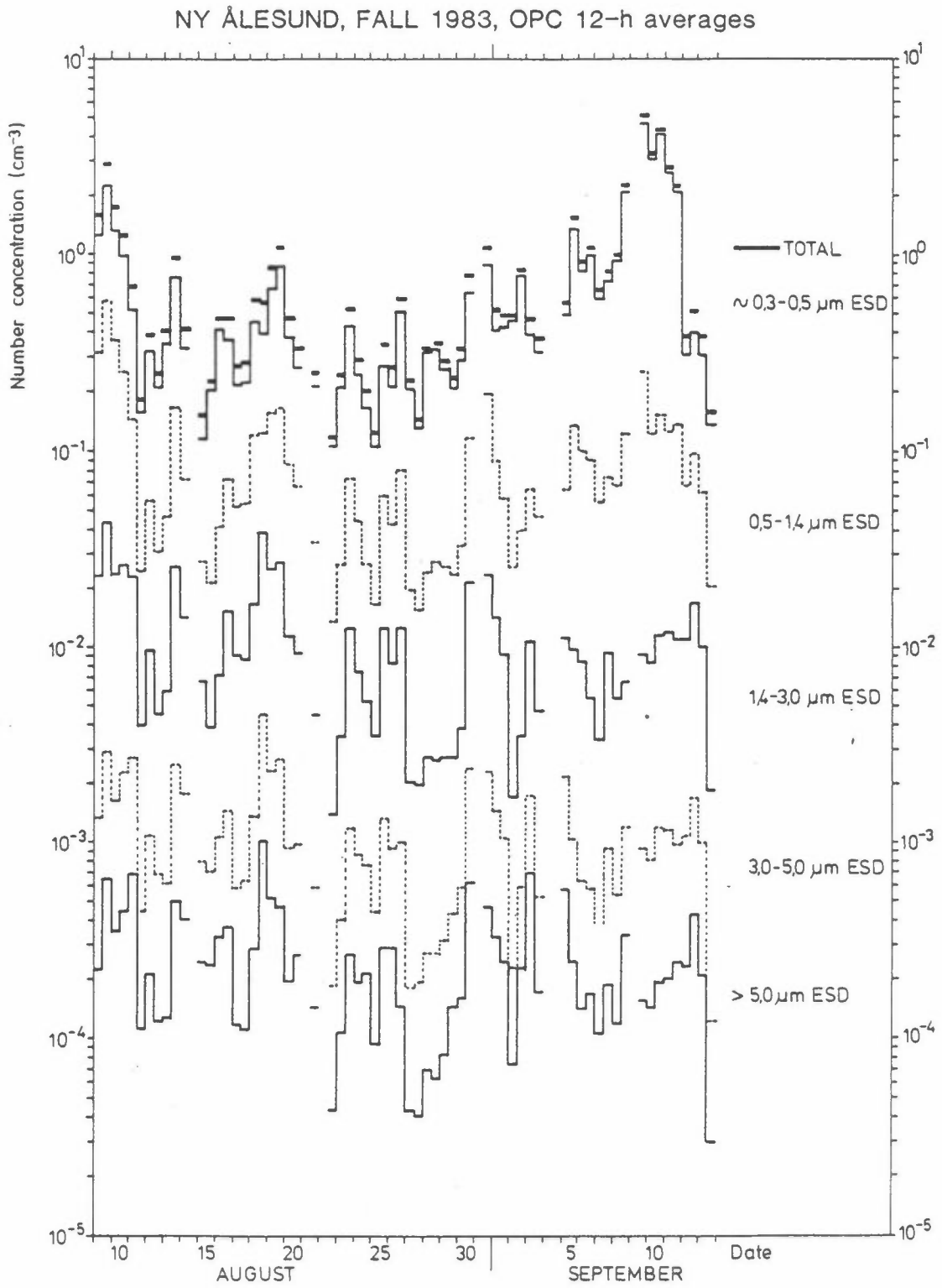

Figure 13: Aerosol particle number concentrations (cm^{-3}) in the 5 size ranges of the Royco 225 OPC, measured during the Fall 1983 campaign at NILU II in Ny Ålesund.

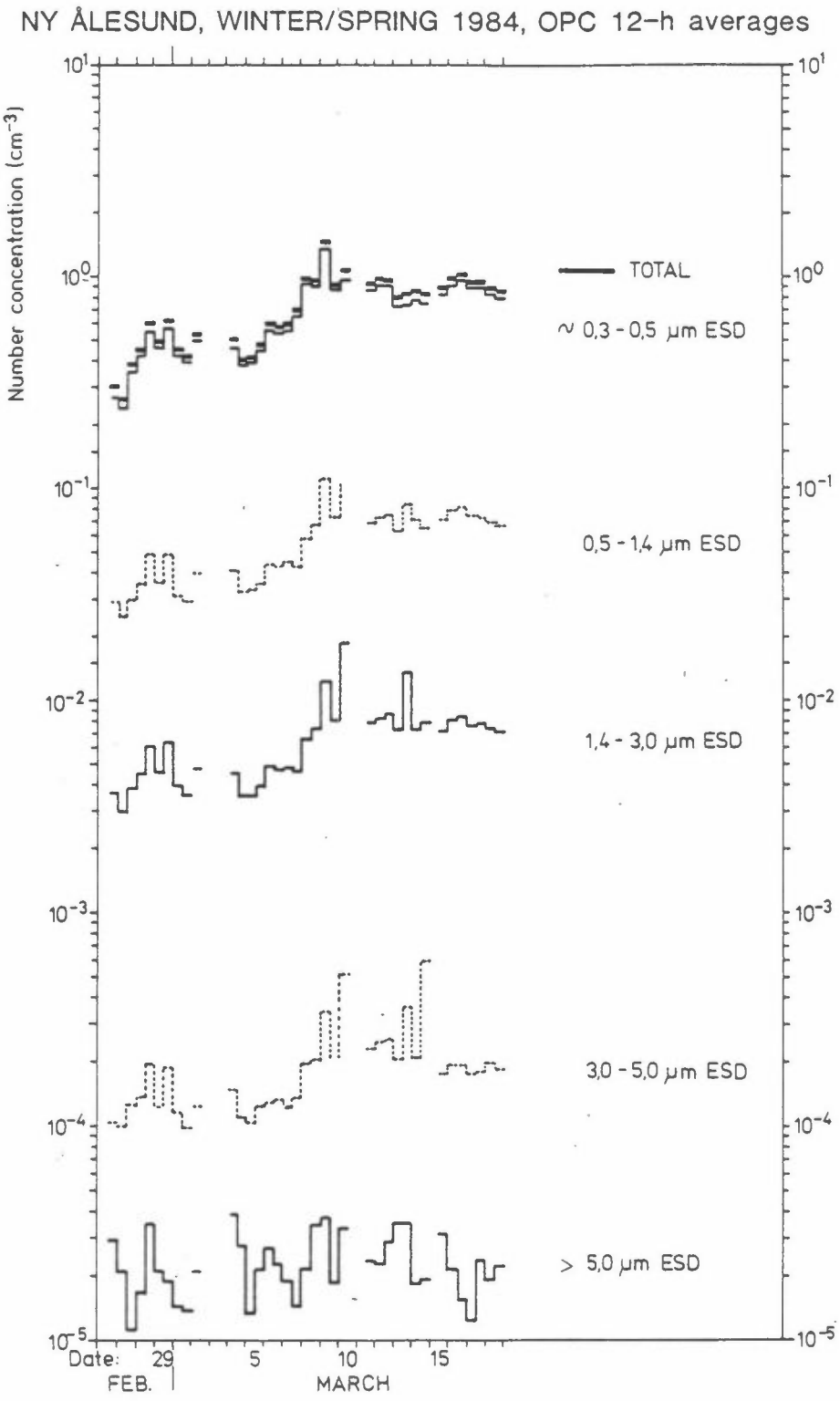

Figure 14: Aerosol particle number concentrations (cm^{-3}) in the 5 size ranges of the Royco 225 OPC, measured during the Winter/Spring 1984 campaign at NILU II in Ny Ålesund.

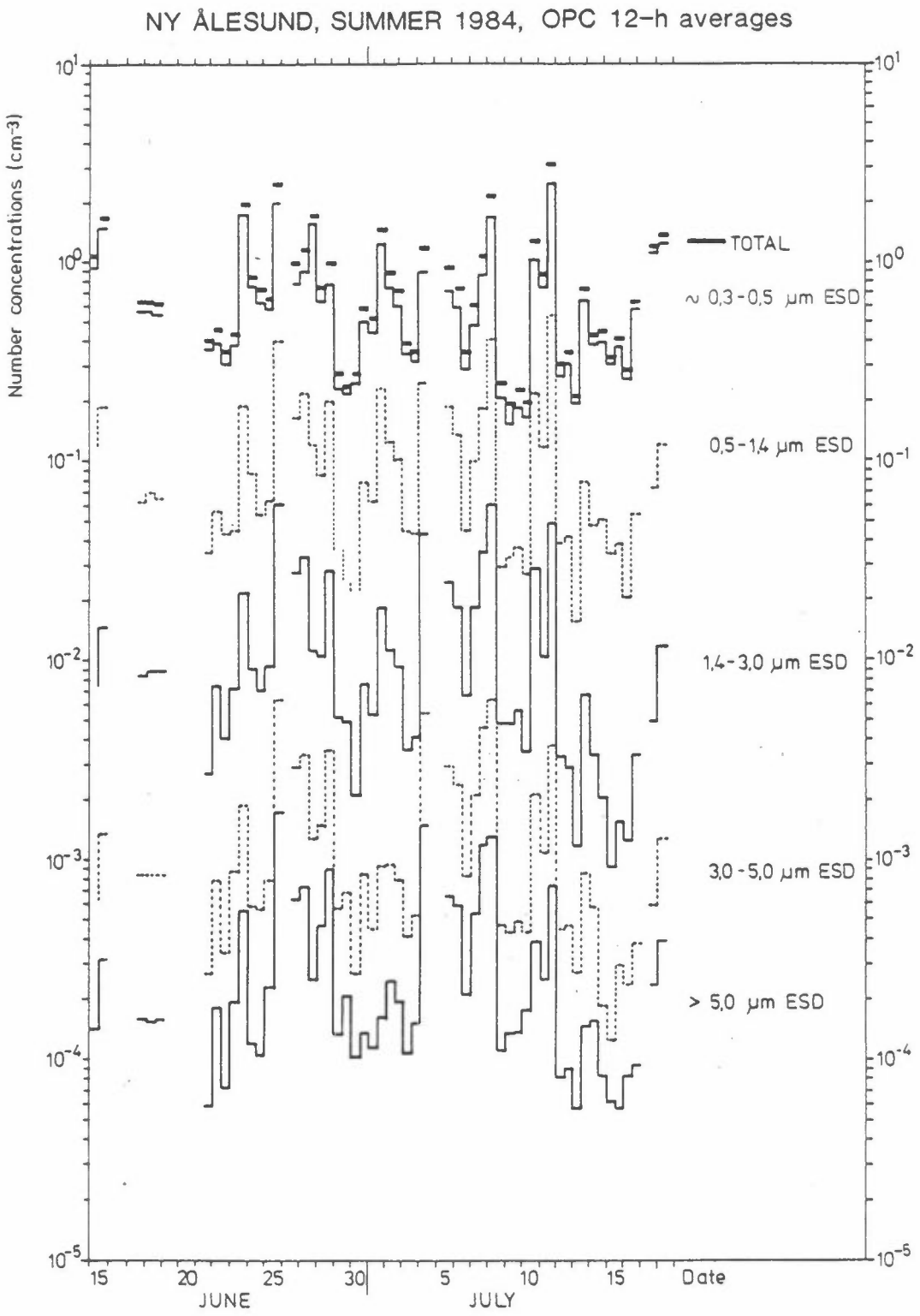

Figure 15: Aerosol particle number concentrations (cm^{-3}) in the 5 size ranges of the Royco 225 OPC, measured during the Summer 1984 campaign at NILU II in Ny Ålesund.

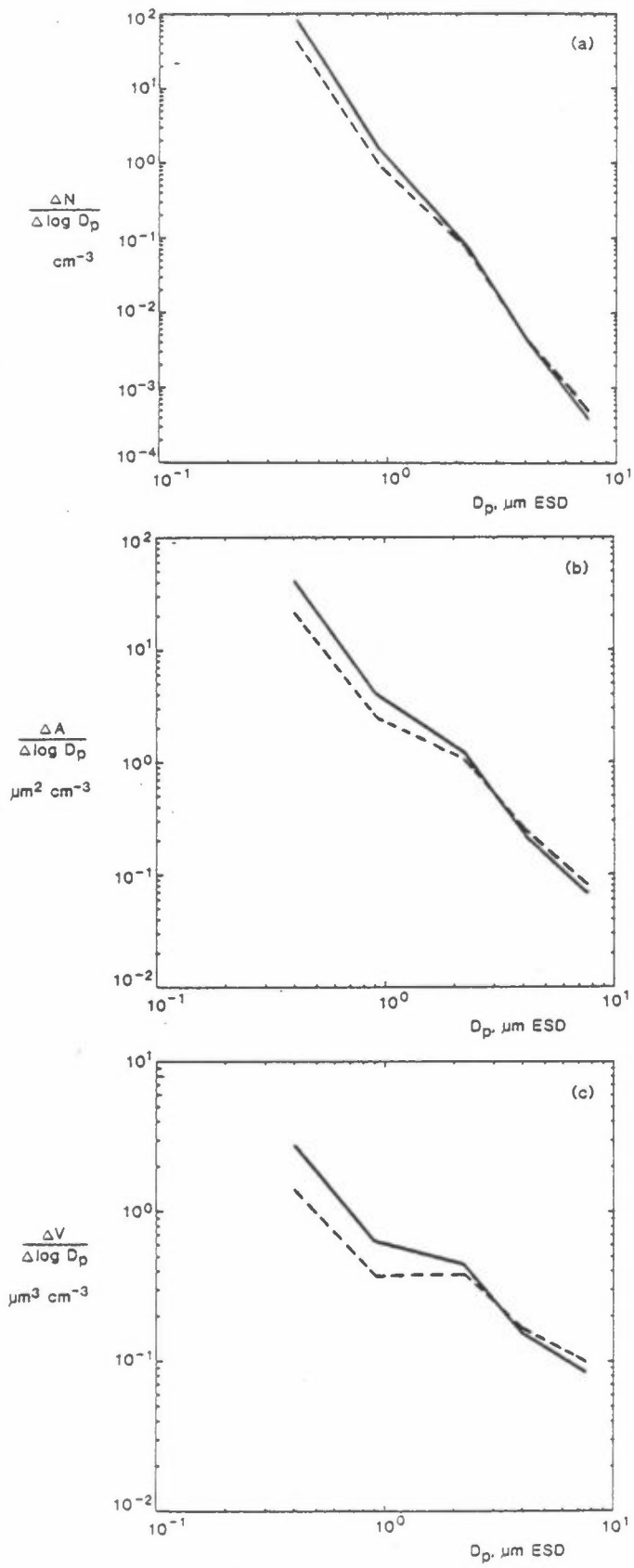

Figure 16: Aerosol average (a) number -, (b) surface -, and (c) volume - distribution spectra at NILU I in Ny Ålesund on 1983-03-11:
—— 0030-0930 MET
--- 1630-2430 MET
(MET = GMT + 1h)

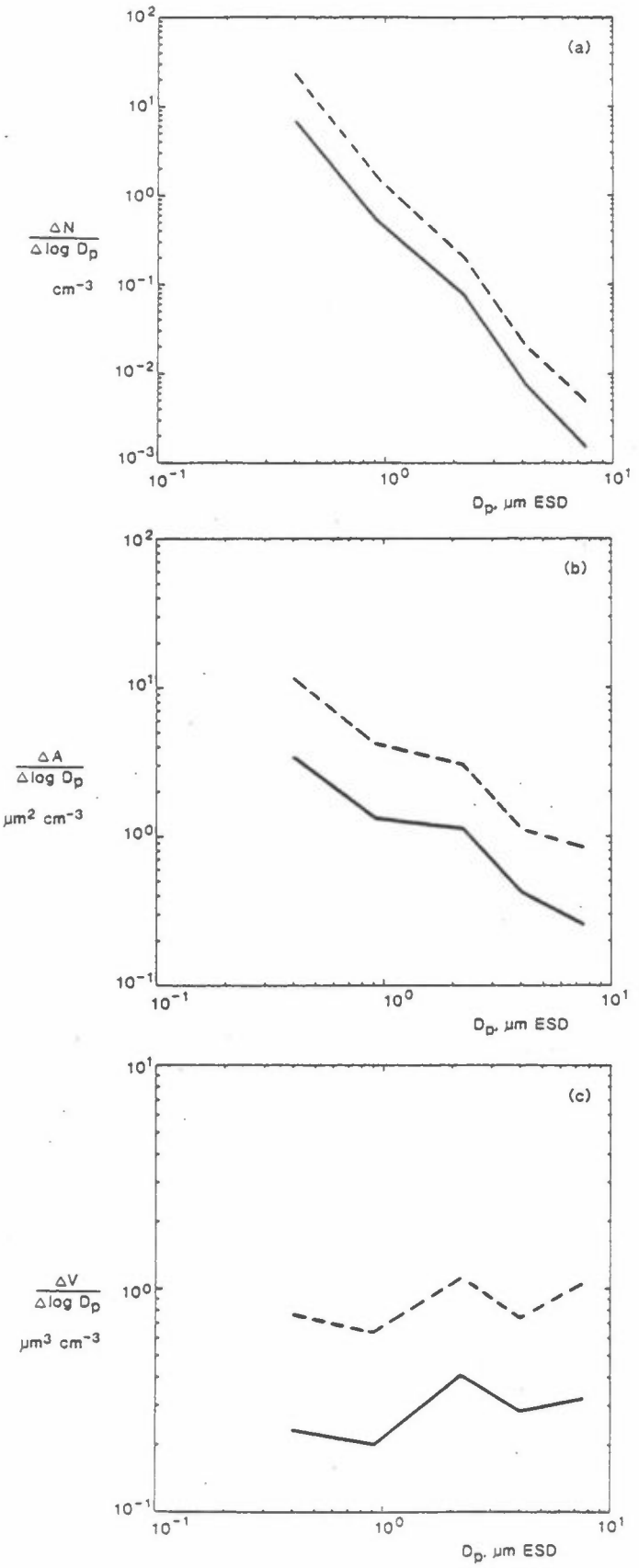

Figure 17: Aerosol12-h average (a) number -, (b) surface -, and (c) volume - distribution spectra at NILU I in Ny Ålesund on 1983-03-18:
—— 0030-1230 MET
--- 1230-2430 MET

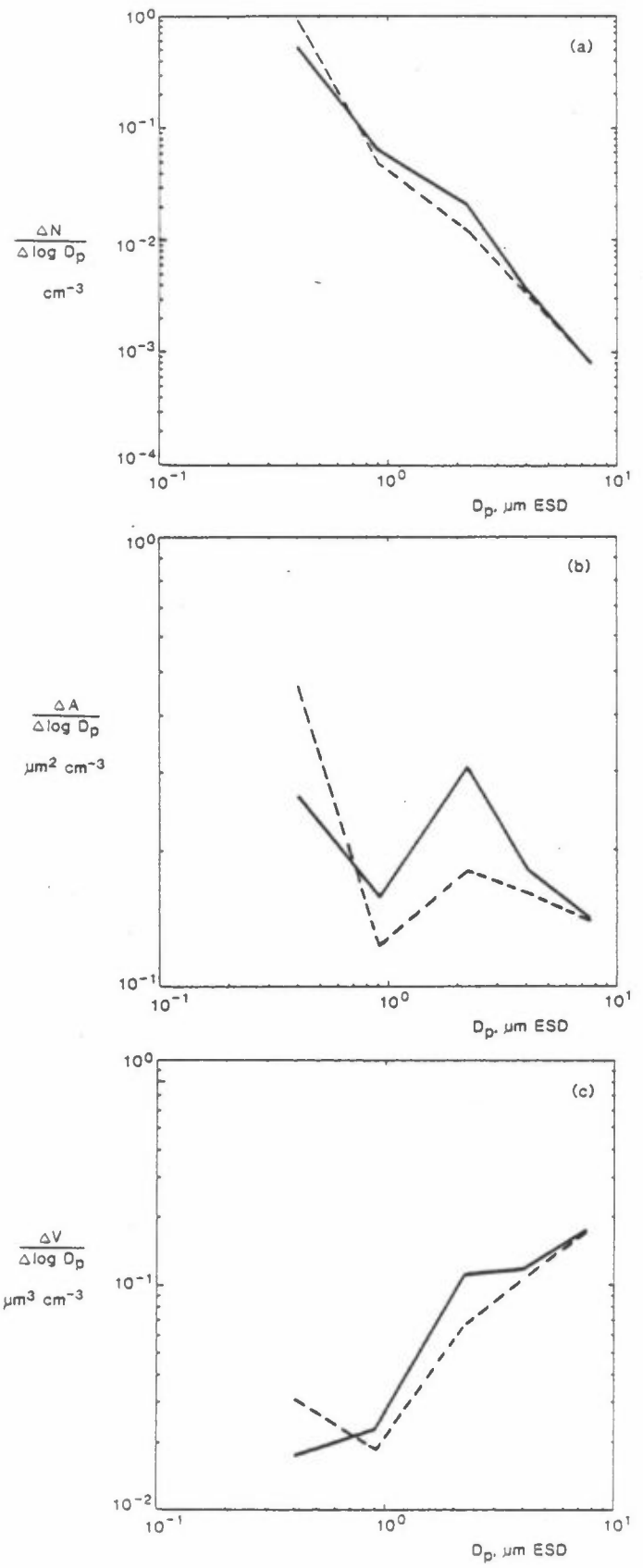

Figure 18: Aerosol 12-h average (a) number -, (b) surface -, and (c) volume - distribution spectra at NILU II in Ny Ålesund on 1983-08-15:
—— 0030-1230 MET
--- 1230-2430 MET

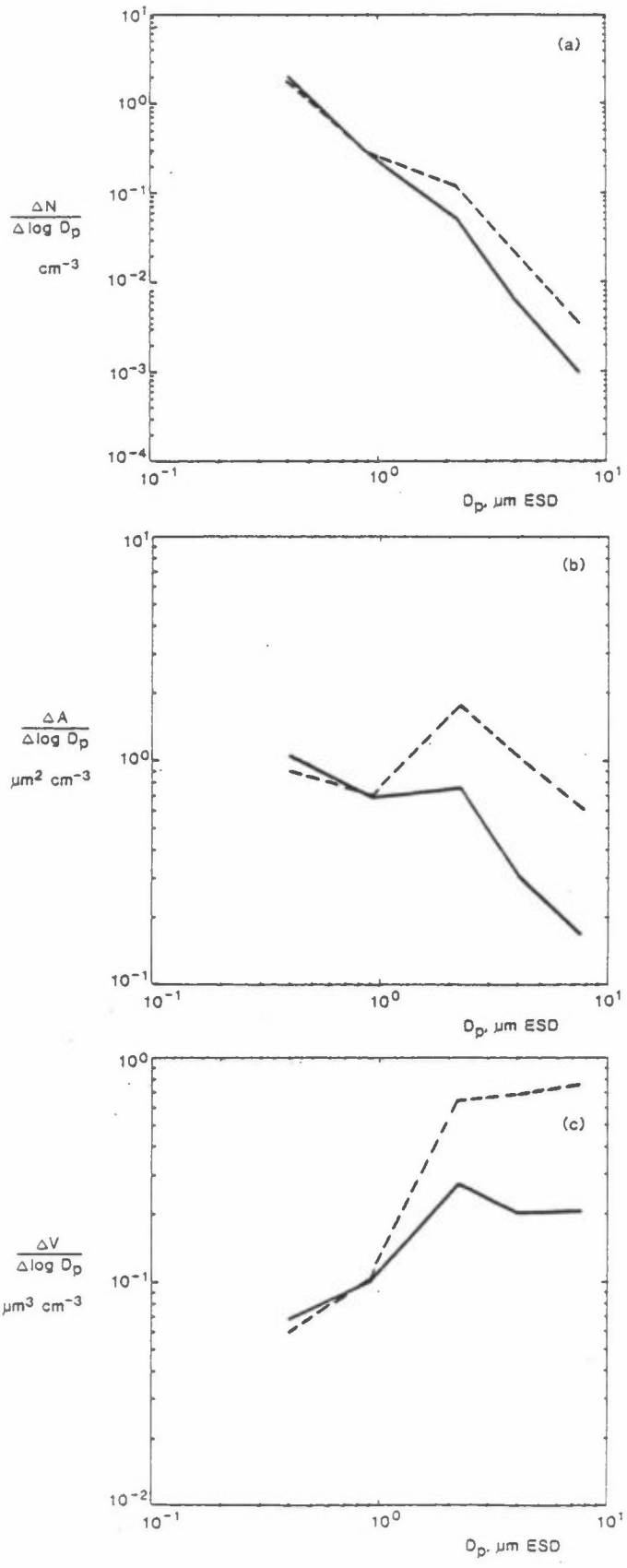

Figure 19: Aerosol 12-h average (a) number -, (b) surface -, and volume- distribution spectra at NILU II in Ny Ålesund on 1983-08-18:
—— 0030-1230 MET
--- 1230-2430 MET

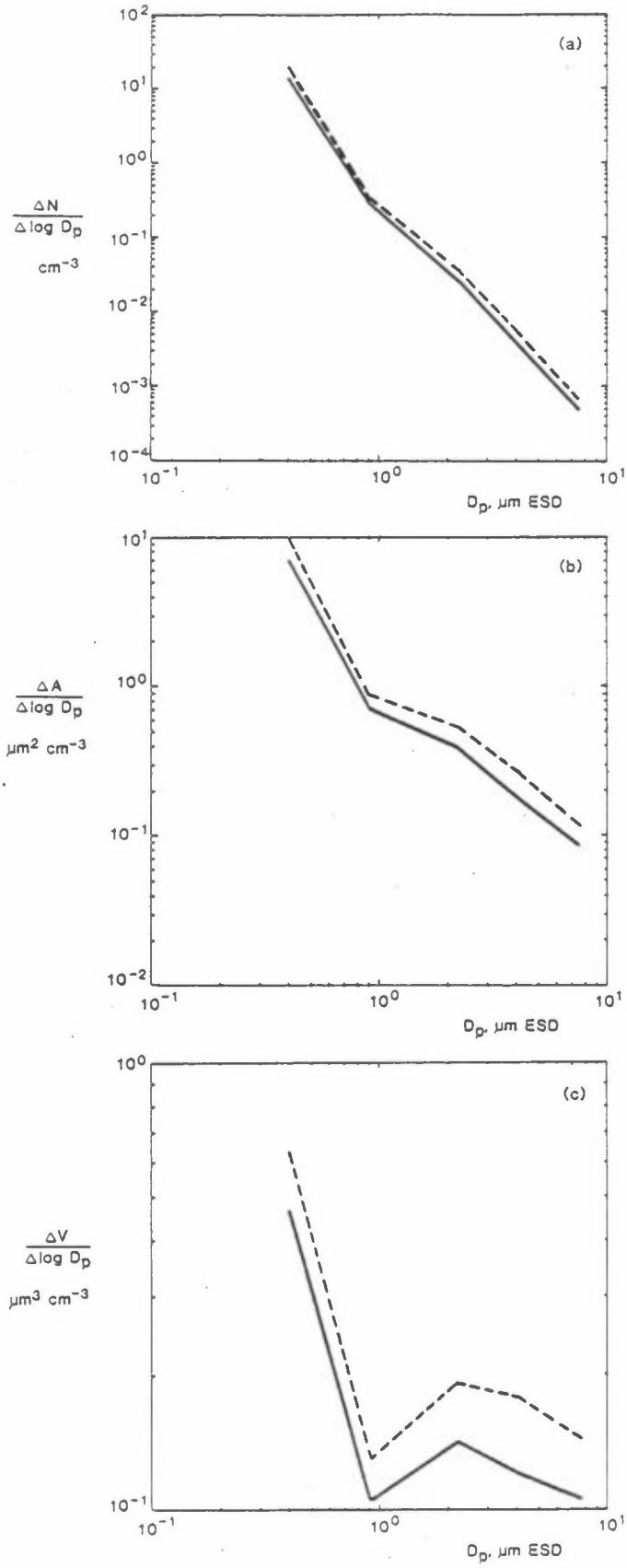

Figure 20: Aerosol 12-h average (a) number -, (b) surface -, and (c) volume - distribution spectra at NILU II in Ny Ålesund on 1983-09-10:
—— 0030-1230 MET
--- 1230-2430 MET

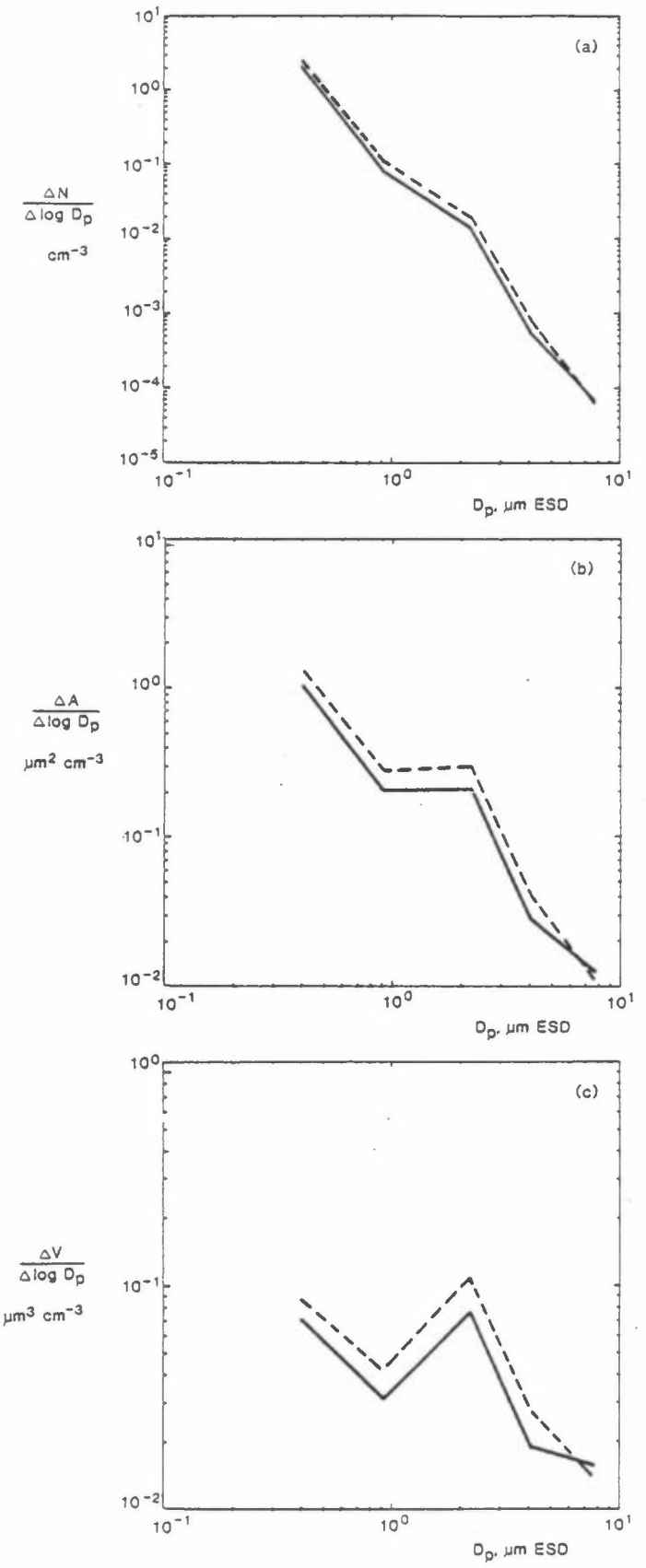

Figure 21: Aerosol 12-h average (a) number -, (b) surface -, and (c) volume - distribution spectra at NILU II in Ny Ålesund on 1984-02-29:
—— 0030-1230 MET
--- 1230-2430 MET

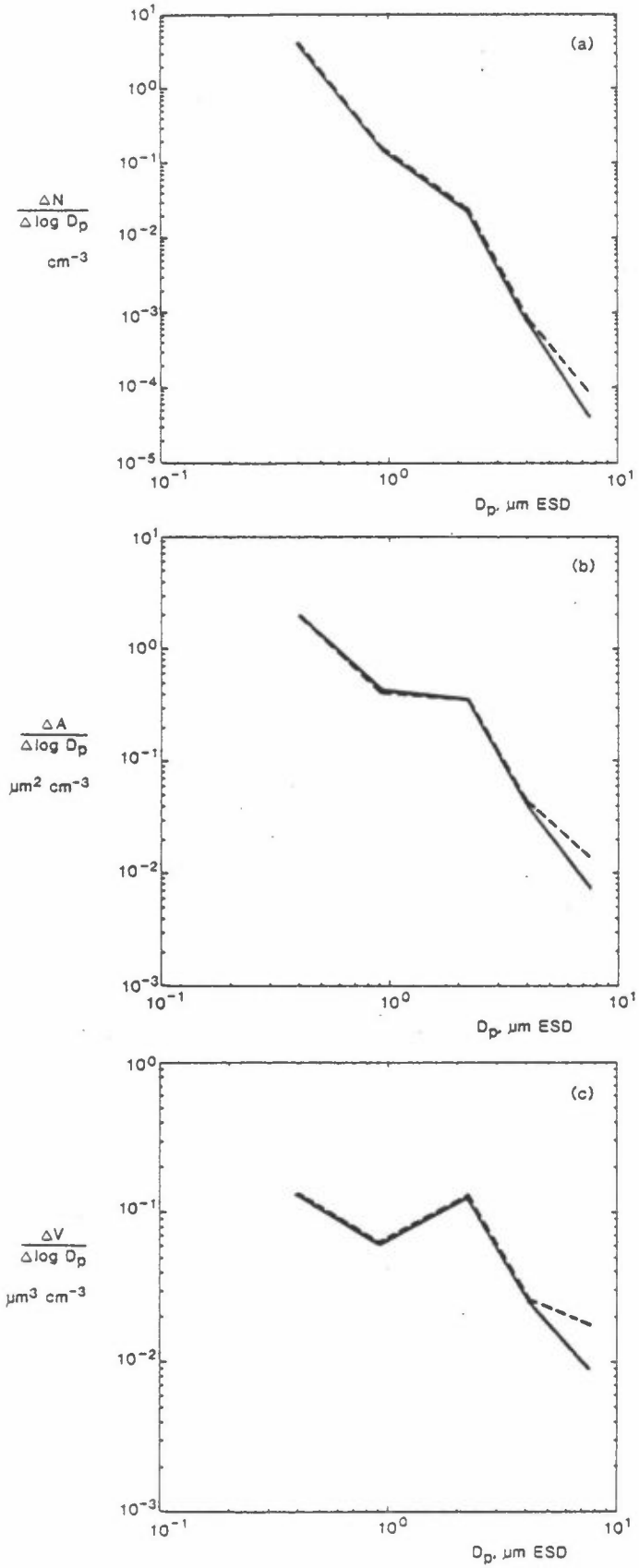

Figure 22: Aerosol 12-h average (a) number -, (b) surface -, and (c) volume - distribution spectra at NILU II in Ny Ålesund on 1984-03-17:
—— 0030-1230 MET
--- 1230-2430 MET

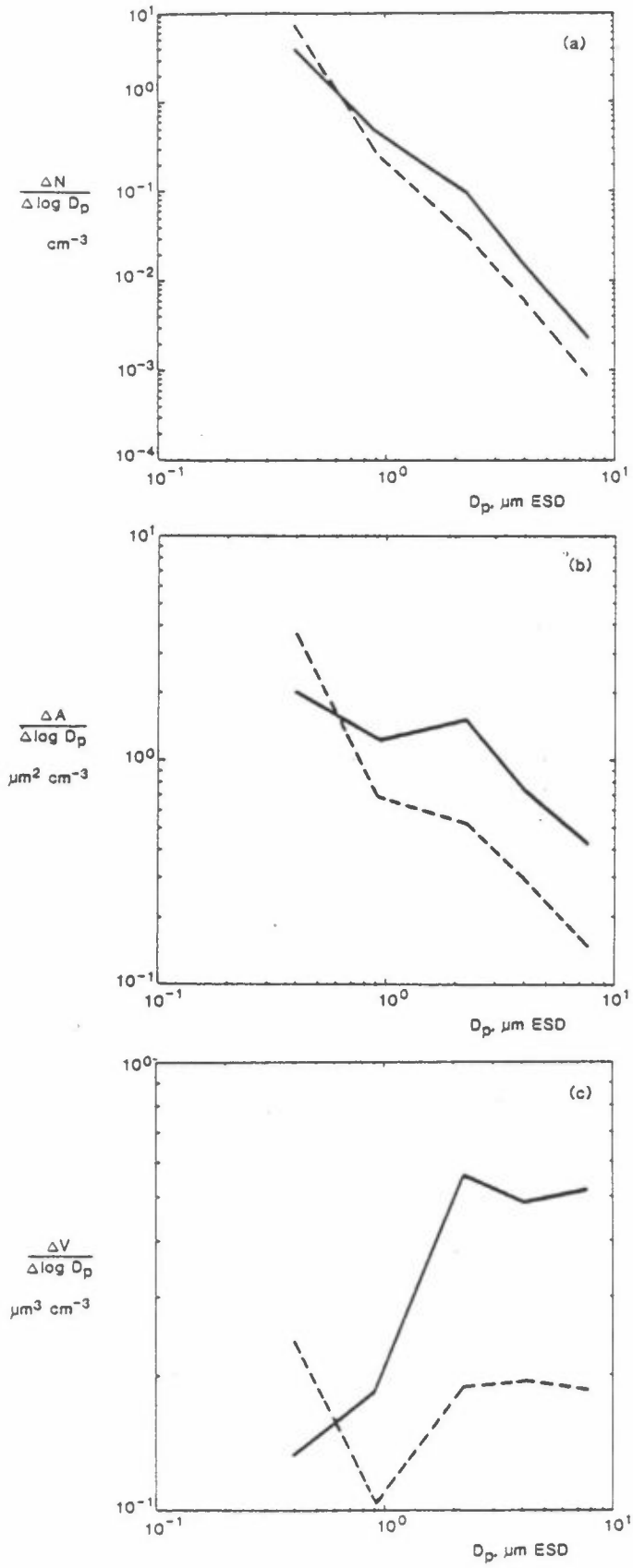

Figure 23: Aerosol 12-h average (a) number -, (b) surface -, and (c) volume - distribution spectra at NILU II in Ny Ålesund on 1984-06-27:
—— 0030-1230 MET
--- 1230-2430 MET

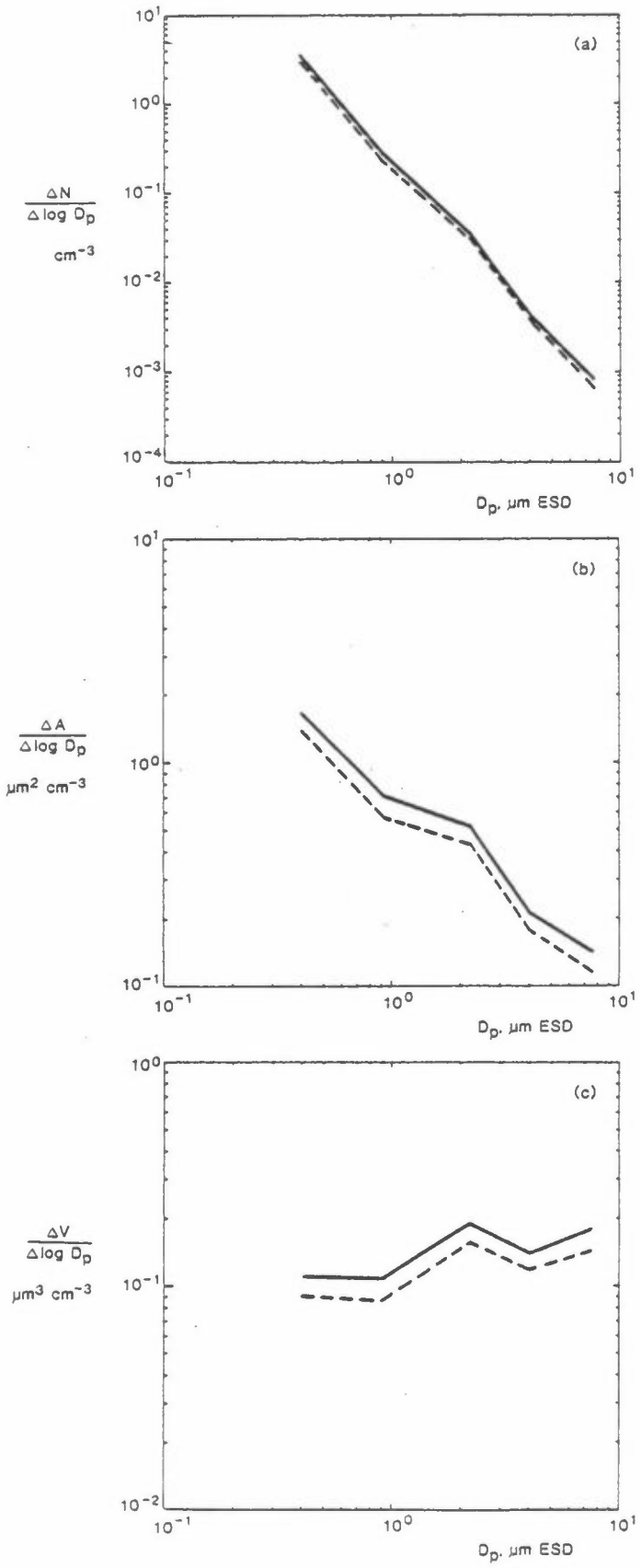

Figure 24: Aerosol 12-h average (a) number -, (b) surface -, and (c) volume - distribution spectra at NILU II in Ny Ålesund on 1984-07-02:
—— 0030-1230 MET
--- 1230-2430 MET

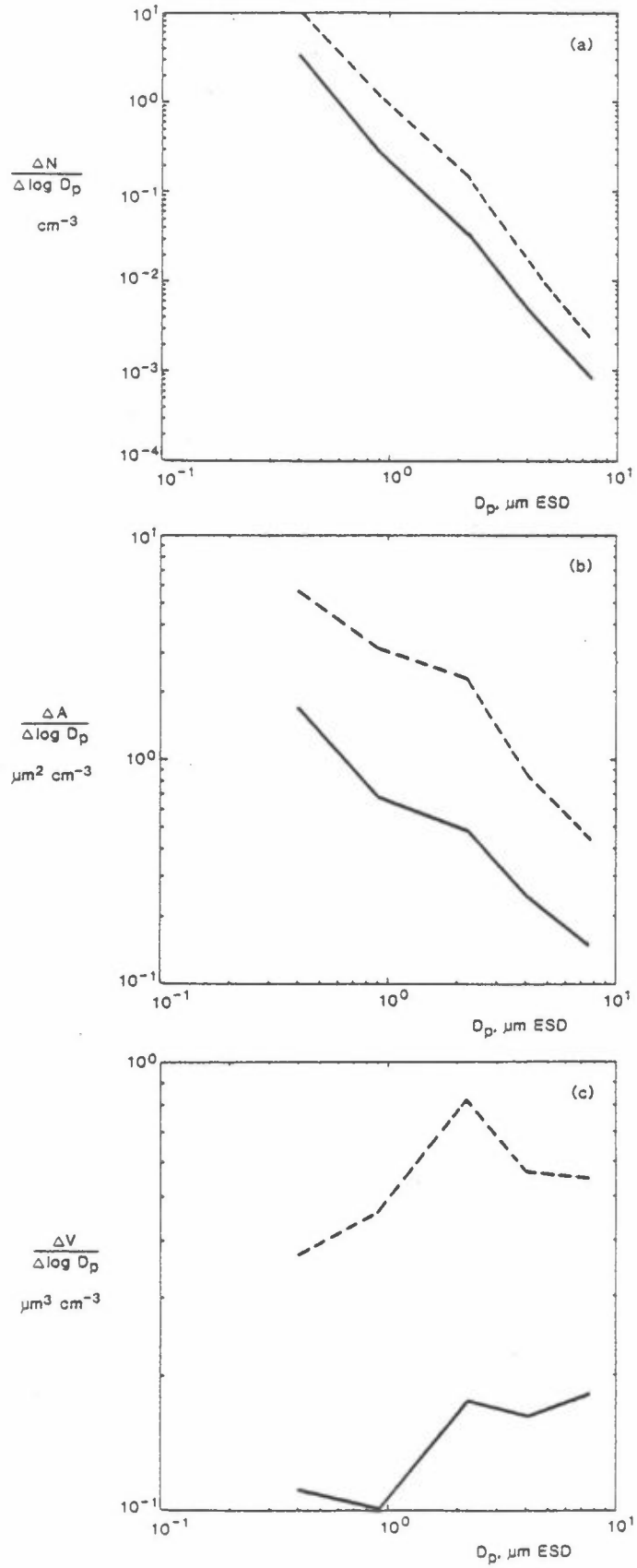

Figure 25: Aerosol 12-h average (a) number -, (b) surface -, and (c) volume - distribution spectra at NILU II in Ny Ålesund on 1984-07-11:
—— 0030-1230 MET
--- 1230-2430 MET

3.2 CHEMICAL PROPERTIES OF AEROSOLS

Two sets of size-differentiated aerosols for chemical composition determinations were independently collected at the NYA reference stations by:

- low-volume cascade impactor (BTL C.I.), and
- parallel-branch fractionation system (P.-B.F.)

The sampling equipment and procedures are described in Vitols and Wasseng (1985). Both sample sets were subsequently analysed* by PIXE (Carlsson et al., 1981) for as many elements, as the collected samples and the sensitivity of the analytical method allowed.

3.2.1 Mass-size differentiation by BTL C.I.

The BTL C.I. is a 6-stage, single round-jet cascade impactor of Battelle-design (Mitchell and Pilcher, 1959), operated at the low sampling rate of 1 l min^{-1}. The 6 impaction stages are coated with a sticky polyethylene glycol substrate, and are followed by a Nuclepore (NP) afterfilter. The filtration efficiency of NP filters has been thoroughly investigated (e.g., Liu et al., 1983). The 0.4 µm pore size NP afterfilters are approximately 100% efficient for particles >1.0 EAD and have filtration efficiencies >80% for all smaller sizes.

The BTL C.I. fractionates the aerosol in seven EAD ranges: <0.25 µm (afterfilter), 0.25-0.5 µm (Stage 5), 0.5-1 µm (Stage 4), 1-2 µm (Stage 3), 2-4 µm (Stage 2), 4-8 µm (Stage 1), and >8 µm (Stage 0). The instrument was used at NILU I and NILU II during four of the BP Project campaigns in the period March 1983 to July 1984. Detailed sampling information is tabulated in Table 1.

---

* by the Department of Nuclear Physics, Lund Institute of Technology, Lund, Sweden.

Table 1: Battelle cascade impactor (BTL C.I.) sampling information for the Spring 1983, Fall 1983, Spring 1984 and Summer 1984 campaigns at NYA.

Sample No.	Start of run (MET*)	End of run (MET*)	Sample volume**, m^3
(1)	(2)	(3)	(4)
1	1983-03-01, 14:30h	1983-03-04, 09:00h	4.38
2	1983-03-04, 14:10	1983-03-07, 09:10	4.41
3	1983-03-07, 15:15	1983-03-09, 08:15	2.51
4	1983-03-09, 14:15	1983-03-11, 08:15	1.41
5	1983-03-11, 17:00	1983-03-13, 09:15	2.02
6	1983-03-13, 09:40	1983-03-14, 13:10	1.61
7	1983-03-15, 11:00	1983-03-18, 08:35	4.04
8	1983-03-20, 12:00	1983-03-22, 09:15	2.25
9	1983-03-22, 09:20	1983-03-24, 09:30	2.52
10	1983-03-25, 13:05	1983-03-27, 08:15	1.01
11	1983-03-29, 09:40	1983-03-31, 10:00	2.61
12	1983-03-31, 10:30	1983-04-01, 09:45	1.15
13	1983-04-02, 11:00	1983-04-03, 16:15	0.99
14	1983-04-05, 08:10	1983-04-06, 08:35	1.28
1	1983-08-11, 09:30	1983-08-15, 08:00	4.07
2	1983-08-16, 17:45	1983-08-19, 10:25	3.95
3	1983-08-19, 14:10	1983-08-22, 08:20	2.56
4	1983-08-25, 23:00	1983-08-29, 10:00	3.12
5	1983-08-29, 12:50	?	Unknown***
6	1983-08-31, 10:15	1983-09-01, 20:10	1.80
7	1983-09-01, 20:50	1983-09-04, 17:45	3.60
8	1983-09-04, 18:45	1983-09-07, 09:00	3.60
9	1983-09-07, 10:30	1983-09-11, 08:15	2.10
10	1983-09-11, 09:15	1983-09-12, 12:15	1.61
11	1983-09-12, 17:00	1983-09-14, 08:30	2.51
1	1984-02-27, 09:45	1984-02-29, 11:35	2.61
2	1984-02-29, 13:45	1984-03-02, 10:45	2.45
3	1984-03-02, 13:00	1984-03-05, 10:05	3.97
4	1984-03-05, 09:15	1984-03-07, 10:20	2.70
5	1984-03-07, 11:00	1984-03-09, 08:45	2.61
6	1984-03-09, 11:00	1984-03-12, 10:05	4.00
7	1984-03-12, 10:50	1984-03-13, 13:05	1.42
8	1984-03-14, 09:55	1984-03-16, 10:05	2.78
9	1984-03-16, 12:40	1984-03-19, 10:45	4.51
10	1984-03-19, 13:55	1984-03-21, 10:15	2.76
11	1984-03-21, 10:55	1984-03-23, 08:15	2.75
12	1984-03-23, 14:30	1984-03-26, 11:25	4.50
13	1984-03-26	?	Unknown***
14	1984-03-28, 13:00	1984-03-30, 12:45	2.87
15	1984-03-31, 11:10	1984-04-03, 12:25	4.73
16	1984-04-04, 08:00	1984-04-06, 08:30	2.75
17	1984-04-06, 09:05	1984-04-09	4.29

* MET = GMT + 1h
** At 760 mm Hg and 298 K
*** Vacuum pump failure

Table 1: Cont.

Sample No.	Start of run (MET*)	End of run (MET*)	Sample volume**, m^3
(1)	(2)	(3)	(4)
1	1984-06-18, 07:10	1984-06-22, 09:30	5.00
2	1984-06-22, 10:20	1984-06-22, 09:30	5.14
3	1984-06-27, 10:10	1984-06-30, 07:00	3.18
4	1984-07-02, 22:20	1984-07-05, 20:30	2.73
5	1984-07-06, 14:30	1984-07-09, 09:00	3.94
6	1984-07-09, 09:25	1984-07-11, 17:15	3.32
7	1984-07-11, 17:50	1984-07-13, 22:40	3.25
8	1984-07-13, 23:10	1984-07-16, 12:45	3.49
9	1984-07-16, 16:35	1984-07-18, 11:30	0.99

* MET = GMT + 1h
** At 760 mm Hg and 298 K

The results from PIXE analyses for the Winter/Spring campaigns are given in Tables 2 and 3, and in Figures 26 and 27 in the form of aerosol constituent mass concentration-size distribution plots. To facilitate plotting of the distributions, the lowest EAD limit for the mass increments of the BTL C.I. afterfilter (<0.25 μm EAD fraction) was arbitrarily taken as 0.06 μm, while 20 μm was assumed the upper limit for Stage 0 (>8 μm EAD). Selected results and discussion of findings from size-differentiated sampling at NYA during the Spring 1983 campaign can be found in Pacyna et al. (1984).

The available results from the Summer/Fall campaigns are summarized in Figures 28 and 29. Because of the generally low aerosol levels and infrequent episodic transport in summertime, the chemical constituents in size-segregated samples from the Summer/Fall campaigns were often below the detection limits of the PIXE method. For these non-episodic periods, only mean concentration distributions can be reported.

Table 2: Concentrations (ng m^{-3}) of Si, Ti, Fe, Cl, K and Ca at NILU I, in Ny Ålesund, March/April, 1983.

Element and fraction	Run No.													
	1	2	3	4	5	6	7	8	9	10	11	12	13	14
Si_o[a]	19.8	*[b]	*	6.91	1.91	37.3	*	6.97	1.38	*	3.28	1.34	51.5	*
Si_1	2.5		*	33.6	7.45	26.0	4.85	36.0	4.33	3.57	4.81	*	13.04	*
Si_2	11.3	23.7	11.5	39.2	17.5	13.6	5.54	4.08	8.94	12.6	1.53	*	12.3	6.53
Si_3	4.01	1.38	24.1	25.3	34.3	27.1	2.74	7.32	6.39	7.45	1.47	*	3.71	*
Si_4	10.6		24.7	47.3	19.6	50.3	7.13	31.0	10.2	25.6	18.0	*		8.79
Si_5		1.24	13.2	17.1	12.6	6.19	12.7	10.1	6.16	29.2	11.4		*	7.31
ΣSi	48.2	26.3	76.5	89.7	93.4	160	33.0	95.5	37.4	78.4	40.5	1.34	80.5	22.6
Ti_o				0.27									*	
Ti_1			0.23	0.62	0.10	0.13		*	0.08	*	*		0.29	
Ti_2		0.11	0.33	0.67	0.38	0.24	0.20	0.15	0.20	0.34	0.13			0.18
Ti_3		0.055	0.43	0.47	0.79	0.51	0.13	0.17	0.22	0.35	*			*
Ti_4		*	0.37	1.32	0.22	0.32	0.07	0.35	0.18	0.61	0.32			0.29
Ti_5		*	0.80	0.82	0.77	0.14	0.24	0.18	0.31	0.48	0.27		*	0.44
T_N			0.53	0.40	0.90	0.82	*		1.14	1.29	0.52			2.37
ΣTi		0.165	2.69	4.57	3.09	1.34	0.64	0.85	2.13	3.07	1.24		0.29	3.78
Fe_o	0.34	0.48	0.46	1.32	0.15	0.05	0.04	0.06	*	*	0.03	0.08	1.38	*
Fe_1	0.08	0.26	1.53	5.27	0.94	0.73	0.24	0.58	0.70	0.87	0.32	*	0.78	0.42
Fe_2	0.40	0.64	3.43	5.99	3.85	1.75	1.13	1.50	2.18	3.46	1.26	0.12	1.27	4.89
Fe_3	0.44	0.36	9.09	5.54	11.7	6.83	1.85	2.18	3.56	4.32	1.28	0.60	1.59	2.09
Fe_4	0.19	0.90	9.52	17.5	6.24	7.21	3.75	4.90	4.75	9.06	7.63	1.10	3.59	7.17
Fe_5	0.05	0.50	16.5	12.5	15.2	4.15	3.65	4.55	6.46	11.9	5.79		4.69	7.50
Fe_N	0.28	0.94	19.0	17.0	16.8	20.3	7.24	7.70	25.5	20.1	12.2	2.43	11.2	6.24
ΣFe	1.78	2.70	59.5	65.1	39.8	41.1	17.9	21.5	43.1	49.7	28.5	4.33	24.5	28.4
Cl_o	137	58.5	1.8	*	1.88	5.29	19.6	8.49	0.89	10.2	7.92	10.5	*	8.96
Cl_1	*	33.8	1.72	9.94	1.06	*	17.0	7.12	3.46	11.2	9.64	2.44	5.25	*
Cl_2	150	35.9	7.96	13.4	2.01	4.48	18.9	6.76	4.10	8.01	9.64	2.65	4.28	1.61
Cl_3	24.5	8.14	91.7	12.6	17.9	10.3	51.4	6.27	6.60	1.96	*	*	3.77	1.78
Cl_4	12.1	56.9	20.5	40.9	11.1	12.5	15.8	7.16	2.29	*	12.7	2.17	6.57	1.84
Cl_5	4.86	6.01	45.1	39.0	19.5	3.72	1.61	16.1	5.21	5.22	3.75		*	4.14
Cl_N	102	135	73.3	29.4	*	*	41.0	28.6	5.84	14.3	19.7	24.2	23.5	21.8
ΣCl	430	334	242	145	53.5	36.3	165	80.5	28.4	50.3	63.4	42.0	43.4	40.1
K_o	2.7	1.32				*	*				*			
K_1		0.34	*	1.85	*	*	*	*	*	*	*			
K_2	3.32	1.03	*	2.70	0.86	*	1.03	*	*	1.24	0.19			*
K_3	0.32	*	4.76	1.84	3.81	3.02	2.05	1.10	1.01	*				*
K_4	*	3.03	0.55	7.57	0.95	4.81	4.28	1.20	*	*	1.24		*	2.13
K_5		*	12.6	9.34	13.2	1.67	0.91	2.96	1.77	4.65	1.16		1.48	3.54
K_N	2.39	43.5	18.5	12.3	26.9	21.0	7.6	5.80	23.5	15.5	15.1			
ΣK	8.73	46.5	36.4	35.6	45.7	30.5	15.9	11.1	26.3	21.4	17.7		1.48	5.67
Ca_o	10.1	1.68	1.11	2.98	1.44	5.97	1.56	2.89	0.34	3.08	1.38	0.71	10.6	1.01
Ca_1	1.1	1.81	8.12	13.4	3.91	9.49	2.23	11.2	0.78	2.24	1.80	1.71	4.96	*
Ca_2	17.2	9.88	4.98	10.9	5.14	3.14	3.30	1.51	2.95	3.73	1.50	*	4.66	*
Ca_3	6.62	2.74	9.24	9.02	8.11	7.81	4.14	2.32	1.93	2.02	1.39	0.80	*	0.69
Ca_4	3.47	2.52	2.35	8.52	2.43	13.9	5.18	6.49	0.38	1.39	2.41	2.97	*	1.07
Ca_5	0.79	1.35	7.09	8.17	5.59	1.54	5.65	3.34	2.99	3.21	2.16		2.03	0.86
Ca_N	4.81	4.84	9.02	11.1	14.4	17.1	6.20	4.65	12.5	7.53	4.58			
ΣCa	44.1	24.8	41.9	64.1	40.9	59.0	28.3	32.4	21.9	23.2	15.2	6.19	22.3	3.63

a - Subscripts denote particle size classes (impactor stage designations)
b - Denotes concentration below detection limit of analytical method.

Table 3: Concentrations (ng m^{-3}) of Si, and Cl at NILU II, Ny Ålesund, in February/March/April 1984.

Element and fraction**	Run No.																
	1	2	3	4	5	6	7	8	9	10	11	12	13	14	15	16	17
Si_0	*	*	*	*	*	15.9	*	10.5	*	3.7	*	2.7		*	5.4	*	2.7
Si_1	79.0	*	2.0	*	7.7	110	4.8	7.7	3.8	7.3	*	4.5		3.9	*	*	*
Si_2	83.6	*	18.4	*	*	13.7	*	178	3.8	9.0	*	13.5		26.9	*	*	5.3
Si_3	*	*	6.6	*	*	20.4	8.9	11.1	3.0	*	*	7.6		*		2.8	3.5
Si_4	17.6	26.2	12.1	*	17.9	*	6.8	16.0	2.6	*	*	11.2		8.3	*	*	4.4
Si_5	97.8	18.2	65.0	*	14.5	10.5	12.3	49.5	11.0	*	*	36.2		*	*	4.2	3.4
S_N (NP)	*	*	13.1	*	*		*			*		8.2		*			
ΣSi	278.0	44.4	117.2		40.1	170.5	32.8	272.8	24.2	20.0		83.9		39.1	5.4	7.0	19.3
Cl_0	*	16.2	1.2	*	97.0	36.8	14.2		12.3	77.8	22.7	28.6		*	23.5	29.8	10.2
Cl_1	21.2	21.2	*	*	137.0	164.0	37.9		35.0	238	62.5	119		*	78.4	30.7	20.4
Cl_2	108.0	25.8	*	5.9	79.8	432.0	65.9		64.7	597	151	315		4.2	154	97.1	36.4
Cl_3	79.7	16.9	*	10.2	22.5	309.0	39.7	3.9	53.2	387	100	132		11.1	122	65.5	26.8
Cl_4	47.5	*	2.7	7.3	53.0	9.3	17.0	11.0	15.9	22.0	19.5	12.7		25.2	71.5	14.2	6.3
Cl_5	447.0	40.4	7.0	21.8	73.4	61.1	54.0	1.9	70.0	153	83.2	87.7		41.4	20.3	60.8	13.4
Cl_N (NP)	*	*	*	*	153.6	134.5	158.5	*	126.6	439	203.0	152.0		*	250.0	133.0	6.1
ΣCl	703.4	120.5	10.9	45.2	616.3	1146.7	387.2	16.8	377.7	1913.8	641.9	847.0		81.9	719.7	431.1	119.6

* below detection limit of analytical method.
** BTL C.I. fractions.

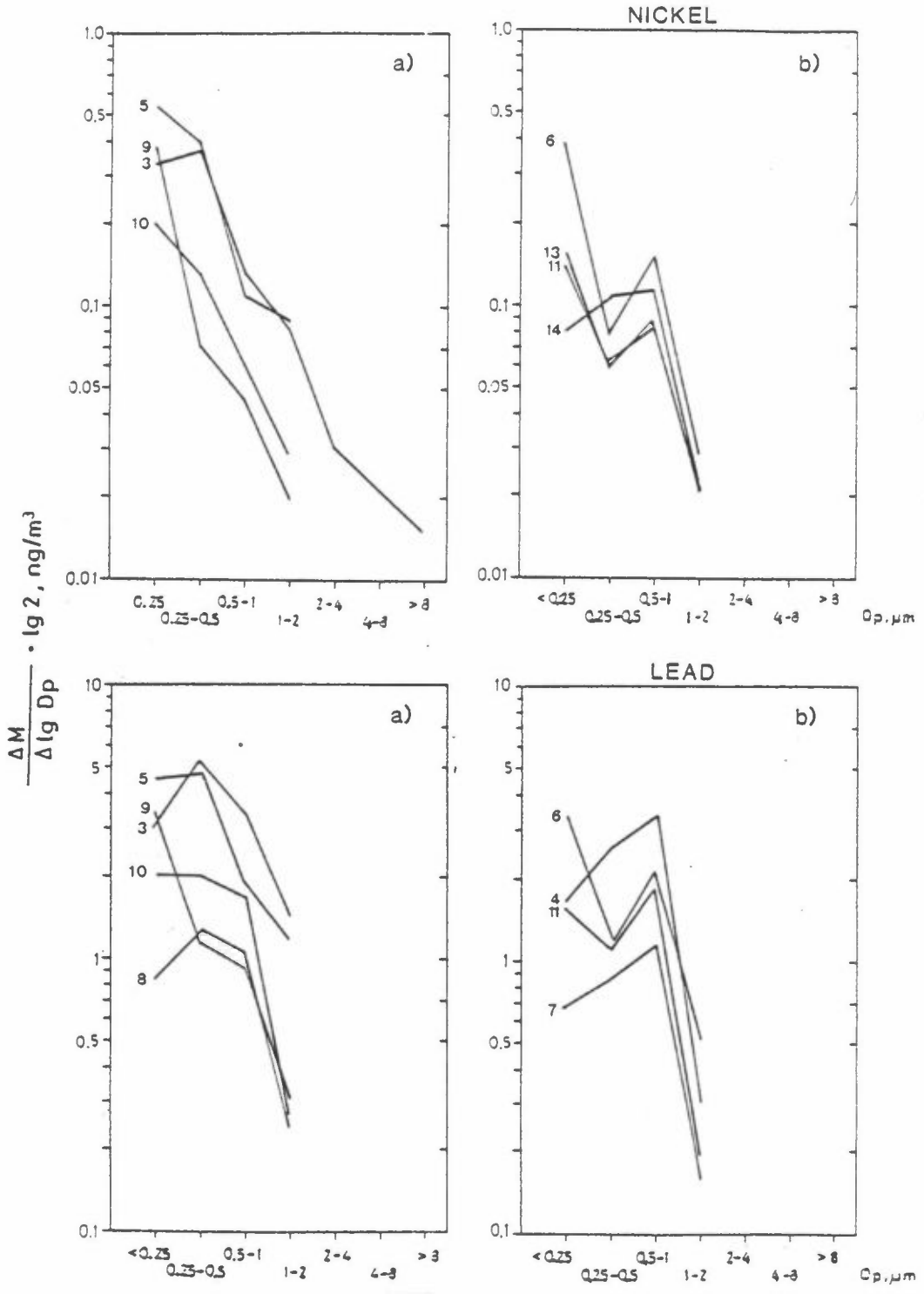

Figure 26: Mass-size distributions of several trace elements, collected with a Battelle low-volume cascade impactor at Ny Ålesund in March/April 1983. The <0.25 µm EAD particles were collected on NP afterfilter.

ΔM represents the amount of a given element in a particular size fraction, and D_p is the particle EAD. Essentially, the value of $\frac{\Delta M}{\Delta \lg D_p} \cdot \lg 2$ represents the concentration of an element in a given size interval, except for the NP afterfilter and >8 µm EAD fractions.

For the meaning of a) and b) see text (p. 83).

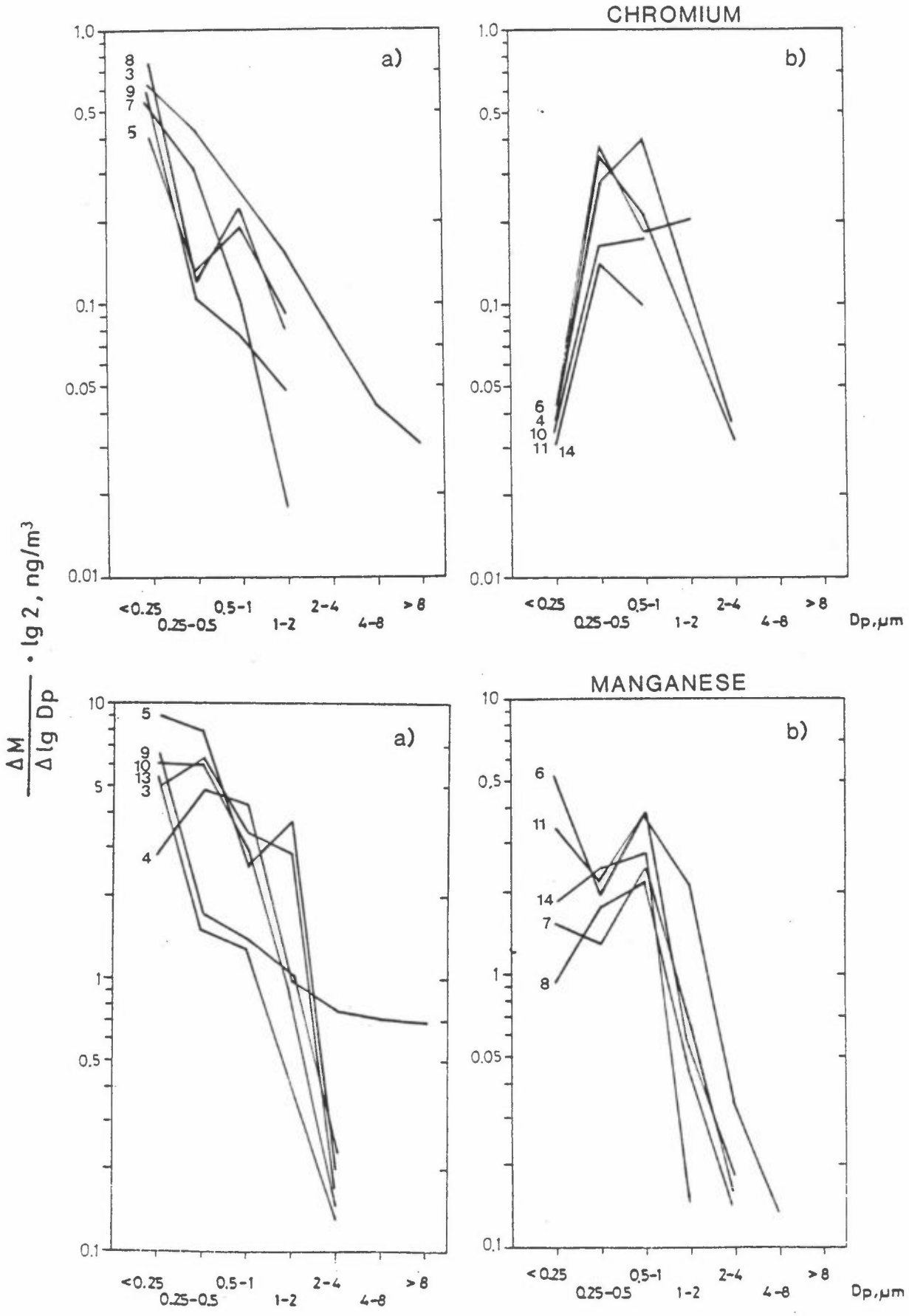

Figure 26: Cont.

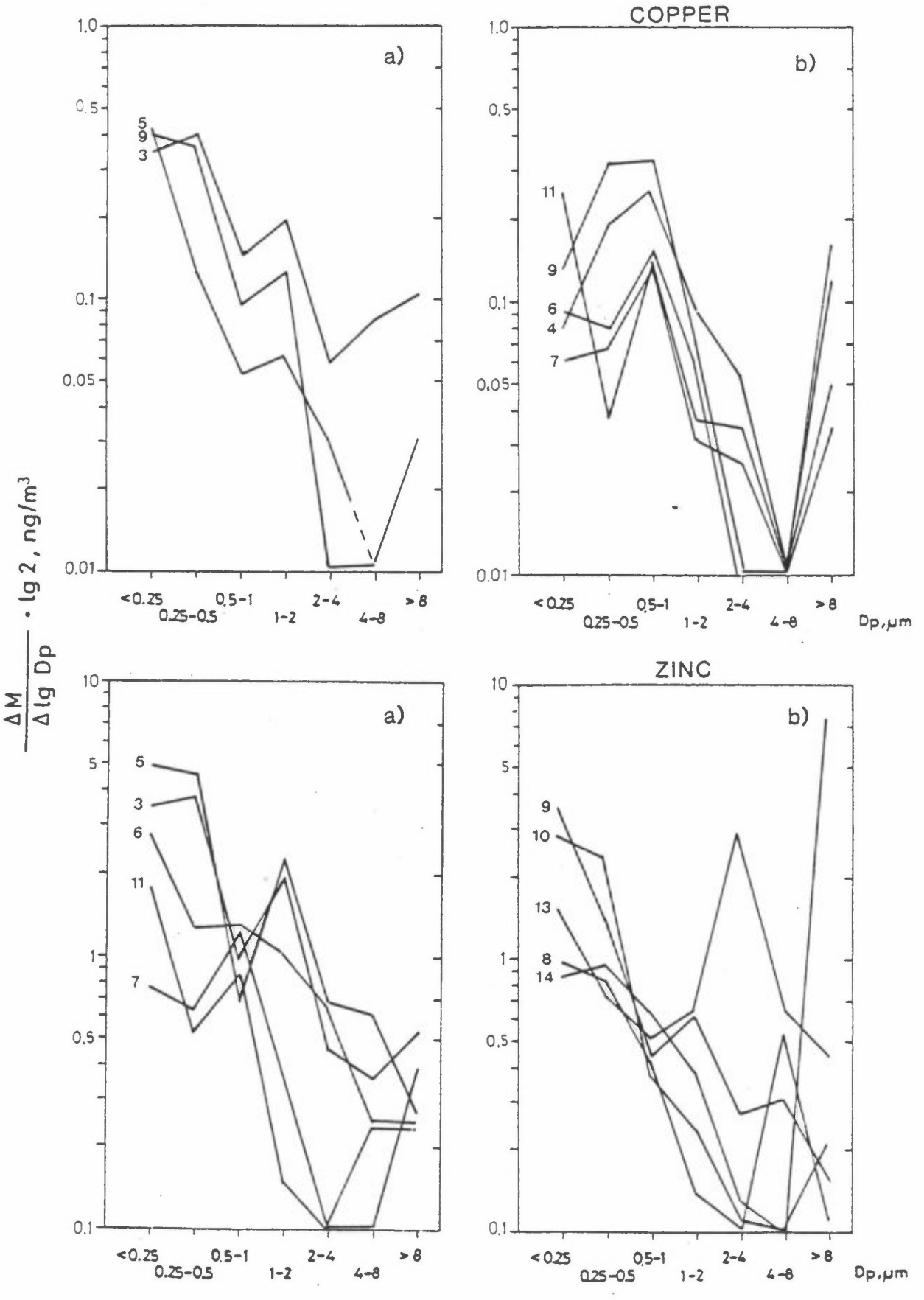

Figure 26: Cont:

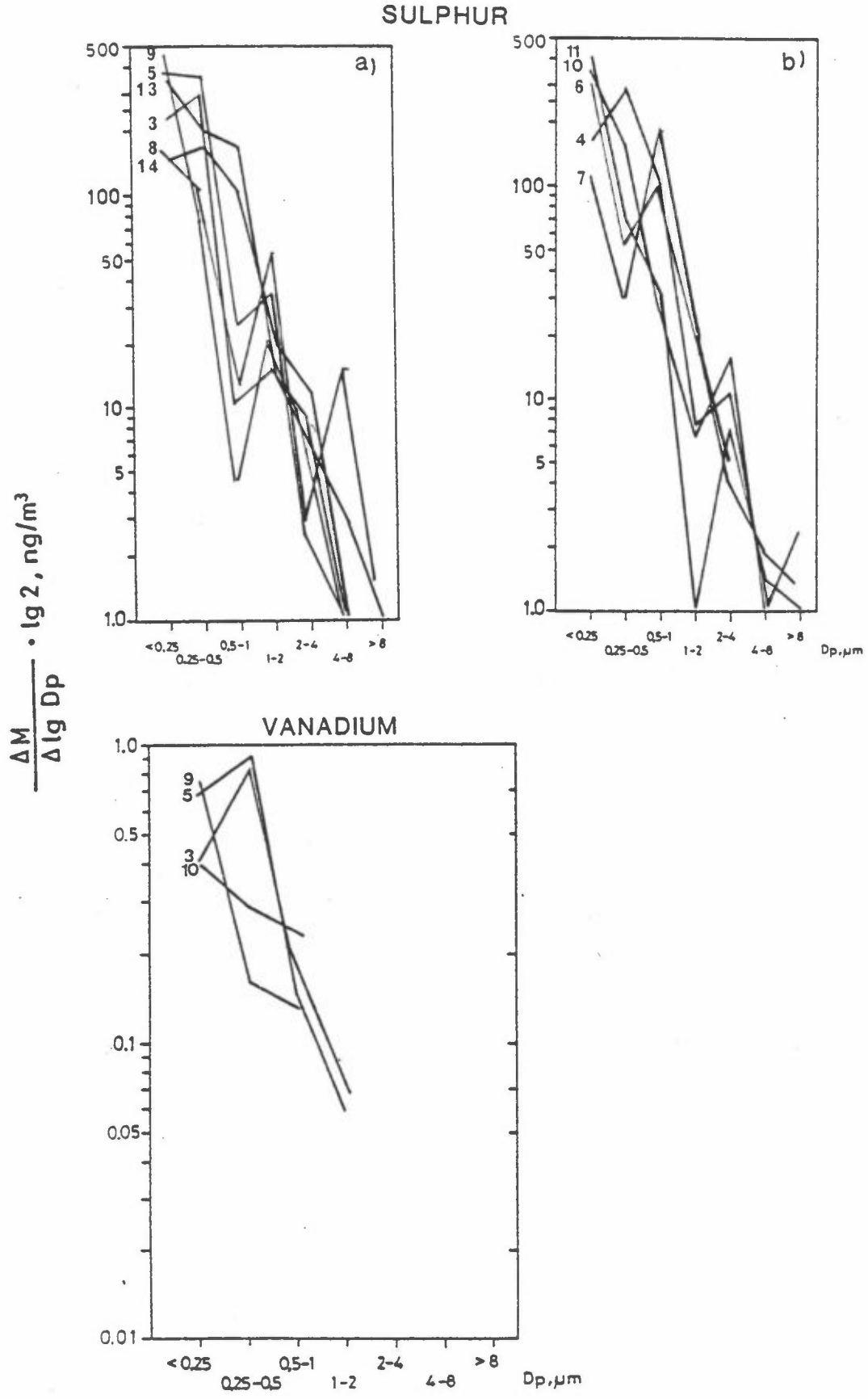

Figure 26: Cont.

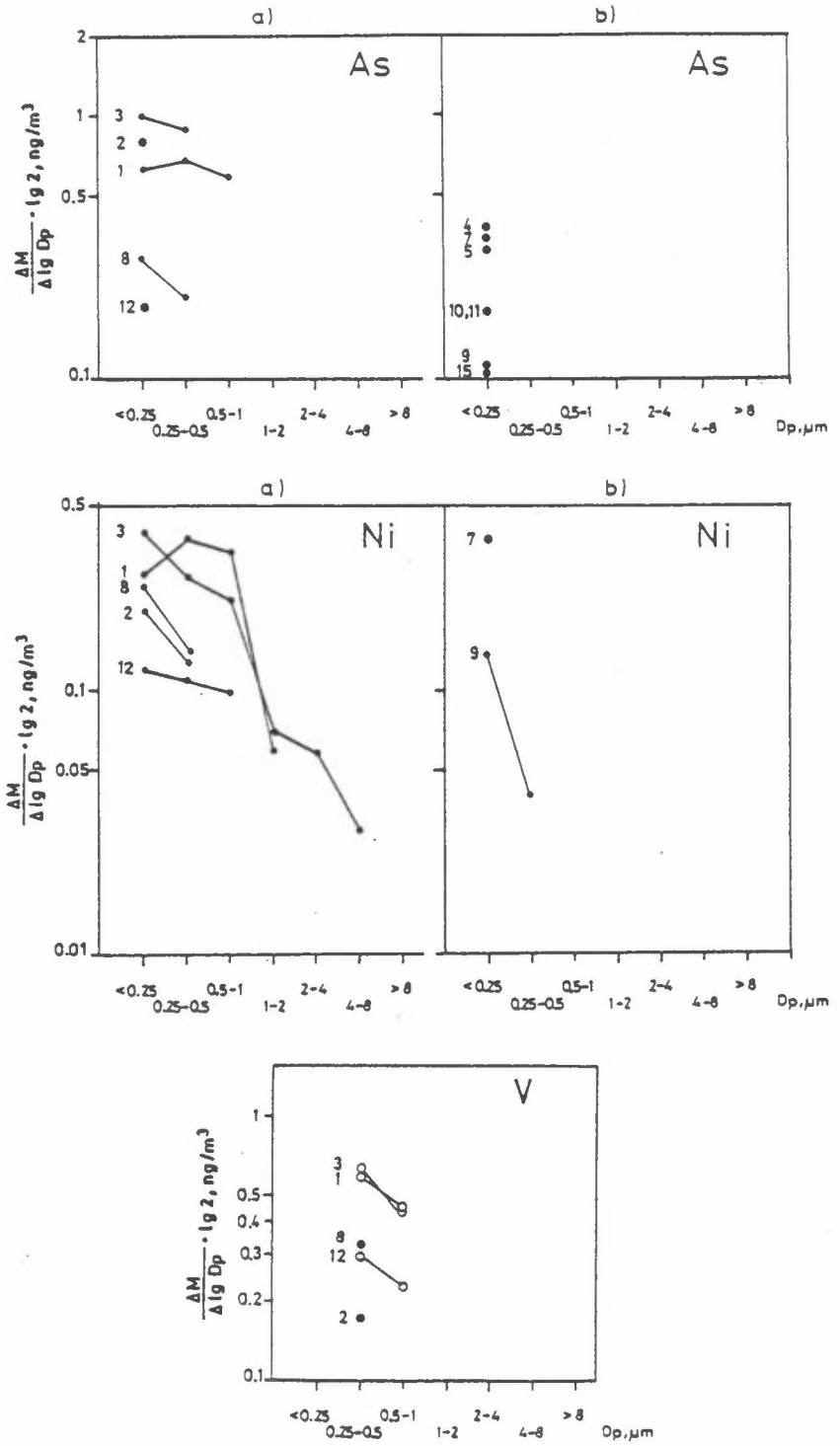

Figure 27: Mass-size distributions of several trace elements, collected with a Battelle low-volume cascade impactor at Ny Ålesund in February/March/April 1984. The <0.25 µm EAD particles were collected on NP afterfilter.

ΔM represents the amount of a given element in a particular size fraction, and D_p is the particle EAD. Essentially, the value of $\frac{\Delta M}{\Delta \lg D_p} \cdot \lg 2$ represents the concentration of an element in a given size interval, except for the NP afterfilter and >8 µm EAD fractions.

For the meaning of a), b), b1), and b2) see text (p. 83).

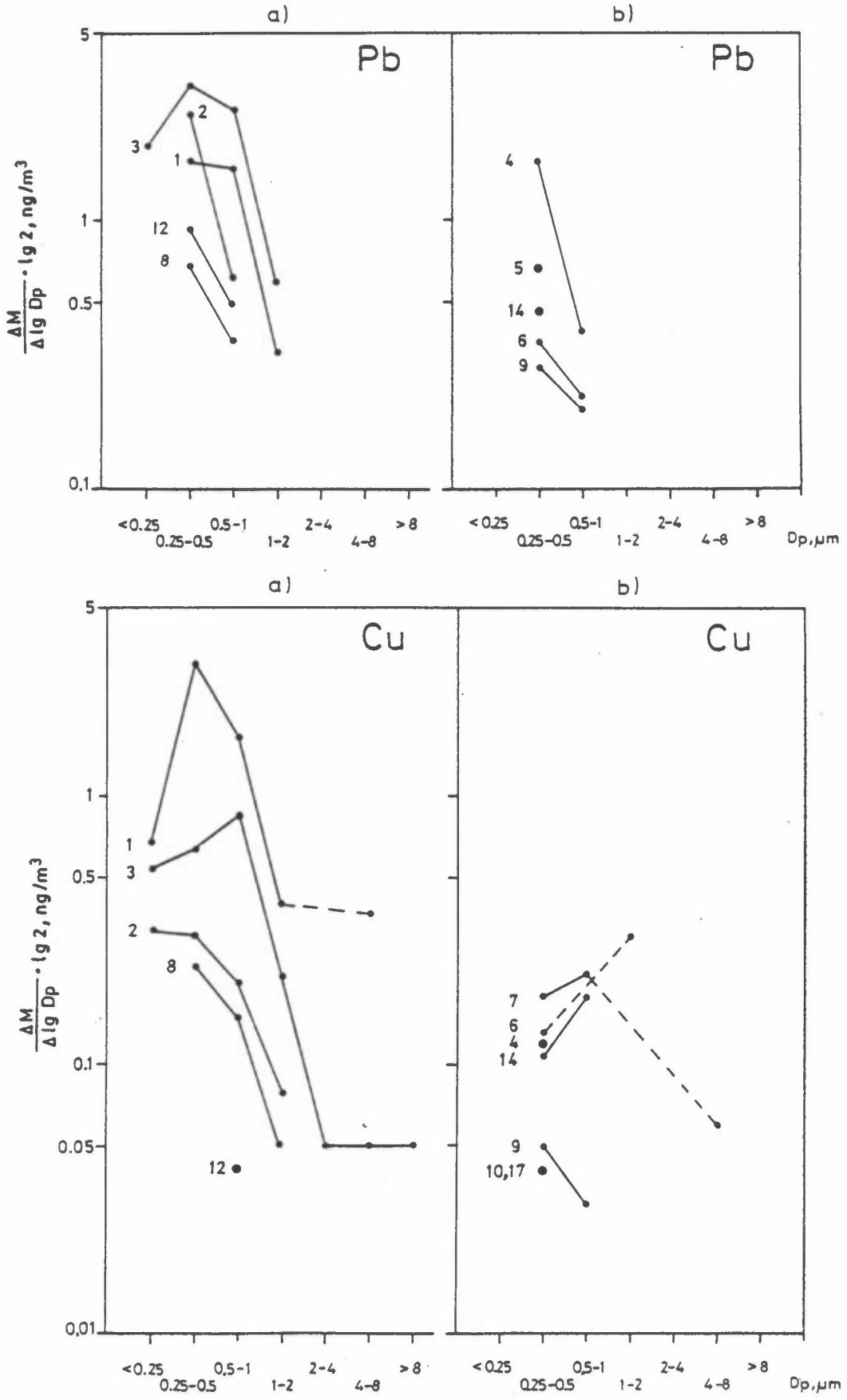

Figure 27: Cont.

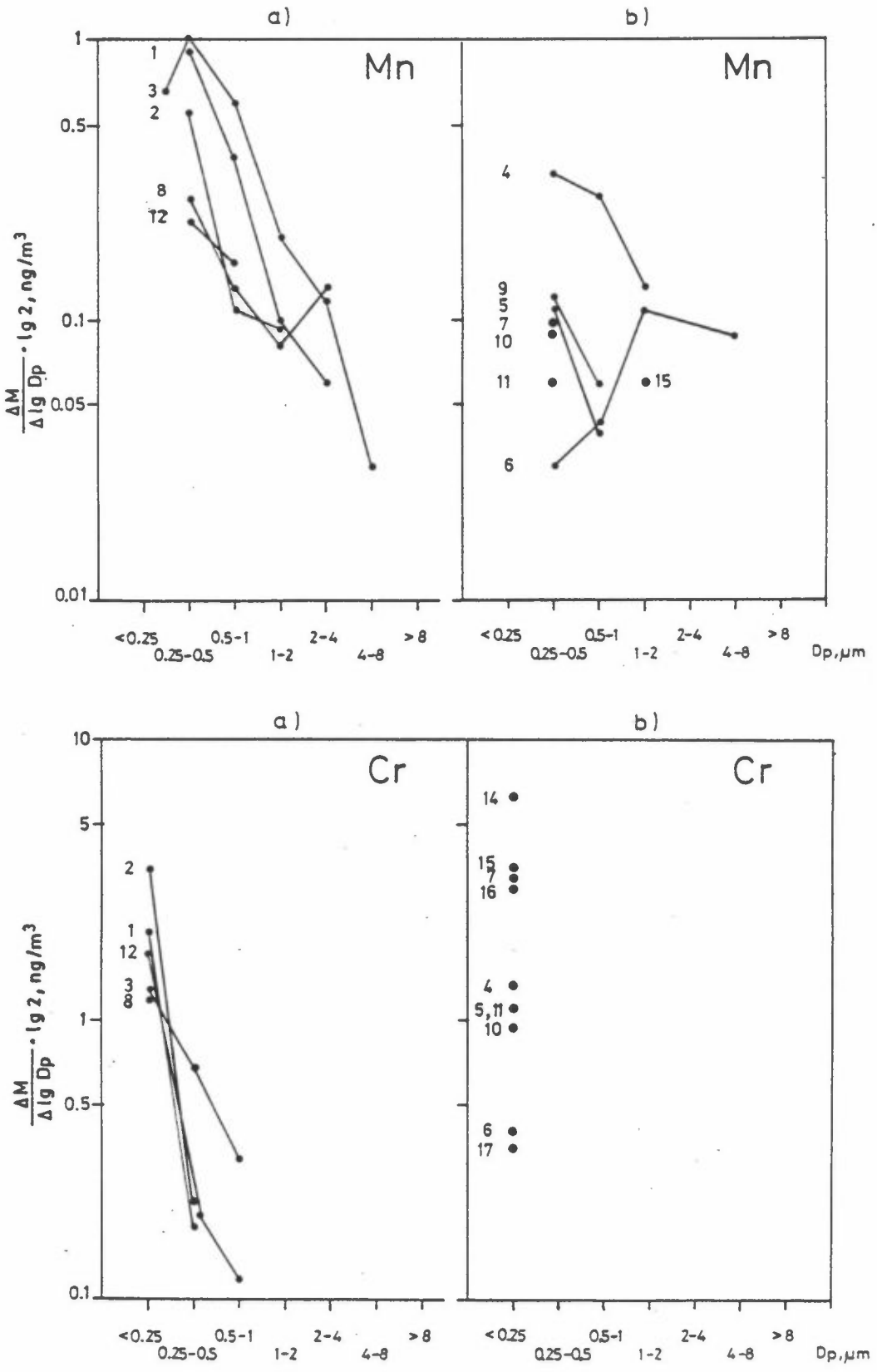

Figure 27: Cont.

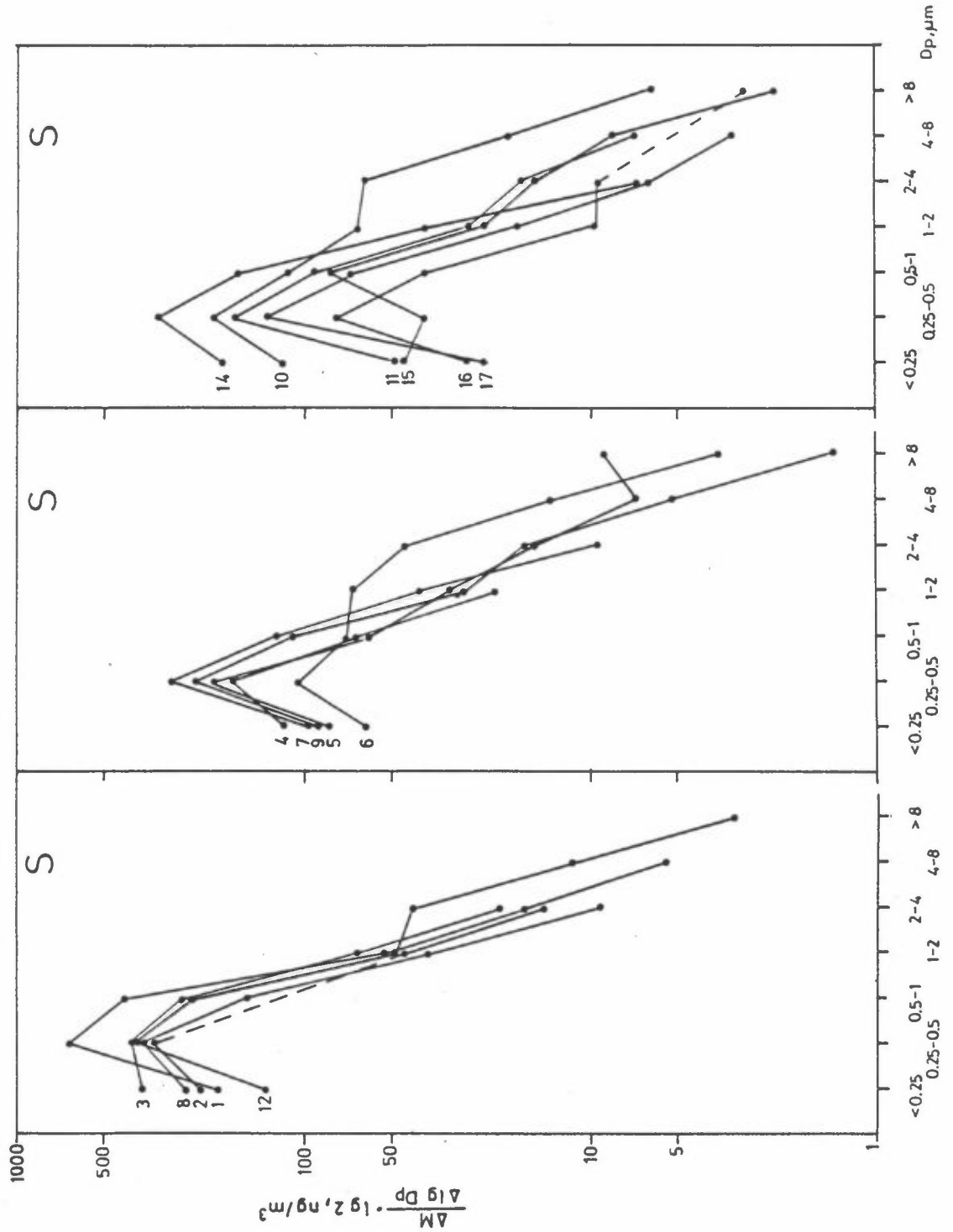

Figure 27: Cont.

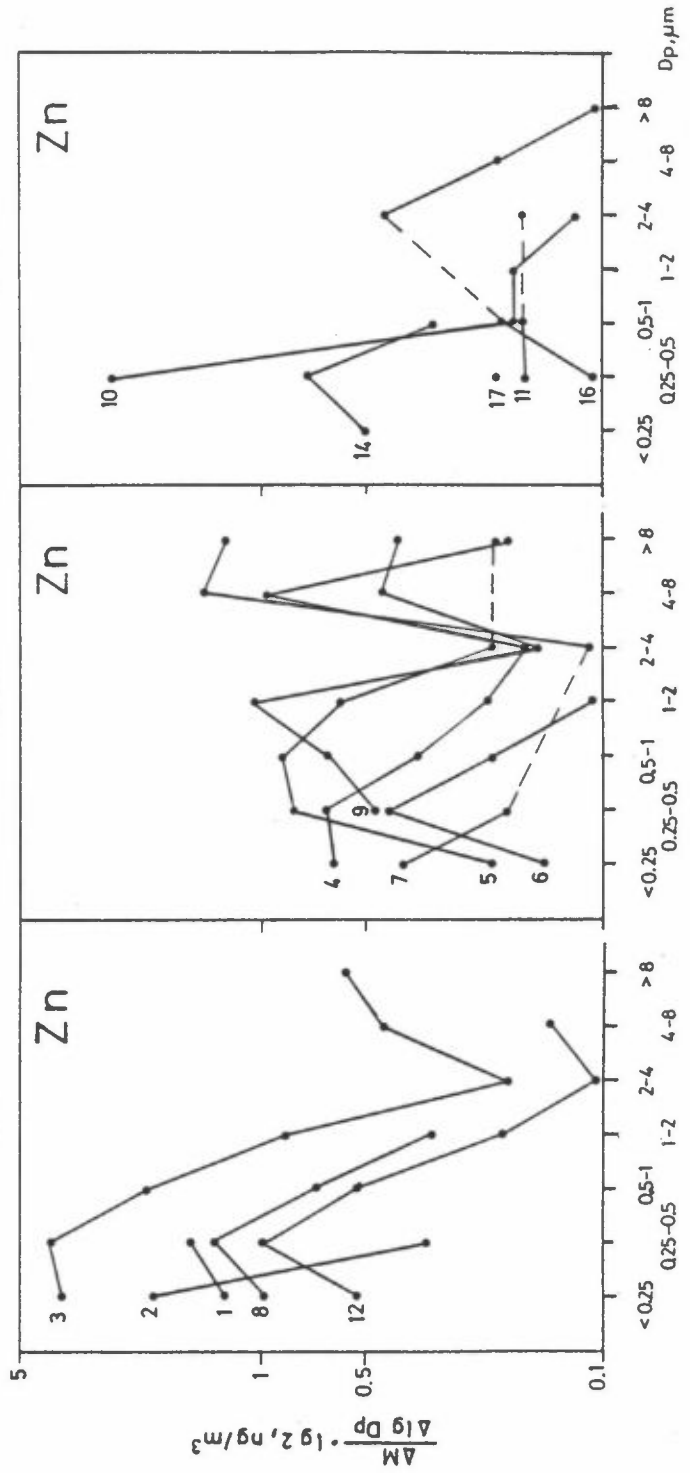

Figure 27: Cont.

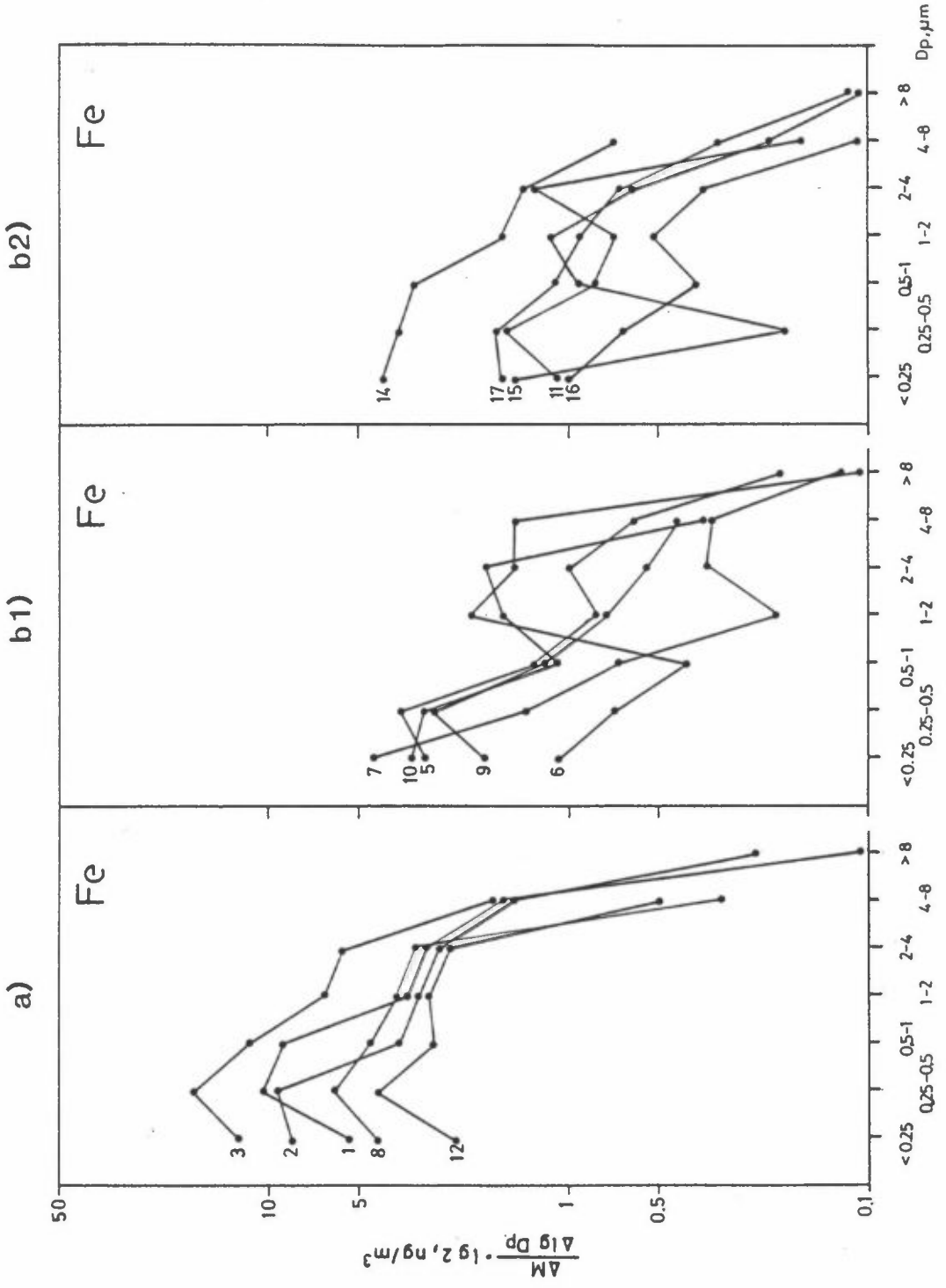

Figure 27: Cont.

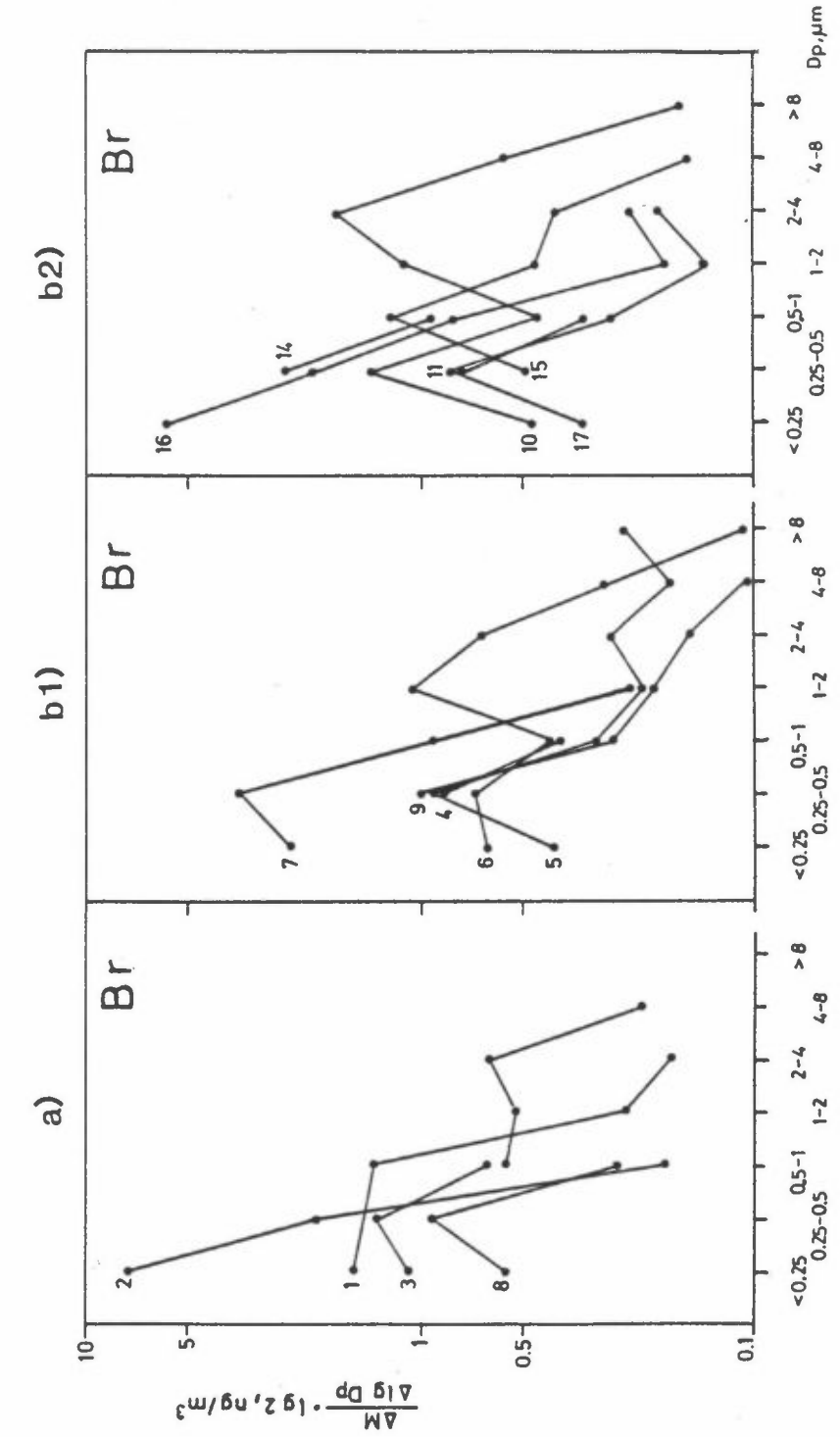

Figure 27: Cont.

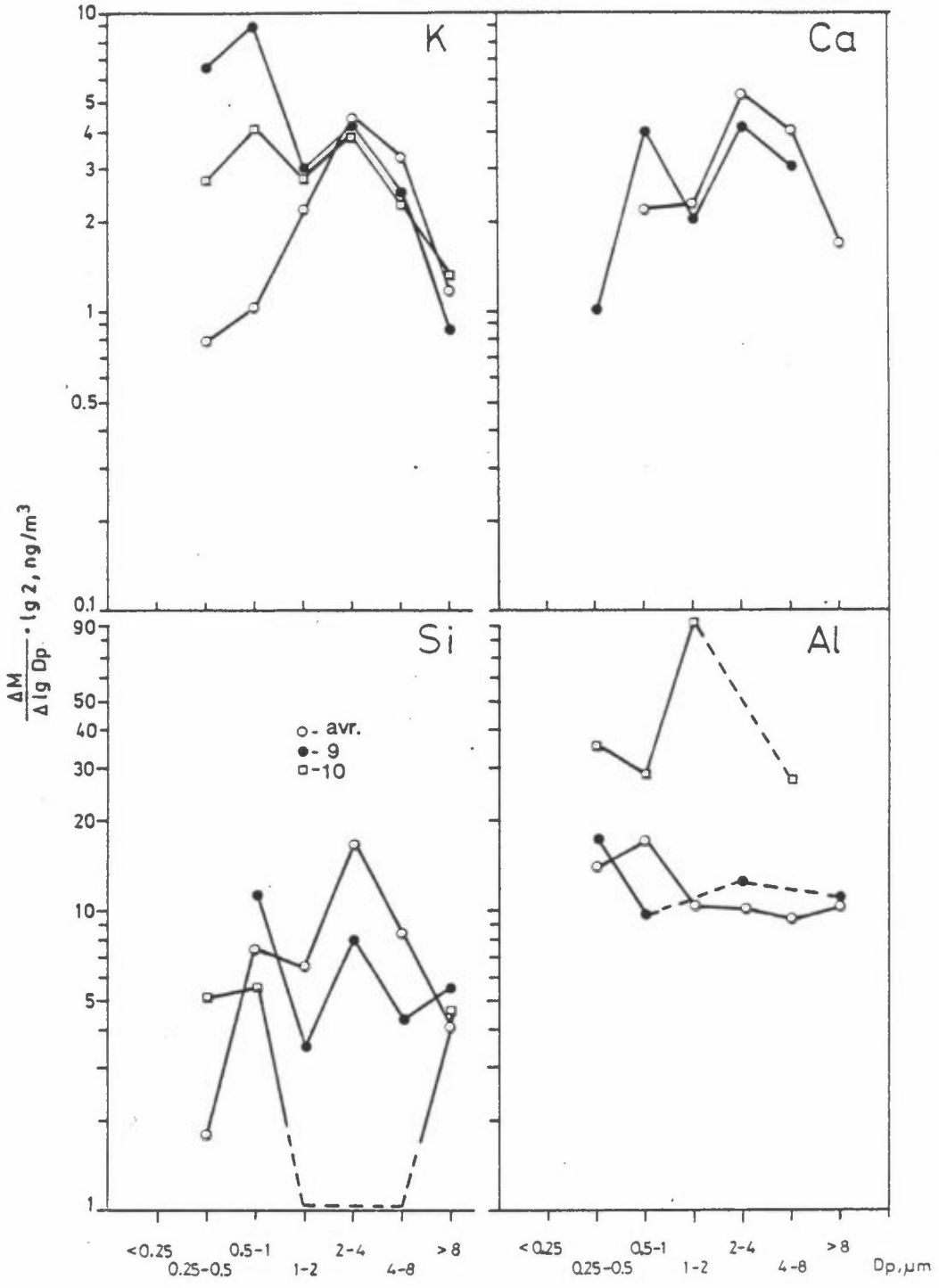

Figure 28: Mass-size distributions of several trace elements, collected with a Battelle low-volume cascade impactor at Ny Ålesund in August/September 1983. The <0.25 µm EAD particles were collected on NP afterfilter.

ΔM represents the amount of a given element in a particular size fraction, and D_p is the particle EAD. Essentially, the value of $\frac{\Delta M}{\Delta \lg D_p} \cdot \lg 2$ represents the concentration of an element in a given size interval, except for the NP afterfilter and >8 µm fractions. The average trace element concentrations in samples other than 9 and 10 are indicated by "avr".

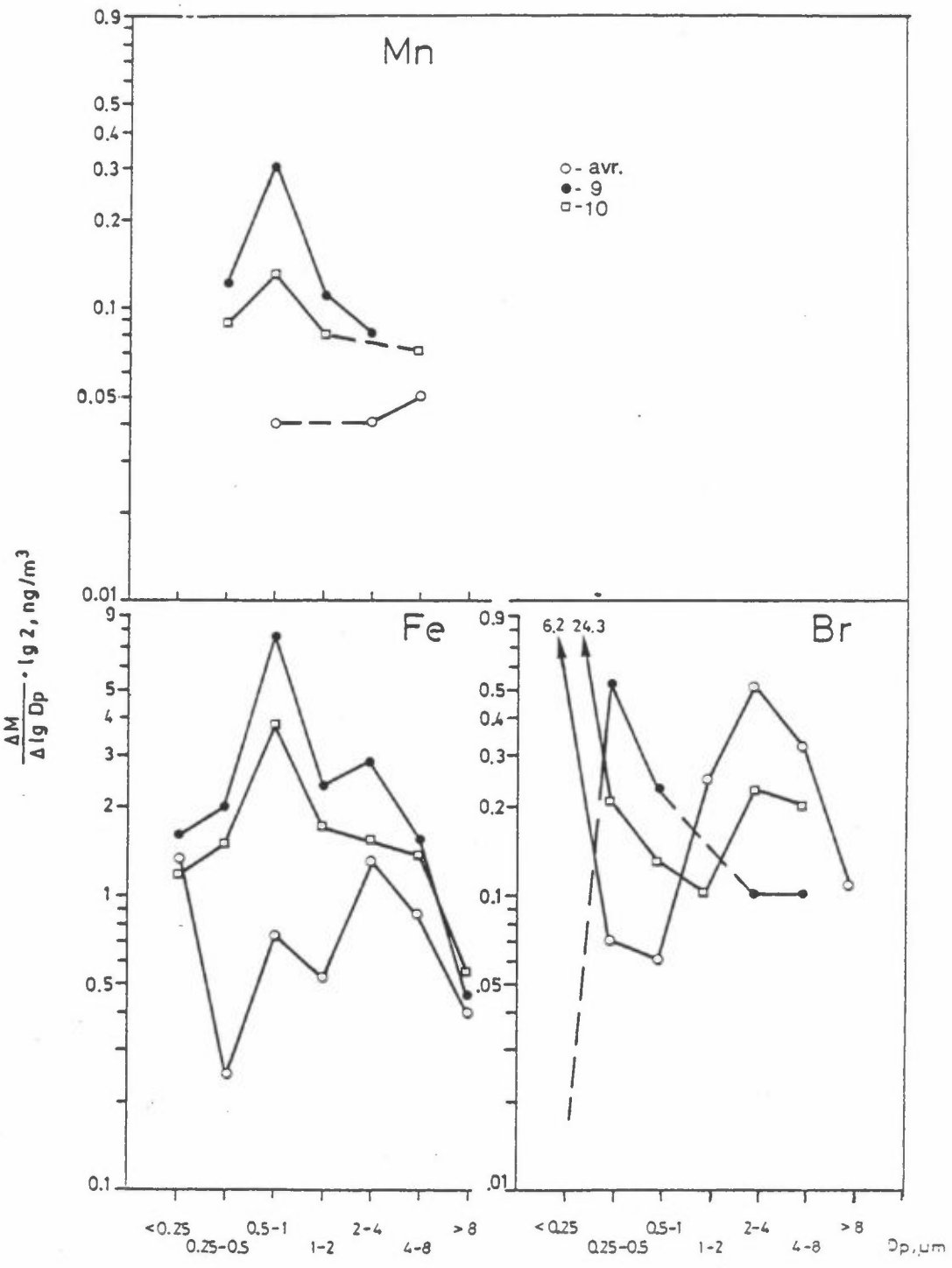

Figure 28: Cont.

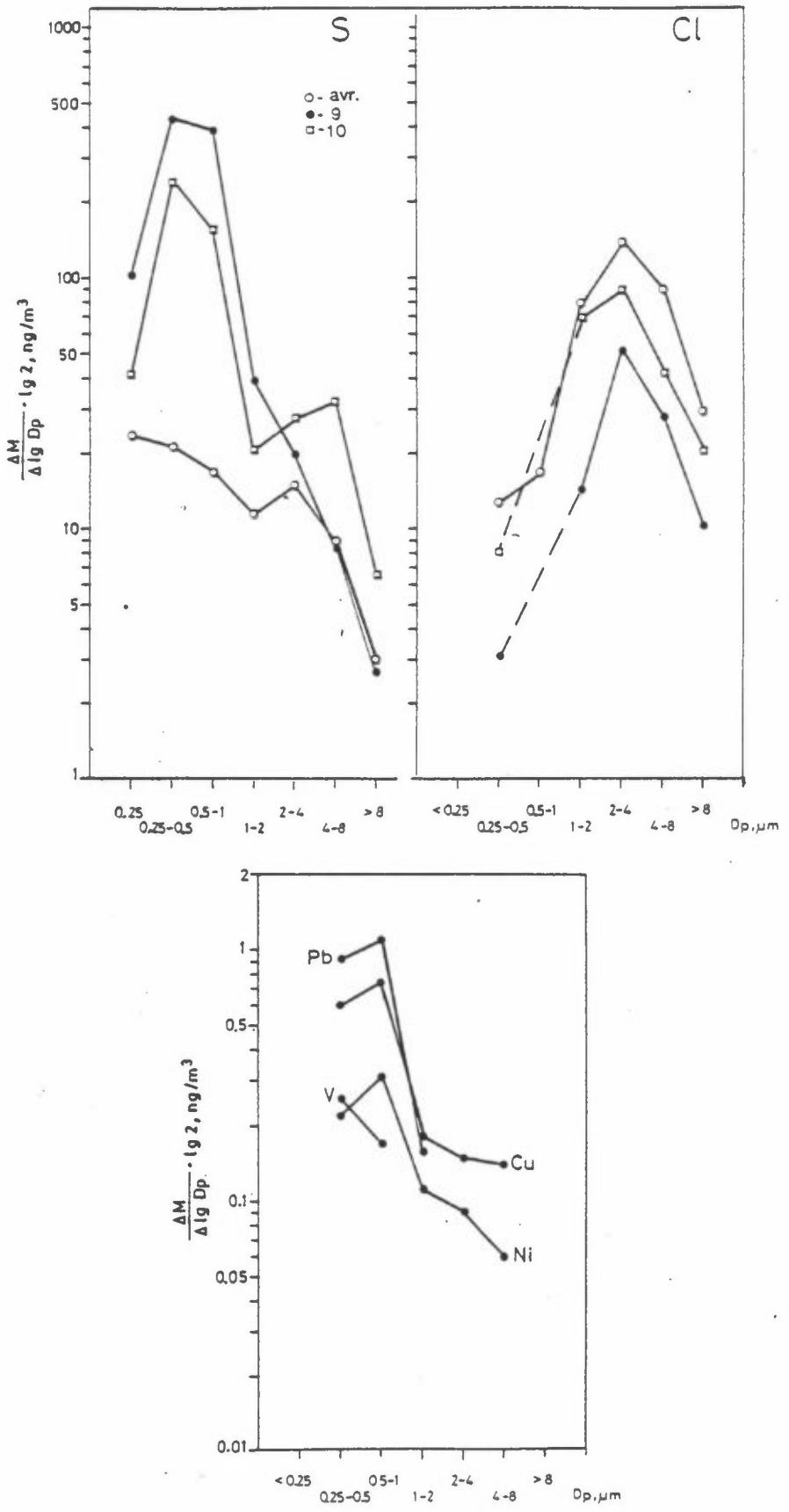

Figure 28: Cont.

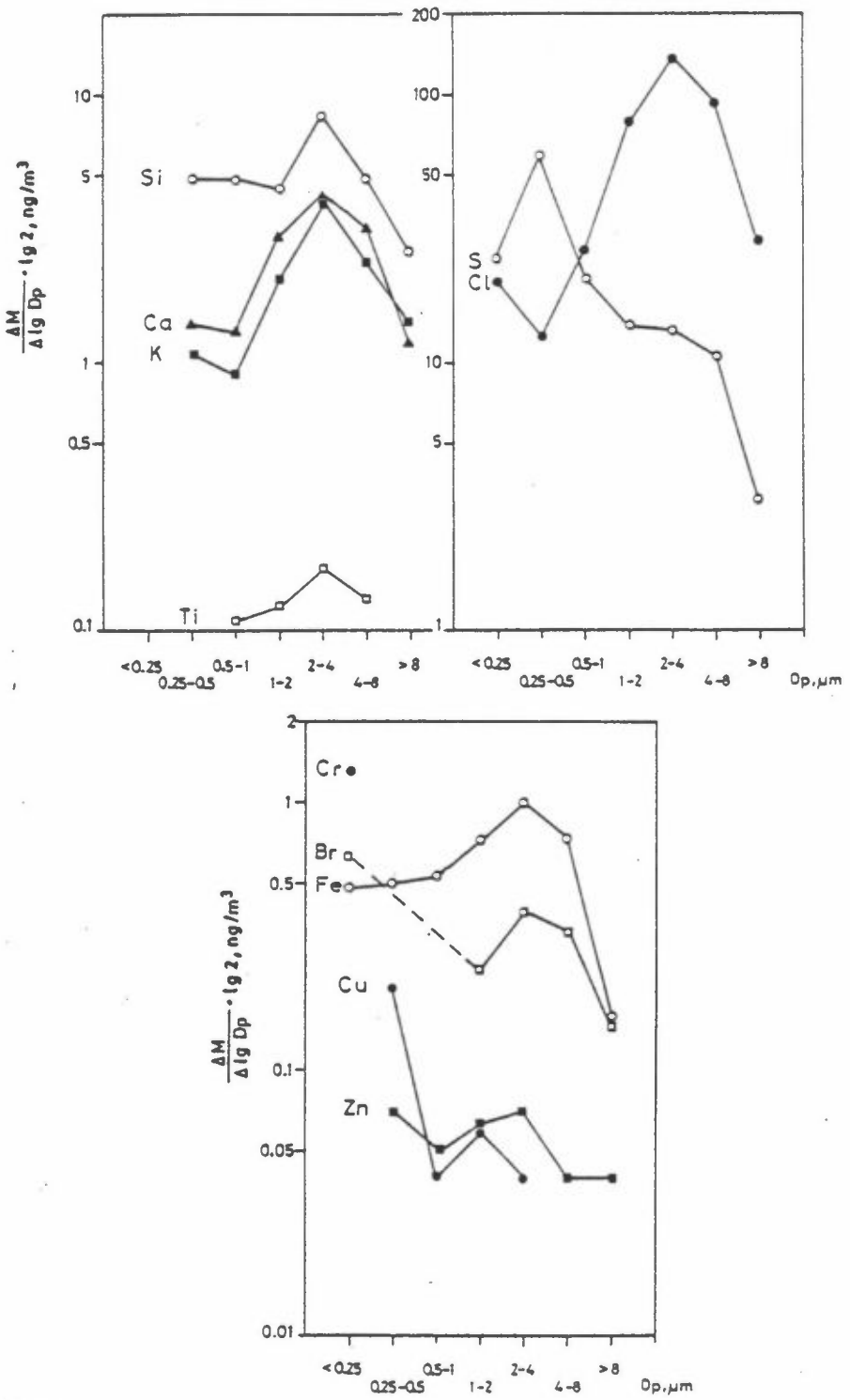

Figure 29: Mass-size distributions of several trace elements, collected with a Battelle low-volume cascade impactor at Ny Ålesund in June/July 1984. The <0.25 µm EAD particles were collected on NP afterfilter.

ΔM represents the amount of a given element in a particular size fraction, and D_p is the particle EAD. Essentially, the value of $\frac{\Delta M}{\Delta \lg D_p} \cdot \lg 2$ represents the concentration of an element in a given size interval, except for the NP afterfilter and >8 µm EAD fractions.

3.2.2 Mass-size differentiation by P.-B.F.

The parallel-branch fractionation (P.-B.F.) system (see Vitols and Wasseng, 1985, for discription),used during the Spring and Summer 1984 campaigns, was similar to the ones reported by Heintzenberg and Covert (1984a; 1984b).

The submicrometre EAD particles penetrating the last impaction stage of the BTL C.I., and collected on the afterfilter, constitute a "lumped" sample, with no details on its structure. Consequently, the P.-B.F. was devised to provide aerosol mass-size differentiation in three additional size fractions down to ca. 0.04 μm EDD. All six aerosol fractions were collected on NP filters, identical to the BTL C.I. afterfilters, and subsequently analysed by PIXE at the Lund Institute of Technology.

Because the parallel branches of the sampling system collect the aerosol particles in overlapping size ranges, it is too complicated to deduce the underlying mass-size distribution from the primary data (from PIXE analysis). Hence, a mathematical inversion is necessary to retrieve the particle mass-size distribution from the primary results. A suitable algorithm has been under development at MISU (Heintzenberg and Covert, 1984a). As of this writing, unfortunately, the algorith is not yet functional*, due to difficulties in "dovetailing" the different equivalent particle diameters, defining the collected particle size ranges. Thus only the primary results are then presented in Tables 3 and 4.

The abbreviated names of the six P.-B.F. branches in the tables mean the following:

DB35: Winkler impactor + 35-screen DB + NP filter;
DB17: " " + 17-screen DB + NP " ;
DB8 : " " + 8-screen DB + NP " ;
FN : " " + NP filter.
BTLF: Stages 0 + 1 + 3 of the BTL C.I. + NP filter;
CYF : Bendix Model 18 cyclone + NP filter.

---

* Personal communication with Dr. Jost Heintzenberg, MISU, November, 1985.

Table 3: Trace element concentrations (μg m^{-3}) in aerosols collected by the six branches of P.-B.F. during the late Winter/Spring 1984 campaign at Ny Ålesund.

Sampling date:		1984-02-07 to 1984-02-29												
Element:		Si	S	Cl	K	Ca	Cr	Mu	Fe	Ni	Cu	Zn	As	Br	Pb
Branch*	Approximate size range **, μm														
DB35	0.16 EDD⁺ - 0.25 EAD⁺⁺	-	63	-	-	-	2.7	-	4	-	-	-	-	4.0	-
DB17	0.09 " - 0.25 "	-	77	-	-	-	.11	-	3	-	-	-	-	4.9	-
DB8	0.04 " - 0.25 "	-	81	-	-	-	4.6	-	3	-	-	-	-	4.0	-
FN	<0.25 EAD	-	100	d.l.	-	-	6.7	-	2	-	-	0.4	-	4.7	-
BTLF	<0.5 EAD	-	624	341	39	38	8.5	4	47	0.8	7.6	64	-	12	8.8
CYF	<2 EAD	d.l.	884	125	43	41	4.3	1	23	1.2	3.1	5.5	0.5	12	4.0
		1984-02-29 to 1984-03-02													
DB35	0.16 EDD⁺ - 0.25 EAD⁺⁺	175	52	-	-	-	3.4	-	1.4	-	-	0.4	-	4.1	-
DB17	0.09 " - 0.25 "	-	83	32	-	-	5.5	-	2.2	-	-	0.4	0.2	5.0	-
DB8	0.04 " - 0.25 "	-	94	-	-	-	3.2	-	2.8	-	-	0.5	0.2	5.1	-
FN	<0.25 EAD	-	99	-	-	-	4.5	-	2.1	-	-	0.6	0.3	5.3	-
BTLF	<0.5 EAD	42	462	73	19	21	6.9	1.0	18	-	0.7	3.9	1.2	8.0	-
CYF	<2 EAD	41	618	21	21	16	5.5	1.0	18	0.6	1.1	5.3	1.5	6.4	3.0
		1984-03-02 to 1984-03-05													
DB35	0.16 EDD⁺ - 0.25 EAD⁺⁺	-	87	26	-	-	2.8	-	6.8	-	0.3	1.0	0.3	2.6	-
DB17	0.09 " - 0.25 "		100	28	-	-	2.4	-	1.5	-	d.l.	0.8	-	3.3	-
DB8	0.04 " - 0.25 "	-	126	25	-	-	4.2	-	2.0	-	d.l.	0.8	-	2.5	-
FN	<0.25 EAD	-	144	d.l.	-	-	2.1	-	2.3	-	d.l.	1.1	0.3	4.0	-
BTLF	<0.5 EAD	70	748	7.2	28	18	2.0	1.4	26	0.7	1.2	7.3	1.6	4.9	4.0
CYF	<2 EAD	93	987	d.l.	37	21	2.0	2.1	36	0.9	1.8	10.7	2.6	5.3	5.7

Table 3: cont.

		1984-03-05 to 1984-03-07													
DB35	0.16 EDD[+] - 0.25 EAD[++]	-	46	37	-	-	8.1	-	1.8	-	-	0.4	-	4.9	-
DB17	0.09 " - 0.25 "	-	60	68	-	-	3.0	-	2.2	-	-	0.5	-	4.6	-
DB8	0.04 " - 0.25 "	-	60	48	-	-	4.5	-	1.8	-	-	0.8	-	4.5	-
FN	<0.25 EAD	-	72	-	-	-	5.6	-	2.4	-	-	0.6	-	3.8	-
BTLF	<0.5 EAD	-	339	77	9.9	7.5	9.2	-	7.7	0.4	0.5	2.3	0.5	7.6	-
CYF	<2 EAD	-	465	20	12	8.1	3.2	-	10.6	0.4	0.4	3.1	1.0	5.2	-
		1984-03-07 to 1984-03-09													
DB35	0.16 EDD[+] - 0.25 EAD[++]	-	49	50	-	-	2.3	-	2.0	-	-	d.l.	-	4.8	-
DB17	0.09 " - 0.25 "	-	55	26	-	-	1.3	-	2.2	-	-	-	-	4.9	-
DB8	0.04 " - 0.25 "	-	67	32	-	-	1.4	-	15	-	-	0.4	-	4.0	-
FN	<0.25 EAD	-	53	-	-	-	3.6	-	2.0	-	d.l.	0.5	-	4.4	-
BTLF	<0.5 EAD	-	215	71	-	-	1.2	-	4	-	-	0.9	d.l.	5.7	d.l.
CYF	<2 EAD	-	320	63	-	6.7	1.0	-	6	-	-	1.1	-	5.9	-
		1984-03-09 to 1984-03-12													
DB35	0.16 EDD - 0.25 EAD	178	30	34	-	-	2.4	-	1.6	-	-	-	d.l.	2.4	-
DB17	0.09 " - 0.25 "	74	36	23	-	-	2.1	-	1.2	-	-	0.3	-	2.9	-
DB8	0.04 " - 0.25 "	85	40	13	-	-	1.8	-	1.4	0.3	-	0.2	d.l.	2.7	-
FN	<0.25 EAD	-	46	-	-	-	4.6	-	1.8	-	0.7	0.3	-	3.0	d.l.
BTLF	<0.5 EAD	-	141	35	-	-	2.0	-	2.4	-	d.l.	0.5	-	4.3	d.l.
CYF	<2 EAD	-	396	94	11	9.3	1.7	-	4.1	0.3	d.l.	0.9	-	6.7	1.2
		1984-03-12 to 1984-03-13													
DB35	0.16 EDD - 0.25 EAD	197	78	56	-	-	8.7	-	d.l.	-	-	-	-	17	-
DB17	0.09 " - 0.25 "	132	85	d.l.	-	-	17	-	8.6	-	-	-	-	24	-
DB8	0.04 " - 0.25 "	102	85	d.l.	-	-	9	-	8.2	0.9	0.9	-	d.l.	24	-
FN	<0.25 EAD	78	70	-	-	-	16	-	9.4	0.8	1.0	0.5	-	22	9.6
BTLF	<0.5 EAD	-	331	135	24	11	31	-	9.7	0.8	d.l.	0.9	-	26	1.6
CYF	<2 EAD	-	631	116	26	13	21	-	14	1.4	1.1	1.8	-	33	2.2

Table 3: Cont.

1984-03-14 to 1984-03-16															
DB35	0.16 EDD - 0.25 EAD	123	107	49	-	-	3.7	-	3.9	d.l.	-	0.5	-	11	-
DB17	0.09 " - 0.25 "	-	167	29	-	-	7.6	-	3.7	d.l.	-	d.l.	-	12	-
DB8	0.04 " - 0.25 "	-	184	20	-	-	11	-	4.9	0.6	-	0.6	-	9	-
FN	<0.25 EAD	-	209	16	-	-	11	-	18	2.8	-	0.6	-	11	1.5
BTLF	<0.5 EAD	-	535	32	d.l.	12	4.4	-	13	0.7	-	2.1	-	10	2.5
CYF	<2 EAD	-	1070	d.l.	26	12	5.8	d.l.	18	0.9	1.0	4.5	-	14	4.6
		1984-03-16 to 1984-03-19													
DB35	0.16 EDD - 0.25 EAD	-	68	32	-	-	9.4	-	2.6	0.3	-	-	-	7.5	-
DB17	0.09 " - 0.25 "	-	92	15	-	-	5.4	-	3.5	0.5	-	0.2	0.2	7.1	-
DB8	0.04 " - 0.25 "	-	109	31	-	-	5.8	-	4.7	0.5	d.l.	d.l.	-	7.3	-
FN	<0.25 EAD	-	136	12	-	-	24	3.1	68	11	1.6	1.4	0.7	8.4	5.3
BTLF	<0.5 EAD	-	267	146	10	10	6	-	5	0.3	-	0.7	-	7.1	0.8
CYF	<2 EAD	-	608	22	15	15	4	d.l.	8	0.4	0.3	1.4	-	8.3	1.9
		1984-03-19 to 1984-03-21													
DB35	0.16 EDD - 0.25 EAD	-	70	27	-	-	6.4	-	3.3	0.4	-	8.1	-	12	-
DB17	0.09 " - 0.25 "	-	82	26	-	d.l.	9.8	-	8.3	0.6	-	-	0.3	10	-
DB8	0.04 " - 0.25 "	-	74	21	-	-	15	-	3.2	-	-	-	0.3	12	-
FN	<0.25 EAD	68	88	-	-	-	8	-	3.3	d.l.	1.0	0.9	-	11	2.8
BTLF	<0.5 EAD	-	505	331	22	23	6	-	7.0	0.5	-	1.0	0.4	12	-
CYF	<2 EAD	-	805	272	35	32	8	d.l.	10	0.4	-	1.7	d.l.	14	1.7
		1984-03-21 to 1984-03-23													
DB35	0.16 EDD - 0.25 EAD	-	39	d.l.	-	-	5.2	-	2.6	d.l.	-	-	-	11	-
DB17	0.09 " - 0.25 "	-	55	39	11	-	8.0	-	3.2	d.l.	-	-	0.2	12	-
DB8	0.04 " - 0.25 "	36	56	16	-	-	5.2	-	3.5	0.5	-	1.0	0.2	11	-
FN	<0.25 EAD	-	64	28	-	-	5.5	-	2.6	d.l.	-	0.4	d.l.	4.9	-
BTLF	<0.5 EAD	-	219	41	-	-	3.4	-	2.4	-	-	0.4	-	5.0	-
CYF	<2 EAD	-	412	21	d.l.	6.5	8.0	-	4.8	-	0.4	1.5	d.l.	5.6	-

Table 3: Cont.

		1984-03-22 to 1984-03-26													
DB35	0.16 EDD - 0.25 EAD	22	49	7.2	-	-	14	-	2.1	0.3	-	-	-	7.8	-
DB17	0.09 " - 0.25 "	33	56	-	-	-	4.5	-	-	1.8	-	-	-	6.9	-
DB8	0.04 " - 0.25 "	44	69	13	-	-	3.9	-	1.8	0.3	-	-	-	7.7	-
FN	<0.25 EAD	-	58	-	-	-	5.9	-	2.9	-	0.2	0.4	0.1	3.3	-
BTLF	<0.5 EAD	-	494	30	11	7.2	3.1	-	4.4	0.4	-	1.1	0.2	7.2	0.9
CYF	<2 EAD	-	675	d.l.	17	8.7	4.0	0.6	7.0	0.4	0.4	2.3	-	4.1	2.2
		1984-03-26 to 1984-03-28													
DB35	0.16 EDD - 0.25 EAD	-	61	-	-	-	7.0	-	3.0	d.l.	-	-	0.2	12	-
DB17	0.09 " - 0.25 "	-	72	d.l.	-	-	6.2	-	3.3	0.4	-	-	d.l.	12	-
DB8	0.04 " - 0.25 "	35	79	139	70	-	30	-	5.0	0.7	d.l.	0.6	0.3	14	-
FN	<0.25 EAD	-	81	-	-	-	12	-	7.1	0.6	-	-	-	12	-
BTLF	<0.5 EAD	-	636	62	23	22	15	d.l.	16	0.5	d.l.	2.4	d.l.	18	1.4
CYF	<2 EAD	-	678	-	14	14	11	-	9.8	0.4	0.6	2.4	d.l.	10	1.3
		1984-03-28 to 1984-03-30													
DB35	0.16 EDD - 0.25 EAD	141	47	53	-	-	3.4	-	2.4	-	-	0.6	-	d.l.	-
DB17	0.09 " - 0.25 "	-	51	d.l.	-	-	11	-	2.3	-	-	0.4	-	1060	-
DB8	0.04 " - 0.25 "	-	50	d.l.	-	-	6.0	-	1.4	-	d.l.	0.5	-	682	-
FN	<0.25 EAD	-	67	d.l.	-	-	1.1	-	1.4	-	-	0.7	d.l.	-	-
BTLF	<0.5 EAD	-	484	46	14	12	1.6	d.l.	8.5	-	0.4	1.9	d.l.	d.l.	-
CYF	<2 EAD	-	610	-	16	11	9.4	-	8.3	d.l.	0.8	2.5	0.5	678	-

Table 3: Cont.

1984-03-31 to 1984-04-03															
DB35	0.16 EDD - 0.25 EAD	48	23	19	-	-	2.6	-	1.6	-	-	0.3	-	-	-
DB17	0.09 " - 0.25 "	43	25	17	-	-	0.9	-	3.7	-	-	0.3	-	-	-
DB8	0.04 " - 0.25 "	38	27	14	-	-	1.8	-	4.6	0.3	-	0.3	-	-	-
FN	<0.25 EAD	79	23	12	-	-	3.1	-	6.5	0.6	-	0.3	-	-	-
BTLF	<0.5 EAD	27	107	158	6.8	7.4	0.8	-	2.3	d.l.	d.l.	0.5	-	d.l.	-
CYF	<2 EAD	26	171	108	5.9	7.9	1.9	-	2.3	-	d.l.	0.7	-	1.2	0.4

* See p. 55 for branch description.
** Approximate 50% penetration (for diffusion batteries) or 50% collection efficiency (for impactors and cyclone) cut points.
\+ EDD = equivalent diffusion diameter (see Vitols and Wasseng, 1985).
++ EAD = equivalent aerodynamic diameter (see Vitols and Wasseng, 1985).
d.l. means at the PIXE detection limit for a given element.
\- means below the PIXE detection limit for a given element.

Table 4: Trace element concentrations (μg m^{-3}) in aerosols collected by the six branches of P.-B.F. during the Summer 1984 campaign at Ny Ålesund.

Sampling date:		1984-06-18 to 1984-06-22							
Element		Si	S	Cl	Cr	Fe	Cu	Zn	Br
Branch*	Approximate size range**, μm								
DB35	0.16 EDD+ - 0.25 EAD++	237	127	83	7.9	4.1	1.0	0.7	31
DB17	0.09 " - 0.25 "	394	163	61	8.7	4.0	-	d.l.	29
DB8	0.04 " - 0.25 "	401	203	83	9.9	4.4	-	0.7	27
FN	<0.25 EAD	429	191	51	8.6	4.1	0.7	0.8	28
BTLF	<0.5 EAD	361	469	43	8.8	4.9	d.l.	1.2	30
CYF	<2 EAD	83	637	66	8.8	7.1	0.8	0.9	32
		1984-06-23 to 1984-06-27							
DB35	0.16 EDD+ - 0.25 EAD++	135	110	50	8.3	6.6	0.7	0.7	25
DB17	0.09 " - 0.25 "	109	175	69	8.5	4.6	0.6	1.0	28
DB8	0.04 " - 0.25 "	101	191	87	11	4.4	-	0.8	28
FN	<0.25 EAD	196	205	50	10	6.1	0.7	1.0	32
BTLF	<0.5 EAD	-	645	53	10	5.0	1.0	1.2	29
CYF	<2 EAD	-	941	164	7	8.3	1.9	1.4	32
		1984-06-27 to 1984-06-30							
DB35	0.16 EDD+ - 0.25 EAD++	1039	90	99	14	7.2	d.l.	d.l.	47
DB17	0.09 " - 0.25 "	811	123	98	15	7.2	-	1.0	49
DB8	0.04 " - 0.25 "	612	124	d.l.	16	8.2	-	1.1	48
FN	<0.25 EAD	741	144	d.l.	20	7.6	-	1.1	48
BTLF	<0.5 EAD	332	449	96	11	7.1	-	1.0	51
CYF	<2 EAD	423	617	107	16	8.9	1.3	1.6	47
		1984-07-02 to 1984-07-05							
DB35	0.16 EDD+ - 0.25 EAD++	263	d.l.	d.l.	14	7.7	-	1.2	53
DB17	0.09 " - 0.25 "	313	99	74	15	6.8	-	1.1	53
DB8	0.04 " - 0.25 "	546	180	137	13	8.7	d.l.	d.l.	51
FN	<0.25 EAD	501	167	82	13	15	d.l.	1.6	52
BTLF	<0.5 EAD	480	310	146	12	8.9	1.3	1.4	54
CYF	<2 EAD	304	446	202	18	8.7	1.6	1.7	57
		1984-07-06 to 1984-07-09							
DB35	0.16 EDD+ - 0.25 EAD++	108	61	-	9.8	20	1.1	d.l.	35
DB17	0.09 " - 0.25 "	272	-	57	12	20	1.5	0.7	35
DB8	0.04 " - 0.25 "	202	56	73	18	37	2.0	d.l.	35
FN	<0.25 EAD	339	d.l.	d.l.	11	57	3.9	1.2	35
BTLF	<0.5 EAD	131	109	124	12	5.0	-	0.8	36
CYF	<2 EAD	-	157	393	13	9.6	-	d.l.	40

Table 4: Cont.

Sampling date:		1984-07-09 to 1984-07-11							
Element		Si	S	Cl	Cr	Fe	Cu	Zn	Br
Branch*	Approximate size range**, µm								
DB35	0.16 EDD+ - 0.25 EAD++	186	d.l.	83	17	6.4	d.l.	1.3	53
DB17	0.09 " - 0.25 "	196	d.l.	77	17	6.5	-	d.l.	45
DB8	0.04 " - 0.25 "	138	95	98	19	6.8	-	-	45
FN	<0.25 EAD	335	125	114	16	8.0	1.1	1.3	45
BTLF	<0.5 EAD	151	187	181	11	5.6	1.0	d.l.	41
CYF	<2 EAD	d.l.	408	311	15	9.4	d.l.	1.1	51
		1984-07-11 to 1984-07-13							
DB35	0.16 EDD+ - 0.25 EAD++	-	80	86	17	5.9	-	-	45
DB17	0.09 " - 0.25 "	151	d.l.	60	11	5.6	-	1.1	40
DB8	0.04 " - 0.25 "	167	85	76	12	5.7	-	1.8	43
FN	<0.25 EAD	281	75	d.l.	20	5.7	d.l.	d.l.	41
BTLF	<0.5 EAD	-	232	85	12	5.6	1.3	1.1	43
CYF	<2 EAD	-	420	-	12	4.6	-	-	45
		1984-07-13 to 1984-07-16							
DB35	0.16 EDD+ - 0.25 EAD++	138	d.l.	60	9.8	5.5	-	0.9	38
DB17	0.09 " - 0.25 "	184	d.l.	69	11	5.3	d.l.	1.0	43
DB8	0.04 " - 0.25 "	195	d.l.	91	13	5.5	-	-	41
FN	<0.25 EAD	235	286	d.l.	9	6.1	d.l.	d.l.	38
BTLF	<0.5 EAD	101	150	d.l.	14	5.5	-	d.l.	38
CYF	<2 EAD	-	310	70	9	6.6	d.l.	1.1	39
		1984-07-16 to 1984-07-18							
DB35	0.16 EDD+ - 0.25 EAD++	2340	328	314	45	24	4.8	4.6	141
DB17	0.09 " - 0.25 "	3970	300	278	38	22	-	5.4	148
DB8	0.04 " - 0.25 "	5330	296	316	53	22	d.l.	-	139
FN	<0.25 EAD	5370	341	205	28	33	3.7	3.3	135
BTLF	<0.5 EAD	3000	556	287	32	19	3.2	3.3	135
CYF	<2 EAD	-	1025	295	37	24	d.l.	3.9	139

* See p. 55 for branch description.
** Approximate 50% penetration (for diffusion batteries) or 50% collection efficiency (for impactors and cyclone) cut points.
+ EDD = equivalent diffusion diameter.
++ EAD = equivalent aerodynamic diameter.
d.l. means at the PIXE detection limit for a given element.
- means below the PIXE detection limit for a given element.

Examination of the data in Tables 3 and 4 reveal frequent inconsistencies concerning the concentrations of elements, collected by the 6 branches of the P.-B.F. Clearly, for a given sampling run, the concentrations should increase from the lowest in the DB35 branch (narrowest particle size range) to the highest in the CYF branch (widest particle size range). The quite frequent deviations from this pattern are suspect, and such erroneous results are likely due to a combination of sampling, sample handling and treatment, and analytical factors. The data in Tables 3 and 4 should, therefore, be used with caution.

3.3 WIND DATA

3.3.1 MISU

The Department of Meteorology, University of Stockholm (MISU) operated a wind "sector meter" (Heintzenberg et al., 1982) in March 1981 at "MISU 1981" (point 4 in Figure 2), and in August 1982 and March 1983 at NILU I (Figure 2).

Average wind direction distributions in eight 45^0 sectors for these periods are shown in Figures 30, together with showing similar information for NILU I in March 1983, plotted from hourly wind sector distributions supplied by MISU*. Recordings of 10-min. average wind speed at the Norwegian Polar Institute (NPI) research station (point 1 in Figure 2) in Ny Ålesund for the same periods are available by special request from NILU**.

3.3.2 NILU W.STA.

During the Fall 1983, Spring 1984, and Summer 1984 campaigns, NILU operated at NILU II (Figure 2) a mechanical "wind station" (W.STA.), for continuous wind speed and direction recording (see Vitols and Wasseng, 1985, for instrument description).

Average wind speed and direction summaries for these periods are presented in Figure 31, 32, and 33.

---

* Unpublished data, courtesy of Dr. Jost Heintzenberg, MISU.
** Contact Forsker E. Joranger, NILU, P.b. 130, N-2001 Lillestrøm, Norway.

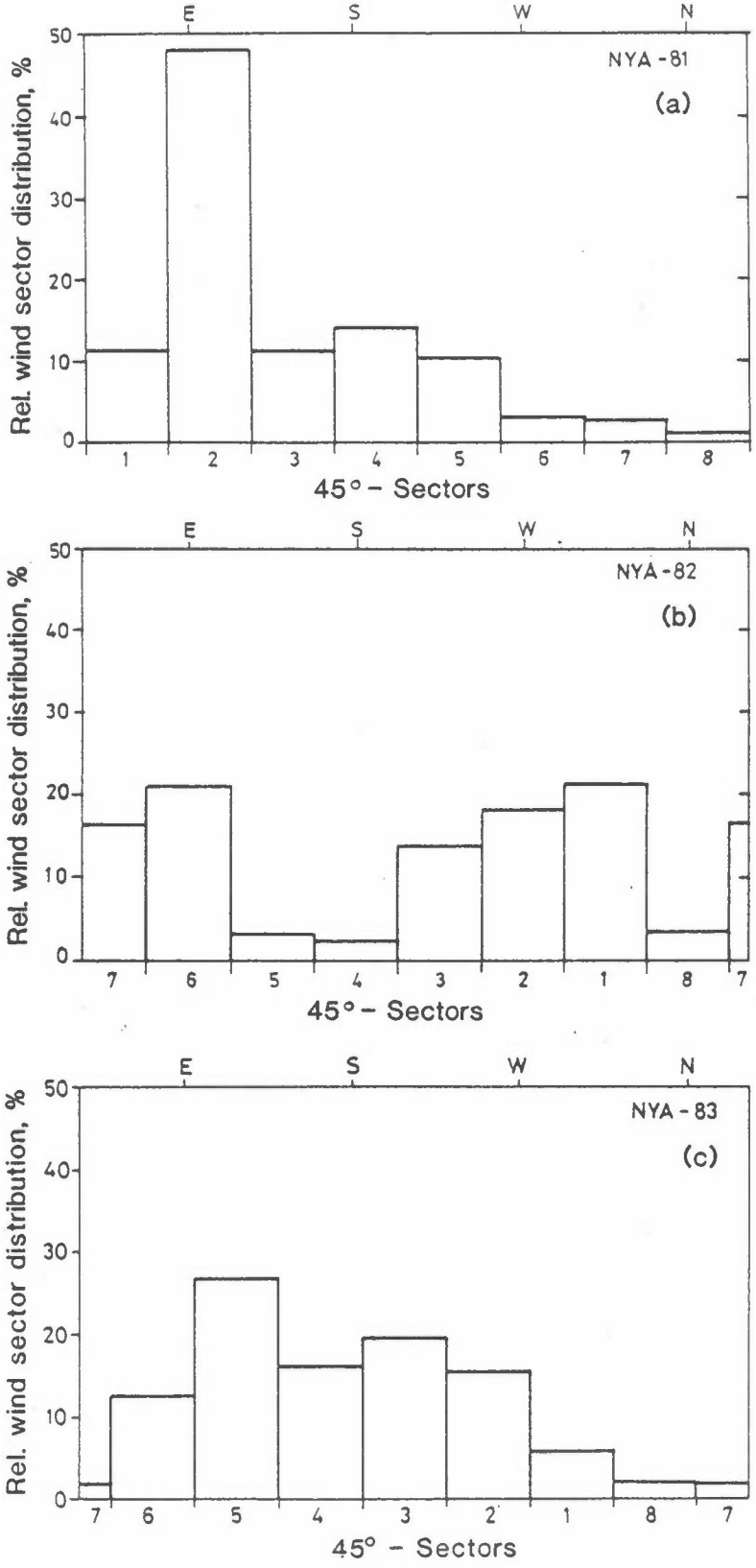

Figure 30: Relative wind sector distributions at Ny Ålesund:
(a) "MISU 1981", March 1981;
(b) NILU I, August 1982.
(Heintzenberg et al., 1983)
(c) NILU I, March 1983
(Data courtesy of MISU)

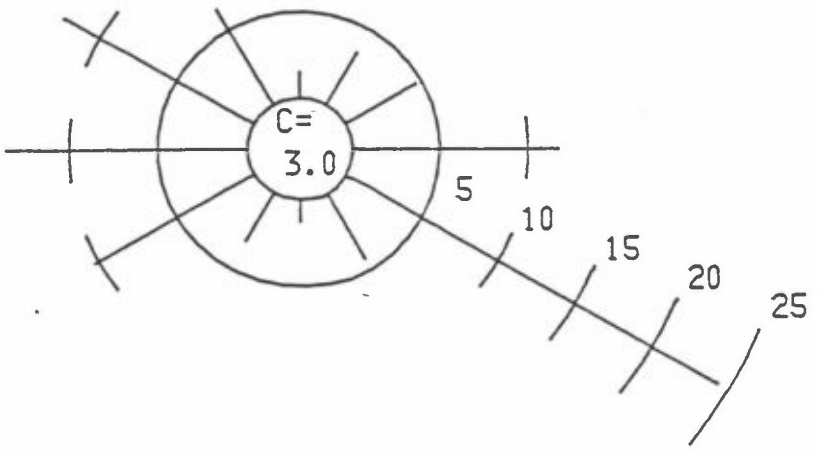

(a)

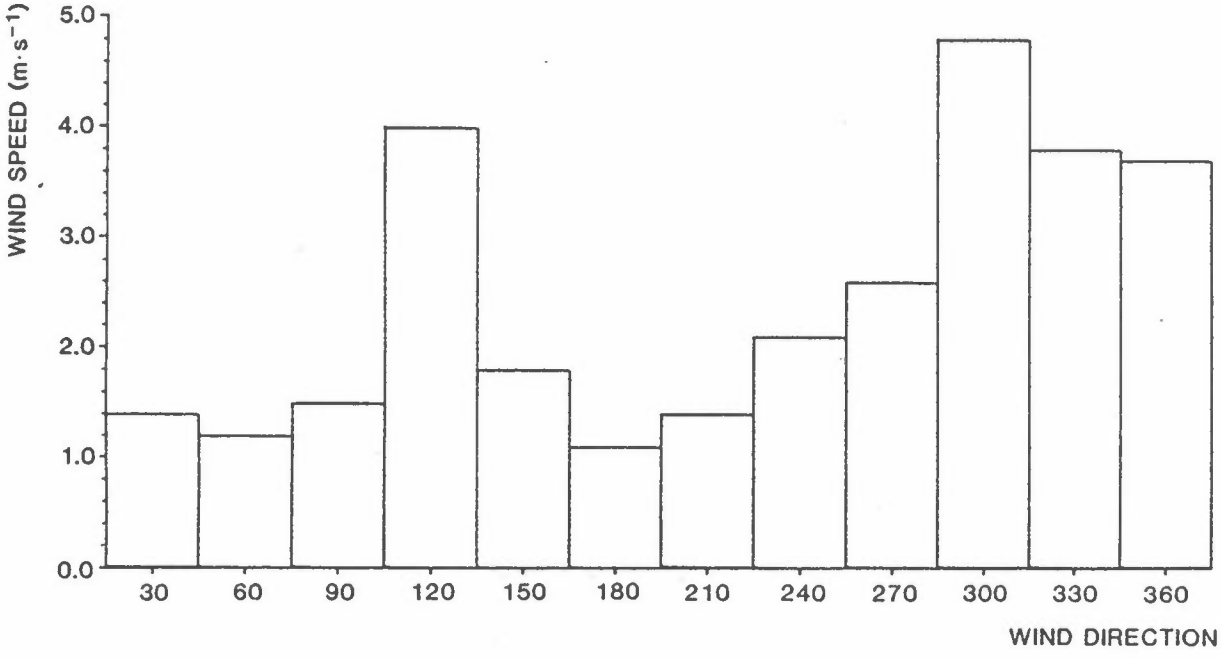

(b)

Figure 31: (a) wind direction, and (b) wind speed distributions at NILU II in Ny Ålesund, 1983-08-08 to 1983-09-14.
(912 hours of observations.)

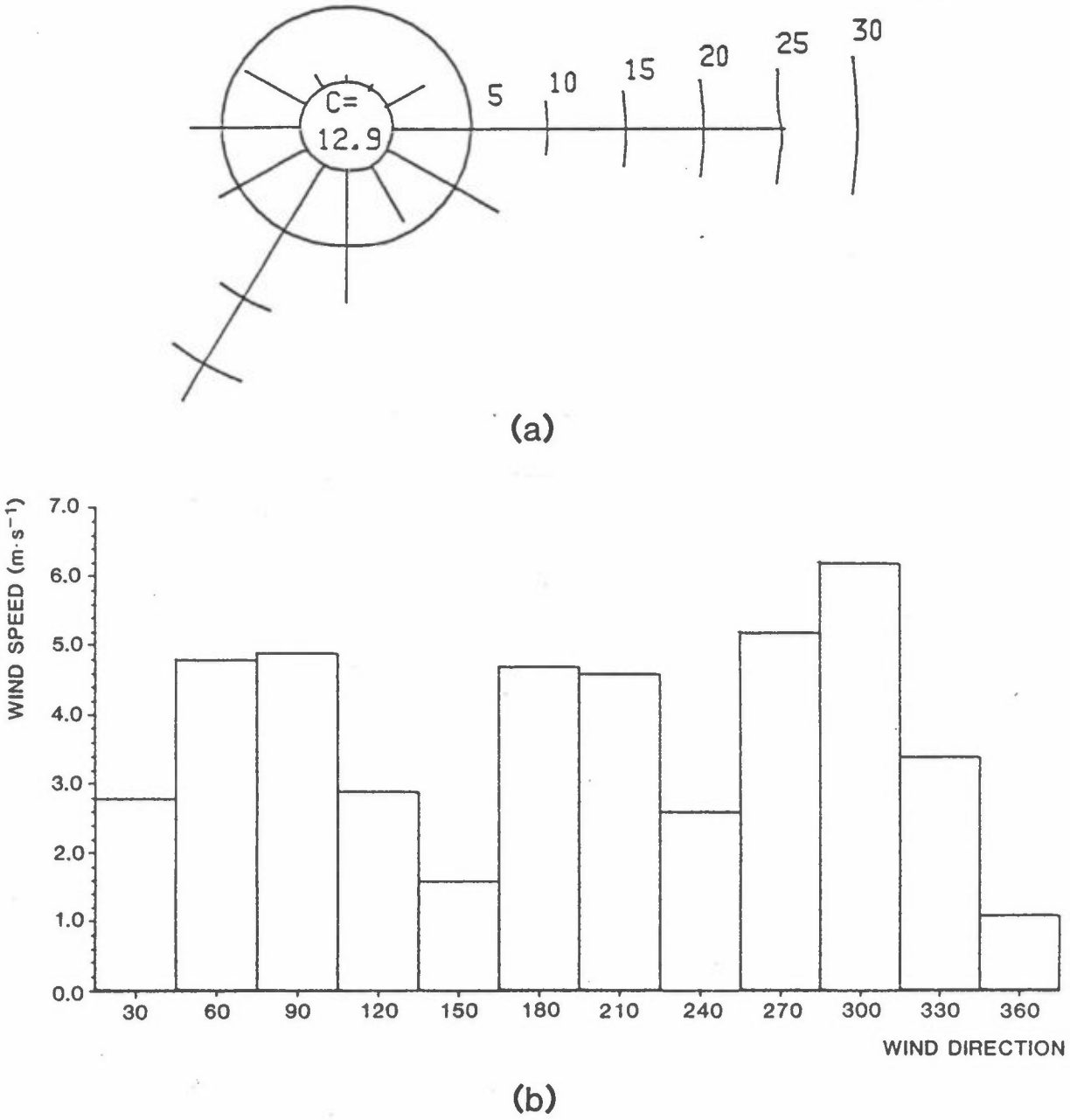

Figure 32: (a) wind direction, and (b) wind speed distributions at NILU II in Ny Ålesund, 1984-02-26 to 1984-04-09.
(972 hours of observations.)

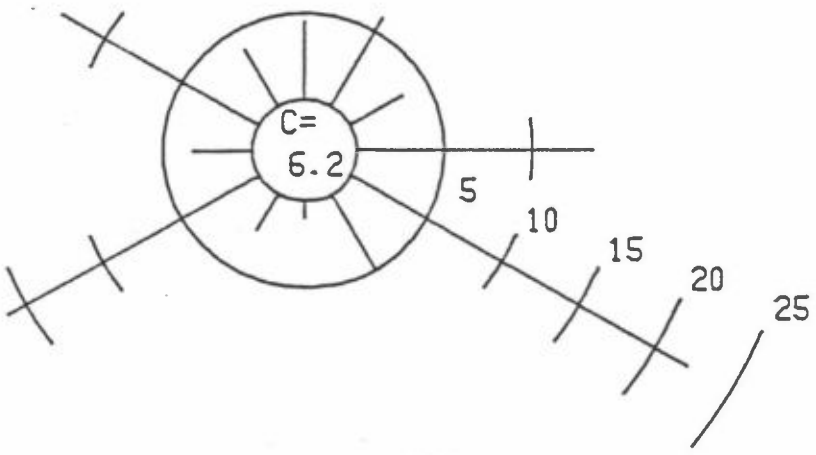

(a)

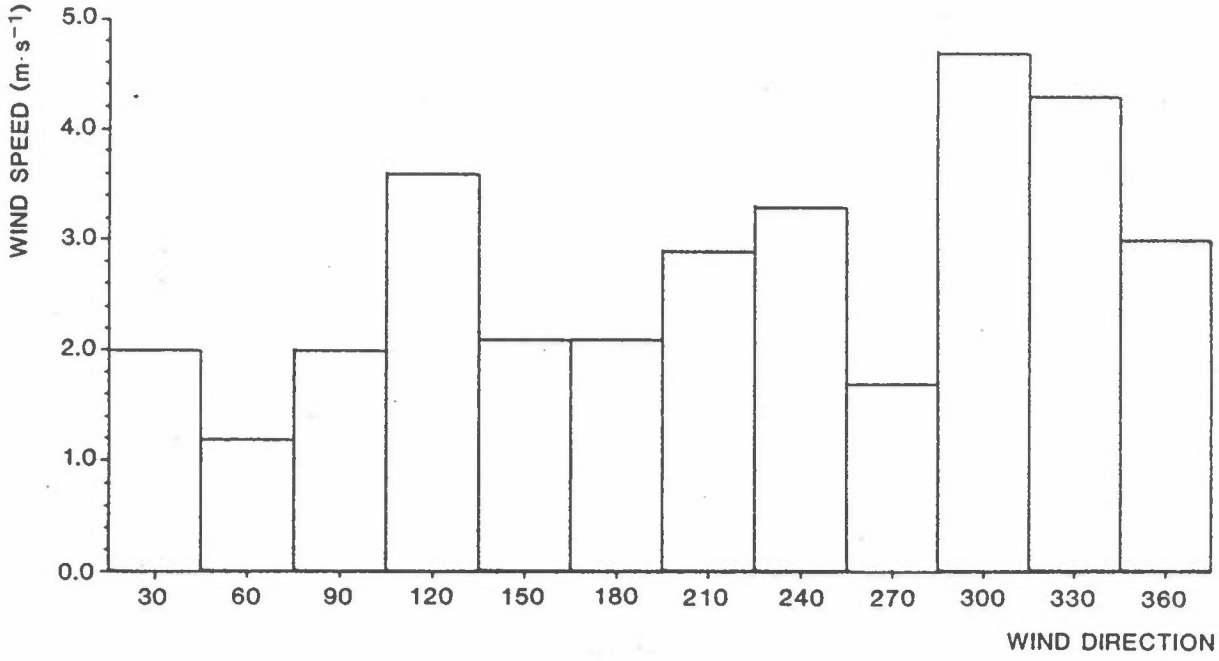

(b)

Figure 33: (a) wind direction, and (b) wind speed distributions at NILU II in Ny Ålesund, 1984-06-23 to 1984-07-18.
(580 hours of observations - observations from 1984-06-15 to 1984-06-23 are missing.)

4 DISCUSSION OF RESULTS

4.1 CNC AND σ_{sp}

The continuous flow CNC (TSI Model 3020), used at NYA for all BP Project and MISU 1981 campaigns, counts Aitken particles reliably down to ca. 0.02 μm diameter, and computes CN concentrations as low as 0.01 cm^{-3} (Agarwal and Sem, 1980; Bartz et al., 1985).

Generally, the CN concentrations, measured during these periods, are in good agreement with other available data from the Arctic (e.g., Jaenicke and Schütz, 1982; Lannefors et al., 1983). During the late winter/early spring campaigns in 1981 and 1983, 12-h medians of CN concentrations remained <500 cm^{-3}, except during air pollutant transport episodes (Figures 3 and 5). In 1984 the wintertime concentrations were considerably lower (Figure 7), never exceeding 200 cm^{-3}, and for the most part remaining <100 cm^{-3}. During the wintertime periods, the range of CN concentrations remained relatively narrow, while the late summer/early fall periods (Figures 4, 6, and 8) were characterized by much greater variability.

A rather unique event occurred on 1982-08-21 during the Fall 1982 campaign, when extremely low CN concentrations were observed at NILU I (Heintzenberg et al., 1985). The weather situation was quite typical of the Spitsbergen summer, with low-lying stratus or fog, light winds, and occasional slight drizzle. These conditions are very effective for scavenging trace substances from the air, and as a consequence the lowest CN concentrations ever reported (around 0.1 cm^{-3}) were measured over many hours (see 12-h median in Figure 4), indicating extremely clean air.

Concentrations this low were not observed at NYA during any of the other campaigns, although in late evening 84-03-02 and in the early morning hours of 84-03-03 during Spring 1984 campaign, CN concentrations dropped below 10 cm^{-3} for about 3 hours. This period had been preceded by driving (>40 kt) south-westerly winds, and falling and blowing snow, apparently resulting in efficient removal of the aerosol. Unfortunately, CN measurements in Spring 1983 had not yet begun when a severe blizzard (with >60 kt. winds) even disrupted operation of filter samplers at NILU I. The lack of CN data

thus presented a verification of enhanced removal effectiveness of driven snow under high wind conditions.

The integrating nephelometers (such as the A-IN at NYA), measuring particle light scattering coefficient σ_{sp}, respond mostly to particles in the 0.1 μm to 1.0 μm diameter range, which are the most efficient light scatterers (Waggoner et al., 1981). These particles also account for the most of the mass in the accumulation mode of aerosol mass-size distributions, representing "aged" particles in the arctic atmosphere, which had enough time to undergo various transformation and removal processes, and stabilize in this size range.

CN concentration and σ_{sp} medians in the late winter/early spring periods are well correlated, as seen in Figure 3, 5 and 7. The simultaneous peaks in 12-h medians of CN concentrations and σ_{sp}s agree well with peaks in trace element mass concentrations, measured at NYA during the same periods (see Section 4.2, and Pacyna et al., 1985a). This also indicates that the TSI Model 3020 CNC responds reasonably efficiently to most accumulation mode aged aerosols (up to ca. 1 μm diameter).

As was the case with CN concentrations, the 12-h medians of σ_{sp} in early spring 1981 and 1983 (Figures 3 and 5, respectively) remained in a rather narrow range (10^{-5} to $10^{-4} m^{-1}$) as well, particularly during the two weeks in March 1981 (ca. 1.0 to 2.6 x $10^{-5} m^{-1}$, in Figure 3). During the Spring 1984 campaign, the σ_{sp} levels also reflected the rather atypical CN concentrations, remaining at all times below 4 x $10^{-5} m^{-1}$ and dropping below the detection limit of the A-IN during periods of low CN concentrations (Figure 7). This agrees well with other evidence (see Section 4.3.1, and Pacyna et al., 1985a) for considerably lower-intensity long-range transport episodes in Winter/Spring 1984, than during the Spring 1983 campaign.

In fall 1983 and summer 1984 (Figures 6 and 8, respectively), σ_{sp}s exhibited large fluctuations, with prolonged periods of sub-detectable σ_{sp} (< ca. $10^{-7} m^{-1}$).

The typical patterns of σ_{sp} distributions during wintertime and summertime can also be recognised in the more continuous σ_{sp} data from the BJO ground station (Figures 9 through 11). Here too the wintertime 12-h median range was confined in the narrow 10^{-5} to $10^{-4} m^{-1}$ band, while during summertime the fluctuations and range widened considerably.

Figure 6 illustrates two contrasting situations during the Fall 1983 campaign. In the first, between ca. 1983-08-15 and 1983-08-25, the 12-h medians show several CN peaks (in excess of 10^3 cm^{-3}) but no detectable σ_{sp} s. In the other, between ca. 1983-09-07 and 1983-09-13, there are nearly coincident peaks in CN ($>10^3$ cm^{-3}) and σ_{sp} (up to 3 x 10^{-5} m^{-1}) medians. Considering the different, particle size-dependent response characteristics of the CNC and the A-IH, the presence of substantial amounts of Aitken particles and a virtual absence of aged particles during the first period is implied. A wide-spread presence of very fine aerosol particles was also observed by BP Project aircraft measurements over Spitsbergen during the same time (Pacyna et al., 1985b). In contrast, during the second period both CNC and A-IH were apparently responding mostly to particles in the accumulation mode size range.

Since the high Aitken particle concentrations during the first period were measured in reasonably well-mixed air, direct transport of local combustion was not their source. Nevertheless, their small size precludes long travel distances and aging times. Thus a nearby, but extensive source of fresh aerosol had to be responsible. Dimethyl sulphide (DMS) from marine biogenic processes is known to be an important part of sulphur compounds in the atmosphere, and a precursor of aerosol sulphur in remote areas (Andreae and Raemdock, 1983). Atmospheric photochemical oxidation of DMS, possible during the arctic summer, may lead to the production of low vapour pressure sulphuric acid and methane sulphonic acid (MSA), primarily in aerosol form in the Aitken particle range (Saltzman et al., 1983; Hatakeyama et al., 1985). These particles are numerous, but because of their very small size contribute little to the aerosol mass. The low trace element concentrations (except for one sampling run, examined below) during the first period (see Figure 6 in Pacyna et al., 1985a) support this view. Since no P.-B.F. data for this period is available, quantitative information on S distributions in the <0.25 μm EAD particles is lacking. Thus, at this time, the possibility of biogenic/photochemical operation of Aitken particles remains only a speculation.

Wind direction and speed measurements at NILU II, shown in Figure 34, indicate that the high CN concentrations coincided with periods of near calm or weak and variable winds. Such weather conditions are conducive to advected aerosol accumulation and recirculations. Although the CNC recordings at these times revealed generally well-mixed air, some "nervousness" (i.e., noise) in the CN trace was evident, which also suggests possible recirculation.

The 2-day interval between 1983-08-17 and 1983-08-18 presents then a somewhat atypical picture. Wind trajectories and aircraft observations (see Pacyna et al., 1985c) identified a brief transport from the USSR, and an aloft layer of aerosols (centred at about 3600 m) over Spitsbergen. The winds (Figure 34) were, however, definitly westerly and relatively strong (ca. 6 m s^{-1}), so that the upper wind direction must have been quite different from that at the 10 m level in Ny Ålesund. The low CN medians (including the lowest one (ca. 20 cm^{-3}) for this campaign, and a 3-h

interval with <10cm^{-3} CN concentrations) and sub-measurable σ_{sp} s during these 2 days (see Figure 6) also suggest that the air pollutants aloft had not mixed down to the ground at Ny Ålesund. The "blips" in Cd and Zn 2-day mean concentrations at this time (see Figure 6 in Pacyna et al., 1985a) may be due to very local and selective contamination, since they coincided with Hi-Vol sampler vacuum pump fire, and an interrupted and significantly foreshortened sampling run. It is conceivable that, while the vacuum pump was exchanged, the concentrated effluent from the motor insulation and plastic material fire (possibly containing the two elements), temporarily trapped inside the station building, could reach the backside of the Hi-Vol filter. This additional "passive" contamination, combined with the small sample air volume for the run, could then very well show up in the calculated concentrations.

During the second, early September 1983 period, the chemical composition of aerosols (Pacyna et al., 1985a) at NYA and all other BP Project ground stations (except JAM) unequivocally confirms the presence of anthropogenic, aged aerosol. The episode was one of the rare, but extensive, summertime meridional transport cases, originating in western and central Europe. The simultaneously high CN concentrations and σ_{sp} s testify to the presence of well-aged aerosol. During two days preceeding the episode at NYA, the winds

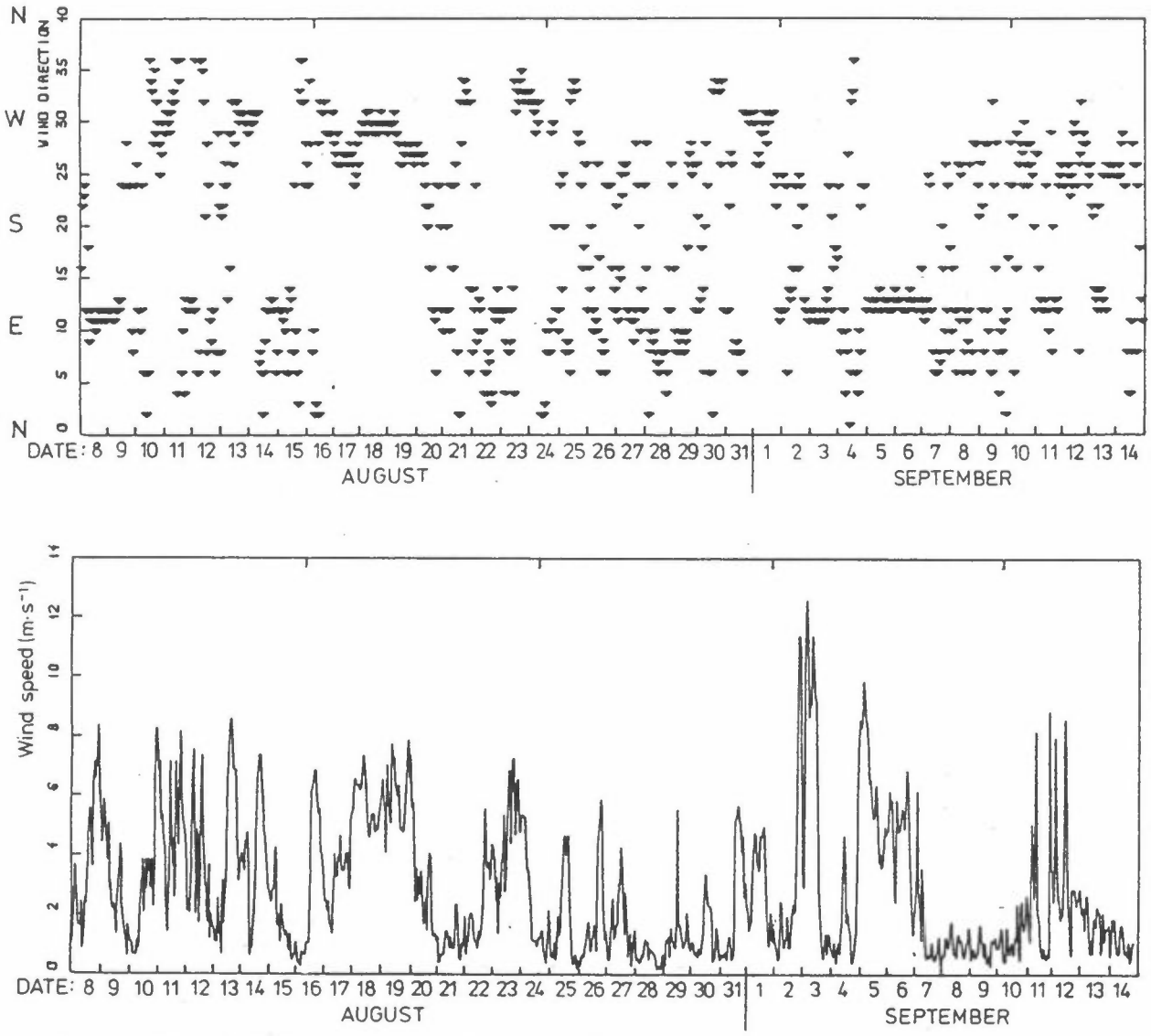

Figure 34: Wind direction and speed distributions at NILU II (10 m above ground) in Ny Ålesund from 1983-08-15 to 1983-09-14.

were clearly easterly and brisk (Figure 34), but subsequent stagnation (average wind speed ca. 1 ms^{-1}) encouraged pollutant accumulation during the episode. The size-differentiated composition of the aerosol (presented in Section 3.2, and discussed in Section 4.2 of this report) shows significant enrichment of anthropogenic trace elements during this time as well.

The characeristics of various particle size distribution spectra during these two periods are examined in Section 4.2.

Relatively high CN concentrations (12-h medians up to 3 x 10^3 cm^{-3}) were also observed during the Summer 1984 campaign (between 1984-06-18 and 1984-07-07), as seen in Figure 8. Unfortunately, concurrent σ_{sp} data for part of this period are missing. Anthropogenic trace element concentrations were generally low at this time, but SO_4^{2-}-S was definitly elevated, suggesting again possible biogenic production (see also Section 4.2). The period was characterized by rapidly changing weather conditions (even snowfall). Although absent with strong and steady winds (see Vitols and Wasseng, 1985), some contributions of combustion aerosol during calms, and weak and variable winds from the spontaneous coal burn site, about 1.5 km to the east of NILU II, cannot be ruled out even in seemingly well-mixed air.

4.2 AEROSOL NUMBER-, AREA-, AND VOLUME-SPECTRA

The relatively narrow-range, white-light OPCs of the Royco Model 225 type have been only rarely used for arctic aerosol measurements. The particle number concentration data from Royco 225 measurements during a short period in March 1983 in the Canadian Arctic (Hoff and Trivett, 1984) agree well with the BP Project OPC wintertime results at NYA. The particle counts in the various size ranges are of about the same magnitude, and show relatively small variation with time.

As seen in Figures 12 through 15, the coarser aerosol particles are few in number, particularly during wintertime, when both airborne sea salt production and dust reentrainment are suppressed. As expected, they show the greatest variability and wind speed dependence in summertime. The total OPC number concentrations are thus largely dominated by the smallest (~0.3-0.5 μm ESD) particles.

A comparison of OPC total particle number concentrations in Figures 12

through 15, to CNC and σ_{sp} values (in Figures 5 through 8 in Section 3.1.1) reveals, for the most part, similar features. The OPC data confirm the considerable differences (ca. one order of magnitude) in aerosol levels during the Spring 1983 and 1984 campaigns, as well as the generally much greater variability during summertime periods.

The highest 12-h average total particle (>ca. 0.3 μm ESD) concentration of 19 cm^{-3} (Figure 12) was measured by the OPC on the morning of 1983-03-11 at NILU I. In comparison, the corresponding 12-h median concentration of particles (>ca. 0.02 μm dia.) by CNC was ca. 2 x 10^3 cm^{-3} (Figure 5). The highest CNC 12-h median of ca. 3.4 x 10^3 cm^{-3} (Figure 8) occured on the morning of 1984-06-27, when the corresponding OPC total particle 12-h average concentration was only 1.2 cm^{-3}. This provides an illustration of the multi order-of-magnitude, size-dependent concentration variations possible in the ambient air under different conditions of aerosol production, transport, aging and removal processes.

As has been noted earlier (Hoff and Trivett, 1984), due to its limited detection range (>~0.3 μm ESD), the OPC will respond much more sluggishly to variations in accumulation mode particles than the A-IN, and cannot, of course, detect the very fine Aitken particles at all. For example, disturbances due to emissions from local combustion sources are missed by the OPC, which makes the instrument unsuitable for sampling control purposes. On the other hand, the OPC counts the coarser, super-micrometer diameter particles beyond the efficient response ranges of both the CNC and the I.N., provided the air inlet does not discriminate against such particles and the OPC conveys them efficiently to its sensing zone. OPCs thus respond to the presence of coarse, reentrained dust and airborne seasalt, which may represent a significant mass fraction of the aerosol. Although particle number distributions are truncated below 0.3 or 0.4 μm ESD by the Royco 225, the two higher moments of particle size distribution, i.e., particle surface area and particle volume distribution spectra (such as those shown in Figures 16 through 25) can help identify directly the aerosol size ranges primarily contributing to such integral aerosol properties, as light scattering and suspended mass, respectively.

Figures 16 and 17 show the 3 size distribution spectra for two days in March 1983. On 1983-03-11, both the CNC and σ_{sp} medians (Figure 5, Section 3.1.1) were the highest for the Spring 1983 campaign. BTL C.I. measurements showed high trace element concentrations (<0.5 μm EAD fraction) as well (Figure 26,

Samples 4 and 5, Section 3.2.1), identifying a significant episodic long-range transport of anthropogenic air pollutants to NYA. This was also a period with light winds and appreciable, apparently regional haziness, which was also observed at Longyearbyen, ca. 100 km south of NYA. Despite the truncated accumulation mode range, the OPC distribution spectra in Figure 16 indicate elevated numbers, area and volume for <1 µm ESD particles, which resulted in the enhanced light scattering and aerosol mass. The slight surface and volume modes in the 2-3 µm ESD range were probably due to residual seasalt, since the period was preceded by enhanced seasalt constituent concentrations (see Pacyna et al., 1985a).

The CNC and σ_{sp} medians (Figure 5, Section 3.1.1) and total OPC count average (Figure 12) on the morning of 1983-03-18 were the lowest for the Spring 1983 campaign. The distribution spectra in Figure 17 reveal much reduced fine particles levels, but increased contribution to aerosol surface and volume from the coarser particles in the afternoon. Snow had been falling throughout the night, turning to rain in the morning. This, and the low clouds and fog had apparently scavenged most of the accumulation mode particles, if any were still remaining in the air from the preceding episode. The wind in the afternoon was brisk from W-SW, so that the higher coarse particle levels were likely due to fresh seasalt particle production, since both Kongsfjorden and the ocean to the west were almost ice-free at this time. The BTL C.I. results for this period (Figure 26, Sample 7, Section 3.2.1) give very low anthropogenic element concentrations, but very high Cl concentrations.

Since particle mass is proportional to volume, the total volume of aerosol particles, calculated from OPC measurements, may be used as a rough but useful estimate of suspended particle mass concentrations, provided the mass of the <ca. 0.3 µm ESD particles is not overwhelming. Assuming an average particle density of 2 g cm^{-3}, the suspended mass concentrations, estimated in this manner, for the 2 days in March discussed above are 2.2 and 2.6 µg m^{-3}, respectively. The direct mass concentration measurements of ≤2 µm EAD particles at NYA by Heintzenberg and Covert (1984b) give ca. 7 and 4 µg m^{-3}, respectively, for sampling periods bracketing these 2 days. Considering all the assumptions and uncertainties inherent in the aerosol volume and mass estimations, the agreement for 1983-03-18 is reasonable, confirming that most of the aerosol mass was due to coarse particles on this day. The substantial disagreement for 1983-03-11, on the other hand, supports the

earlier suggestion, that on that day the aged aerosol fraction "ignored" by the OPC (i.e., <0.3 μm ESD), contained substantial mass.

Estimation of light scattering from the total surface area of particles is not as straight-forward, because the nature of the surface, i.e., the shape and particularly the chemical/optical properties of the particle, determine to a large extent the scattering intensity.

Figures 18 through 20 relate to the two intersting periods during the Fall 1983 campaign, already discussed in Section 4.1.

Figure 18 shows the OPC particle distribution spectra for 1983-08-15, when on the afternoon the 12-h CNC median climbed past 10^3 cm^{-3}, while the σ_{sp} s remained below the detection limit of the A-IN (Figure 6, Section 3.1.1). The distribution spectra for 1983-08-21 and 1983-08-24, the two other days in August with such unusual CNC and σ_{sp} patterns, are virtually identical to those on 1983-08-15, and are not shown. The total OPC count concentrations on these days (Figure 13) were only about 0.2 cm^{-3}, and the particle spectra were about an order-of-magnitude lower and have entirely different shapes than during the high CNC period in Spring 1983. The aerosol surface distributions have a low magnitude and the well-resolved mode for the >1 μm ESD particles is outside the useful response range of the A-IN. The volume spectra indicate a depleted accumulation mode, with essentially all of the low magnitude particle volume due to >1 μm ESD particles. The latter particles were likely reentrained dust and airborne seasalt. The 3 days were characterized by very light winds (see Figure 34, Section 4.1), but all were preceded by periods of strong winds. Aerosol chemical composition measurements during this time (see Pacyna et al., 1985a) indicated a virtual absence of anthropogenic trace elements, but somewhat elevated seasalt ions. The negligible particle volume in the portion of the accumulation mode, covered by the OPC (Figure 18) then supports the suggestion (in Section 4.1), that the high CN levels could have only come from nearby or regionally-produced Aitken range particles.

The lowest concentrations (and sub-detectable σ_{sp} s) during the Fall 1983 campaign were measured on 1983-08-18 (Figure 6, Section 3.1.1). Judging from Figure 19, however, the situation appears to be only a modification, due to different weather, of the conditions prevailing during the August period just discussed. The strong winds (average ca. 6 m^{-3}) on this day were

westerly, resulting in increased coarse particle (likely seasalt) surface and volume spectra. At the other end of the spectrum, snow shower and low stratus scavenging kept the smaller accumulation mode and Aitken particles at low levels.

The OPC aerosol spectra in Figure 20 for 1983-09-10 typify the one strong episodic transport period at NYA during the second week in September. It was preceded by brisk (ave. ca. 5 ms^{-1}) easterly winds, but subsequent frequent calms with no precipitation gave poor ventilation in the Kongsfjorden "bowl" and were favourable to advected pollutant accumulation, which resulted in quite hazy conditions. The CNC and σ_{sp} medians (Figure 6, Section 3.1.1) indicated enhanced levels of accumulation mode particles, and the size-differentiated BTL C.I. samples (Figure 28, Section 3.2) contained high concentrations (for summertime) of anthropogenic (<1 μm EAD) sulphur. Both the surface and volume spectra in Figure 20 indicate enhanced scattering and suspended mass in the accumulation range. The rising coarse particle volume on the afternoon of 1983-09-10, probably reflects the influence of the freshening wind (Figure 34, Section 4.1) on dust reentrainment.

All OPC spectra remained remarkably similar throughout the Winter/Spring 1984 campaign at NYA. 1984-02-29, 1984-03-03 and 1984-03-04 were the three days with the highest CNC and σ_{sp} 12-h medians. Although they, as well as OPC total particle concentrations, were, on the average, almost an order-of-magnitude lower than in Spring 1983, anthropogenic sulphur and trace element concentrations in BTL C.I. samples (Figure 27, Samples 1, 2 and 3, Section 3.2) were at similar levels. The OPC aerosol spectra in Figure 21 for 1984-02-29 are typical also for the two other days above (not shown), but are almost on order-of-magnitude lower than even during the September 1983 episode, the spectra of which they resemble. The distinct volume mode in the 2-3 μm range persisted throughout this period, even though the winds were easterly, and Kongsfjorden was frozen over at the time. The Hi-Vol samples from the period (see Pacyna et al., 1985), however, showed a seasalt ion concentration peak.

Figure 22 for 1984-03-17 represents one of the days with the lowest CNC and σ_{sp} medians for the Winter/Spring 1984 campaign (Figure 7, Section 3.1.1). The BTL C.I. results(Figure 27, Sample 9, Section 3.2) indicate low levels of anthropogenic constituents. The general features of the aerosol spectra had changed little from Figure 21, but the surface spectrum for <1 μm ESD

particles points to lower light scattering. Snow, driven by strong SE winds, probably caused the decline in accumulation mode particles. The volume mode in the 2-3 μm ESD range, however, is still present, but at this time Kongsfjorden had some open waters opposite NYA, and the Hi-Vol seasalt ion concentrations (Pacyna et al., 1985a) indicate an airborne seasalt "episode".

The first two-thirds of the Summer 1984 campaign were a difficult time for sampling well-mixed air at Ny Ålesund. Frequent intervals with very light and variable winds caused interruptions in sampling, due to local source interferences. As seen in Figure 8 (Section 3.1.1) several instances with high CN concentrations (2-3 x 10^3 cm^{-3}) were experienced during this time, reminiscent of those during the Fall 1983 campaign. The BTL C.I. samples generally contained trace element concentrations below or at the analytical detection limit, and Hi-Vol sampling was frequently disrupted. Due to the A-IN breakdown during about the same period, simultaneous σ_{sp} data are lacking as well. Two of the high CN days were selected to examine the OPC particle spectra for possible clues of the high concentrations.

Figure 23 shows rather different distributions for the morning and the afternoon of 1984-06-27. The day began clear, and sunny, with very light and variable winds (19 hours with windspeed <2 ms^{-1} during the day). The OPC particle surface and volume spectra until noon are dominated by the >1 μm ESD particles, suggesting that (as on 1983-08-15) the very fine particles, detected only by the CNC, may have again had their origin in biogenic production and/or local combustion aerosol recirculation. The presence of the coarser particles is not suprising, with the bare ground in summertime and no precipitation before and during the period. An abrupt change to SE wind in the afternoon, resulted in substantial alterations in the OPC particle spectra. The OPC and CN concentrations decreased appreciably, and the <1 μm ESD particle surface and volume began to grow, thus indicating enhanced influence of accumulation mode particles. The weather conditions on 1984-07-02 were quite similar to those during the first part of 1984-06-27, except for a very unusual (for NYA) N-NE wind direction. The shapes of the OPC particle distributions in Figure 24 have some similarity to the before-noon spectra in Figure 23. Figure 24, however, also bears a strong resemblence to Figure 17 (with low wintertime CN concentrations on 1983-03-18), so that the nature of the high CN episode on 1984-07-02 remains unclear.

The last OPC spectra in Figure 25 for 1984-07-11 illustrate OPC aerosol characteristics on a day when both CNC and σ_{sp} medians were elevated (Figure 8, Section 3.1.1). The before-noon NW to SW winds on this day were fairly brisk, but weakened and became shifty in the afternoon. There were pronounced differences (90^0 to 180^0) in visually-observed wind directions between NILU II, the NYA settlement and the airstrip windsock (points 1 and 5, respectively, in Figure 2). Although Figure 25 shows significantly increased particle surface and volume spectra in the afternoon for all size ranges, only the >1 μm ESD particles showed a declining surface and volume trend in the afternoon. This is inconsistent with the increased σ_{sp}s in Figure 8, which imply increased surface of the <1 μm ESD range particles.

From the foregoing, it appears that because the Royco 225 OPC cannot provide sufficient information in the important accumulation mode size range, the usefulness of the OPC spectra for aerosol behaviour interpretations is seriously limited. An OPC having better fine particle detection capability, e.g., the PMS LAS-X used in the NILU aircraft, would be better suited for this purpose. It was also felt, that the narrow range of the Royco Model 225 OPC did not justify an attempt to fit the number concentration data to a power-law relationship. The nearly flat volume (and thus mass) distribution, found by Hoff and Trivett (1984) during a short winter period in the Canadian Arctic, is not evident in the NYA volume spectra, which invariably show a modal structure.

4.3 AEROSOL SIZE-DIFFERENTIATED CHEMICAL COMPOSITION

Size-differentiated chemical composition of aerosols provides valuable information for the assessment of the origin of the aerosols and the importance of various emission sources. Until 1983, information on size-differentiated chemical composition of arctic aerosols was either lacking, or was available only for "fine" and "coarse" particle fractions (e.g., Heintzenberg et al., 1981). This data was not always adequate for explaining differences in the behaviour of various trace elements in aerosols, and the partitioning of the aerosol into more size fractions, followed by multi-component chemical analyses (e.g., Winchester et al., 1984; Heintzenberg and Covert, 1984a; 1984b), was desirable.

At the present time, chemical composition data for seven size-fractions of aerosols, obtained with the BTL C.I. at the NYA ground stations during four BP Project campaigns, are available.

4.3.1 The winter aerosol

The PIXE analyses results of 14 fractionated aerosol samples from March/April 1983 and 17 samples from February/March/April 1984, shown in Tables 2, and 3, and in Figures 26 and 27, are discussed.

4.3.1.1 Concentrations and size distributions

During both winter/spring measurement campaigns, Si showed bimodal mass-size distributions with a minimum abundance on Stage 3 (1-2 μm EAD). It is now generally accepted that due to the different production processes of coarse and fine particles the mass-size distributions of ambient aerosols are bimodal, with a minimum at about 1-2 μm EAD, and that the particles above this diameter are usually derived from seasalt, natural erosion processes and reentrained dust (Lee and Goranson, 1976; Whitby, 1978). This is borne out by the Si data presented here. Winchester et al. (1984) from aircraft measurements of size-differentiated aerosols during the AGASP programme have discussed the existence of coarse soil dust in the arctic aerosol in March/April 1983. They compared ratios of elements in the >2 μm EAD aerosol fraction with geochemical average shales (Turekian and Wedepohl, 1961), geochemical average earth crust (Mason and Moore, 1982), Chinese loess (Heller and Liu, 1982), and stratospheric samples of El Chichon volcanic ash (Kotra et al., 1983), still in the arctic stratosphere during the measurement period (Shapiro et al., 1984). The comparison is shown in Table 5, together with the median ratios for elements on BTL C.I. Stages 0-2 (>2 μm EAD) from the March/April 1983 BP campaign, and geochemical average sandstones (Bower, 1961).

Table 5: Ratios of crustal elements in coarse particle fractions (>2 μm EAD).

Sample	Si/Ca	Si/Fe	K/Ca	K/Fe	Ti/Fe
Median for AGASP[1] aerosol, March/ April 1983	1.34	1.46	0.51	0.56	0.10
Median for NYA in March/April 1983 (this work)	2.67	16.50	0.18	1.50	0.10
Shales [2]	3.30	1.55	1.20	0.56	0.10
Earth's crust [3]	7.64	5.54	0.71	0.52	0.09
Loess [4]	50.00	10.15	2.69	0.55	0.14
Volcanic ash [5]	-	-	1.46	2.55	0.32
Sandstones [6]	9.41	37.50	0.27	1.10	0.15

[1] Medians by Winchester et al. (1984).
[2] Averages of Turekian and Wedepohl (1961).
[3] Averages of Mason and Moore (1982).
[4] From Nanking, China (Heller and Liu, 1982; Tyler et al., 1983).
[5] Stratospheric ash from El Chichon eruptions, May 1982 (Kotra et al., 1983).
[6] Averages of Bower (1966).

The NYA ratios of Si to Ca are compatible with a clay mineral source, while other ratios are close to those for sandstones. Winchester et al. (1984) hypothesized that the initially fine clay mineral particles (from shales) during transport to the Arctic, under suitable atmospheric conditions of moisture and temperature, may have served as nuclei for ice crystals (Mason, 1961). These ice crystals (snow flakes) can aggregate, and upon sublimating could conceivably coalesce into larger, aggregated clay particles. They suggested Asian dust as the possible source of the fine particles. Desertification is a known problem in Asia, resulting in frequent injection of dust into the atmosphere. The general atmospheric circulation of the Arctic in March/April is occasionally favourable for transport of this desert dust into the Arctic (Rahn et al., 1977).

Winchester et al. (1984) also advanced an alternative explanation for the presence of soil particles in the arctic air: emissions from volcanoes, geysers, or other surface/ocean-floor disruptions. Indeed, on 1983-02-18, satellite observations revealed a large plume of aerosols venting from the flank of Bennett Island (76.7^0N, 149.3^0E) in the Eastern Siberian Sea

(Kienle et al., 1983). Similar aerosol emissions from Bennett Island were also observed in early April, 1983. These volcanic aerosols had an estimated residence time of ca. 48 hours, during which time they could have travelled about 3500 km (assuming an average wind speed of 20 ms^{-1}). The chemical composition of the arctic aerosol measured by BTL C.I. at NYA, however, did not show elevated concentrations of Cd, As, Co and Pb, which are normally associated with volcanic releases.

Concentrations of Si in the >2 μm EAD fractions in wintertime, shown in Tables 2 and 3, are surprisingly high, with a maximum at about 0.5-1.0 μm EAD. Heintzenberg et al. (1981), using a two-stage sampler at NYA in April/May 1979, found Si concentrations of about 40 ng m^{-3} in the ca. <1 μm EAD particle fraction, and 68 ng m^{-3} in the ca. >1 μm fraction. Since Si is a typical soil-derived element, its high concentrations in the fine fraction of the arctic aerosol suggest that natural processes, especially erosion, can generate not only coarse, but relatively fine particles as well. The size distributions of K and Ca (see Table 2), two other elements of crustal origin, seem to confirm this. High concentrations of Si, K, and Ca in the 0.1-1.0 μm size fraction have also been observed during dust storms over desert areas of Rajasthan, India (Joshi et al., 1984).

The size distribution of Fe-containing aerosols shows high concentrations in the <2.0 μm EAD fractions, indicating a significant contribution of anthropogenic sources to the total iron load in the Arctic. (Note that Fe concentrations observed during March/April 1983 are shown in Table 2, while those for February/March/April 1984 are shown in Figure 27, together with the concentrations of anthropogenic elements.) Contribution from coal combustion may be more significant than from steel and iron production in this respect. Measurements, carried out in a large coal-mining and steel-producing area in Poland, have shown that the effect of steel industry on atmospheric Fe concentrations may be rather low, compared to that of coal combustion (Tomza et al., 1982). Although coal combustion effluents, due to their high Fe emission factors (Pacyna, 1980), may in general contribute significantly to iron content of aerosols, the Fe enrichment factors, calculated from the NYA BTL C.I. data, do not point to this (see Section 4.3.1.2).

Marine sources in March/April 1983 had a rather small influence on the arctic aerosol, when Cl concentrations were generally low because of the

largely ice-covered waters. During February/March/April 1984, however, Kongsfjorden at NYA and the ocean to the west were open most of the time, which may explain the high Cl concentrations measured by BTL C.I. at that time. Cl, Na and Mg in Hi-Vol samples showed the same trend (Pacyna et al., 1985a). The $\Delta M/\Delta \log D_p$ vs. D_p plots of Ni, Pb, Cr, Mn, Cu, Zn, V, and S for March/April 1983 in Figure 26, and for the same elements plus As, Fe, and Br during February/March/April 1984 in Figure 27, suggest two types, or groups, of distribution curves for all elements. The graphs in Group "a" represent distributions during episodic, long-range transport conditions, while those in Group "b" typify samples collected under "normal" non-episodic conditions in the Arctic. Thus, Group "b" can be regarded as representing the "normal" distributions of elements among the measured fractions of the arctic aerosol. To avoid confusion with too many graphs on the same figure, the "normal" concentrations of Zn, S, Br and Fe in February/March/April 1984 (shown in Figure 27) were split into two groups: "b1" (Samples 4 to 9, except 8) and "b2" (Samples 10 to 17, except 12). Only Group "a" distributions of V were observed.

The mass-size distributions of Ni show the highest concentrations in the finest particles, and a clear peak in the 0.5-1.0 μm EAD range for samples from March/April 1983. Generally, the trace element concentrations in the various size fractions of aerosols were higher in March/April 1983 (Figure 26), than in February/March/April 1984 (Figure 27), particularly during the episodic periods, in agreement with other BP Project findings (Pacyna et al., 1985a; Pacyna et al., 1985b; Iversen, 1985). During episodes, Ni concentrations in the two finer fractions increased, indicating an additional contribution from certain sources or source areas. Because there is no simple way of relating the size of particles measured in chimney emissions to the sizes of particles collected in the Arctic, it is impossible to judge, which sources may be reponsible for the increases. However, there are two possibilities: nickel ore smelters and oil combustion. Since Ni is reportedly concentrated mostly on the smallest flyash particles in oil-fired power plant effluents (NRCC, 1981), it could be assumed that the additional amount of Ni in the 0.25-0.5 μm EAD fraction during the episodes at NYA originated from the emissions from nickel smelters. As can be seen from Figures 26 and 27, almost all of the measured Ni was found in the <2 μm EAD fractions.

The distributions of As and Pb have shapes similar to those of Ni. The March/April 1983 period was characterised by peak Pb concentrations in the 0.5-1.0 μm EAD fraction, lower values in the 0.25-0.5 μm fraction, and the highest concentrations in the <0.25 μm EAD fraction. Such distributions can be regarded as "normal" in the Arctic. In the February/March/April 1984 plots, Pb in the <0.25 μm EAD fraction was below detection limit. During the episodes at NYA, Pb concentrations increased significantly in the <0.25 μm fractions in 1983, while in 1984 the increase occurred in the 0.25-1.0 μm EAD fraction.

Generally, the concentrations of anthropogenic pollutants in the <0.25 μm EAD fraction during the February/March/April 1984 episodes were very low or below detection limits. Other BP Project results (Pacyna et al., 1985a) implicate different emission sources, contributing to the pollutants measured at NYA during the March/April 1983 and the February/March/April 1984 episodes. In both periods, the relevant emission sources were traced to the USSR, and in 1983 the industrial activities on the Kola Peninsula appeared to have contributed most to the episodic concentrations at NYA. For 1984, other sources in western and central USSR, as well as the Norilsk smelter complex, must be considered. Accordingly, the pollutants measured at NYA in 1984 must have travelled longer distances than in 1983. Since a part of <0.25 μm EAD particles falls into the accumulation mode range, these small particles thus had a longer aging time during the episodic long-range transport in February/March/April 1984. This may be a partial explanation for the observed shift in particle mass towards larger particle sizes during the 1984 episodes (see also Heintzenberg and Larssen, 1983). The BP Project aircraft measurements (see Pacyna et al., 1985c) showed that polluted air layers over Spitsbergen during March 1984 were almost twice as thick, and particle volume concentrations significantly lower, than during March 1983. This is thought to be due to atmospheric stability variations, with the transported pollutants better dispersed (and thus the concentrations lower) in March 1984 than in March 1983.

The origin of aerosol Pb during 1983 and 1984 winter/spring episodes is difficult to assess. In the USSR petrol combustion is estimated to contribute about 56% of total Pb emissions (NILU, 1984). Two other high-temperature processes: non-ferrous metal production, and iron, steel and ferroalloy manufacturing, release about 26% and 3% of the total lead, respectively. All three sources could affect the Pb concentrations measured

at NYA.

Very clear differences between the concentrations during the "normal" and episodic periods existed for Cr in the <0.25 EAD fraction during March/April 1983. While these concentrations remained usually very low, during episodes they increased by a factor of 10. This "additional" Cr in the finest particles comes definitely from high-temeperature sources, i.e., fuel combustion, and /or iron, steel and ferroalloy manufacturing. Lee et al. (1975) found that Cr in coal-fired power plant chimney gases was predominantly concentrated in the <1.0 µm diameter particles, only 6% of which came from electric arc furnace emissions. Thus fuel combustion can be suspected as the main cause of the increased Cr concentrations. The same source can also be responsible for the high concentrations of Mn in the <0.5 µm EAD fractions during the same 1983 episodes. However, the equally high fine fraction Cr concentrations during both episodic and non-episodic periods are puzzling.

The observed elevated Cu concentrations during the 1983 and 1984 winter episodes are most likely due to long-range transport from regions with non-ferrous metal production. The interpretation of the mass-size distributions for Zn is more complicated. The high concentrations in the <0.5 µm fractions could come from emissions of non-ferrous metal production. A study by Pacyna et al. (1981) of trace element emissions from copper and lead smelting complexes identified large Cu, Pb and Zn releases concentrated in the finest particle fractions. The size distributions of aerosol Cu and Zn at NYA have interesting shapes in the >2 µm EAD fractions. Although often extremely low concentrations of Zn and Cu were measured in the 2-4 µm and 4-8 µm EAD ranges, the concentrations increased significantly in the >8 µm particle size fraction. The coarse fraction Zn and Cu comes probably from natural sources, particularly the erosion of earth's crust. Pacyna et al. (1984a) have estimated the global emissions of Cu from windblown dust as almost equal to the total anthropogenic emissions of the metal in Europe (1.2×10^4 ta^{-1}). The anthropogenic emission flux of Zn in Europe (8×10^4 ta^{-1}) is almost three times higher than from windblown dust.

Long-range transport to NYA added also to S concentrations in the <0.5 µm EAD fractions. Vanadium in measureable concentrations at NYA was present in the <0.5 µm EAD fractions only during episodes. Oil combustion has been identified as the only source of airborne V.

Judging from the size distribution graphs for Br, the element had no significantly different size distribution features during the episodic and non-episodic periods, confirming its predominantly marine origin in remote areas.

4.3.1.2 Enrichment factors

From the above discussion on the size-differentiated chemical nature of the arctic aerosol, two samples from 1983 (Samples 3 and 5) and four from the 1984 campaign deserve further attention. The size distributions of all of these samples in Figure 26 and 27 are of Group "a" type, i.e., they likely represent episodic conditions. To be able to verify this supposition and trace the origin of the episodic transport, enrichment factors were calculated for Cr, Mn, V, Zn, Pb, Ni, Cu, S and Fe for the 1983 and 1984 periods, and additionally for Si in 1983, and As and Br in 1984.

The enrichment factor, EF, for an element X in the aerosol, relative to the reference material, is defined by:

$$EF(X) = \frac{(X/Ref)_{aerosol}}{(X/Ref)_{reference\ material}} \qquad (1)$$

where X/Ref is the concentration ratio of element X to the chosen reference element.

Titanium (Ti), a typical soil-derived element, was selected as the reference element for the 1983 data. From the BTL C.I. measurements, its concentrations were **evenly** distributed with respect to particle size and time. Thus, Ti seems to be a very good reference element for enrichment factor calculations. Ti concentrations were not available from the 1984 campaigns, and silicon (Si) was used instead. Schütz and Rahn (1982) report bulk crustal rock, bulk soil, and the fine fraction of soil as the most commonly used reference materials. The latter seems to be the best choice. Bulk soil can be inappropriate, because the composition of its fine fraction may differ from that of the bulk. The problem of obtaining a representative composition of rock is due to its slow weathering. However, Schütz and Rahn (1982) suggest, that the composition of the fine fraction of desert soil is quite similar to bulk crustal rock. The latter, therefore, can be an

acceptable reference for calculating aerosol-crust enrichment factors. Several geochemical average compositions of crustal rock can be found in the literature (e.g., Taylor, 1964; Lawson and Winchester, 1979; Mason and Moore 1982).

The calculated enrichment factor are shown in Figures 35 and 36 for the 1983 and 1984 spring campaigns, respectively. Graph A in Figure 35 represents the average values of EFs calculated for all samples, except Samples 3 and 5. The EFs for Cr, Mn, V, Zn, Pb, Ni, Cu, Fe, Si and S, calculated for the finest fractions of Samples 3 and 5, are much higher than those obtained for the others. Additionally, the EFs for V, Mn and Zn in the 0.25 - 0.5 µm EAD fraction in Samples 3 and 5 are also higher than in Graph A for the same fraction. Thus, the episode from 1983-03-07 to 1983-03-13 was associated with increased Cr, Mn, V, Zn, Pb, Ni and Cu concentrations in the <0.5 µm EAD fraction. Since the increase in S concentrations in these fractions is not as high as for the above elements, only the two finest fractions were apparently affected by the episodic transport to the Arctic during March 1983. Although Si does not normally have high enrichment factors, the EFs for Samples 3 and 5, plotted in Figure 35, show interesting Si "de-enrichment" for the 0.25 - 0.5 µm size fraction, which is difficult to explain. Both Si and Ti have the same main source, i.e., crustal rock and soil.

The decreased EFs for the 0.25 - 0.5 µm EAD fraction of Samples 3 and 5 suggest that Ti in the <0.5 µm fractions had an additional source. Steel and ferroalloy production is a possibility, but the low enrichment factors of Fe (see Figure 35) do not implicate these processes. There appear to be no other important anthropogenic sources of fine particle Ti. If the Ti in the <0.5 µm EAD particles is indeed anthropogenic in origin, a stage-by-stage enrichment factor analysis of BTL C.I. data (with Ti as the reference element) will be limited to naturally generated >0.5 µm EAD particles. Perhaps a measurement artifact, e.g., the much higher accuracy of the analytical method for Si in fine fractions, than for other pollutants, may account for the apparent Si de-enrichment. It is also somewhat puzzling that Sample 4 should be different from Samples 3 and 5, since the wind tracjectories indicated the same origin for transport during 1983-03-07 to 1983-03-13.

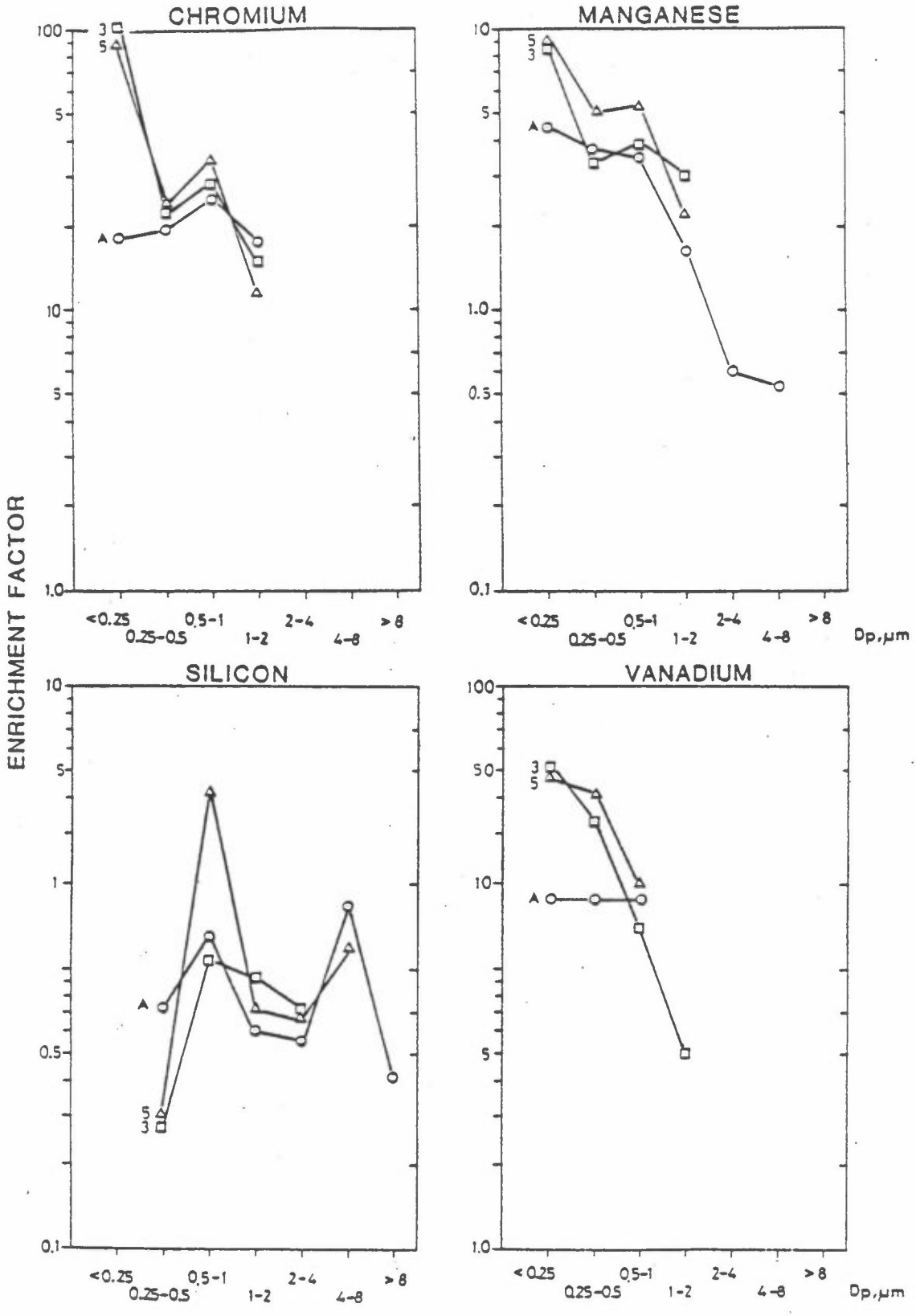

Figure 35: Enrichment factors of several trace elements in a given size fraction, in samples collected at Ny Ålesund in March/April 1983. The <0.25 µm EAD particles were collected on NP afterfilter.

Curve A represents average enrichment factors for samples other then 3 and 5.

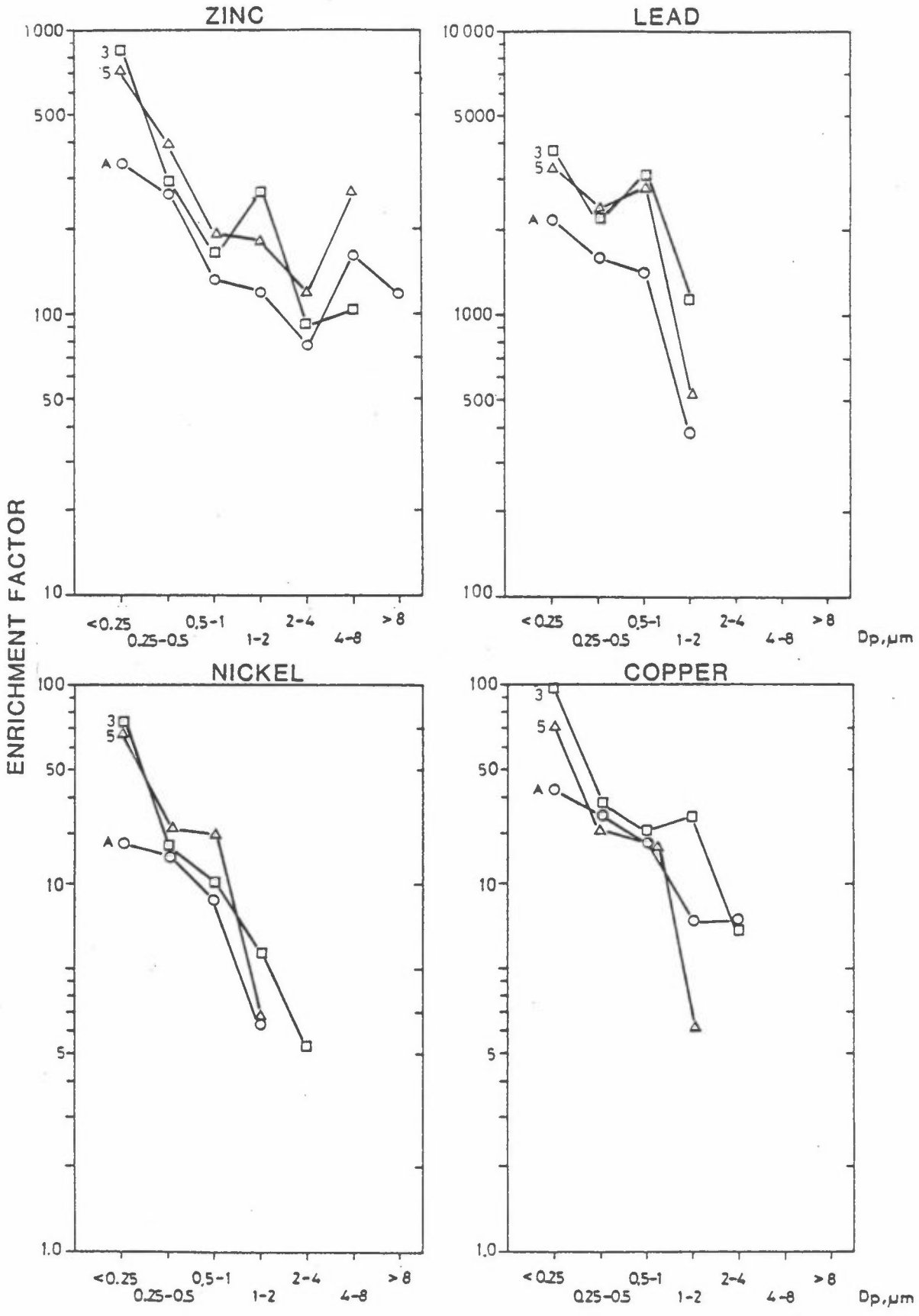

Figure 35: Cont.

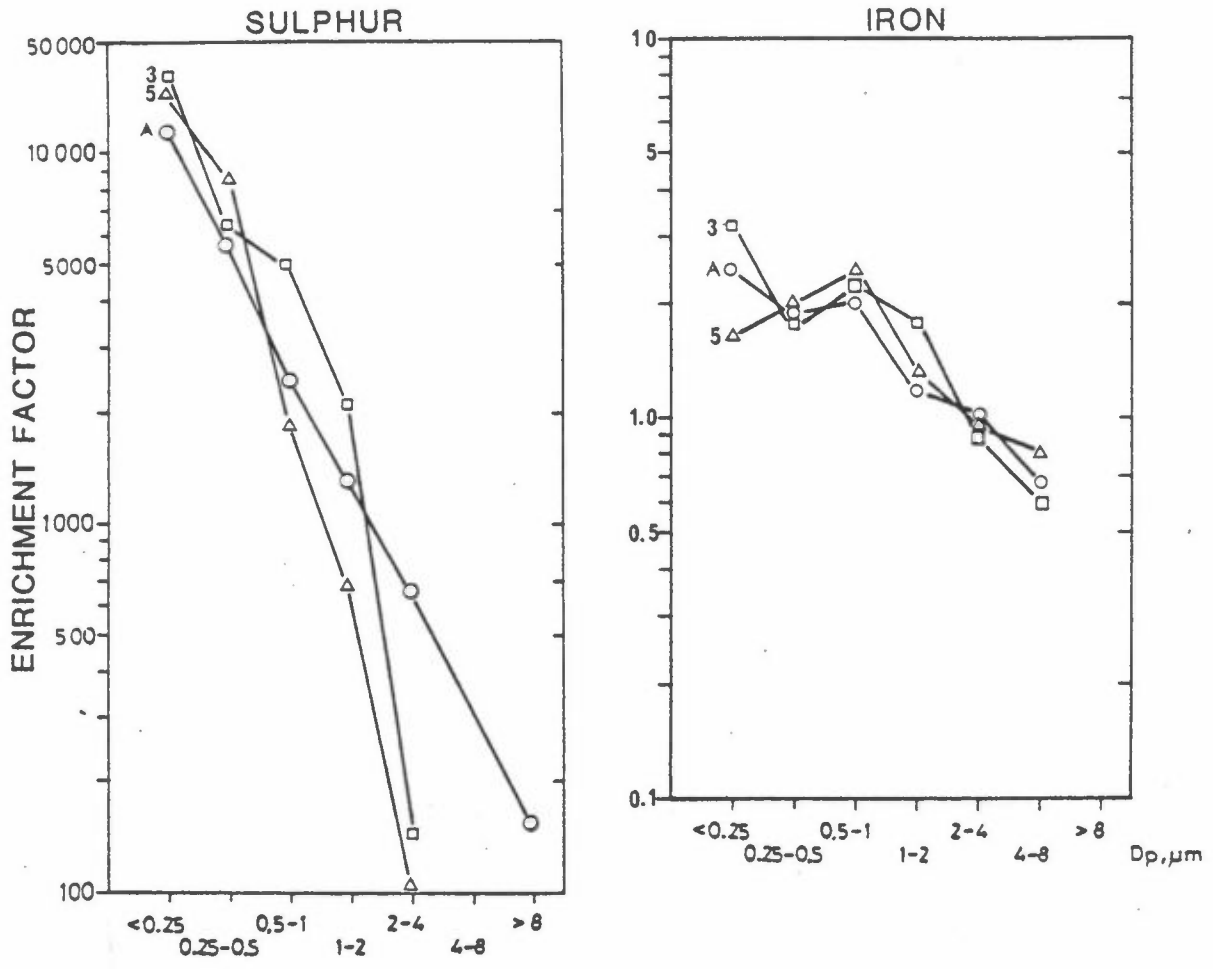

Figure 35: Cont.

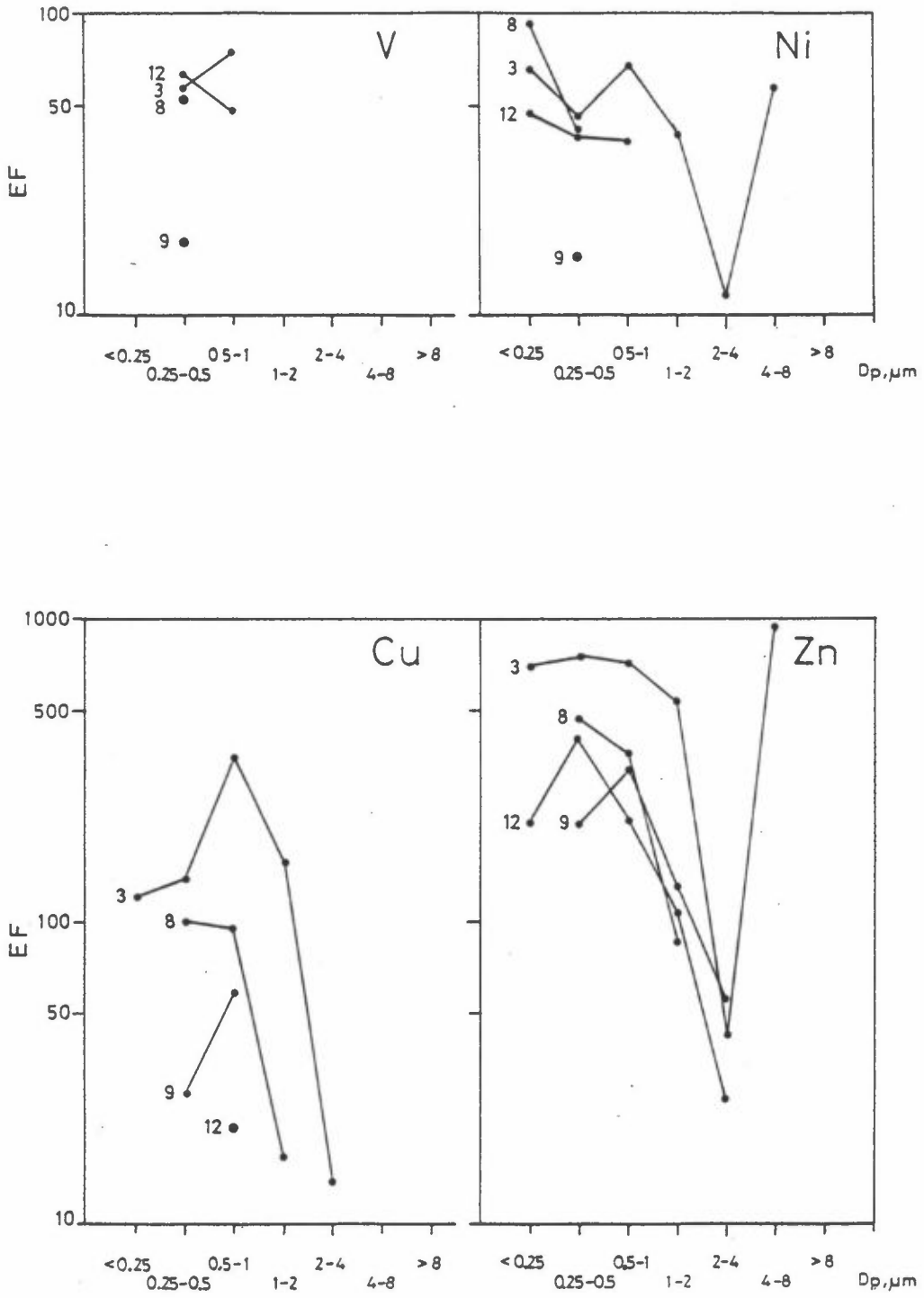

Figure 36: Enrichment factors of several trace elements in a given size fraction, in samples collected at Ny Ålesund in February/March/April 1984. The <0.25 µm EAD particles were collected on NP filter.

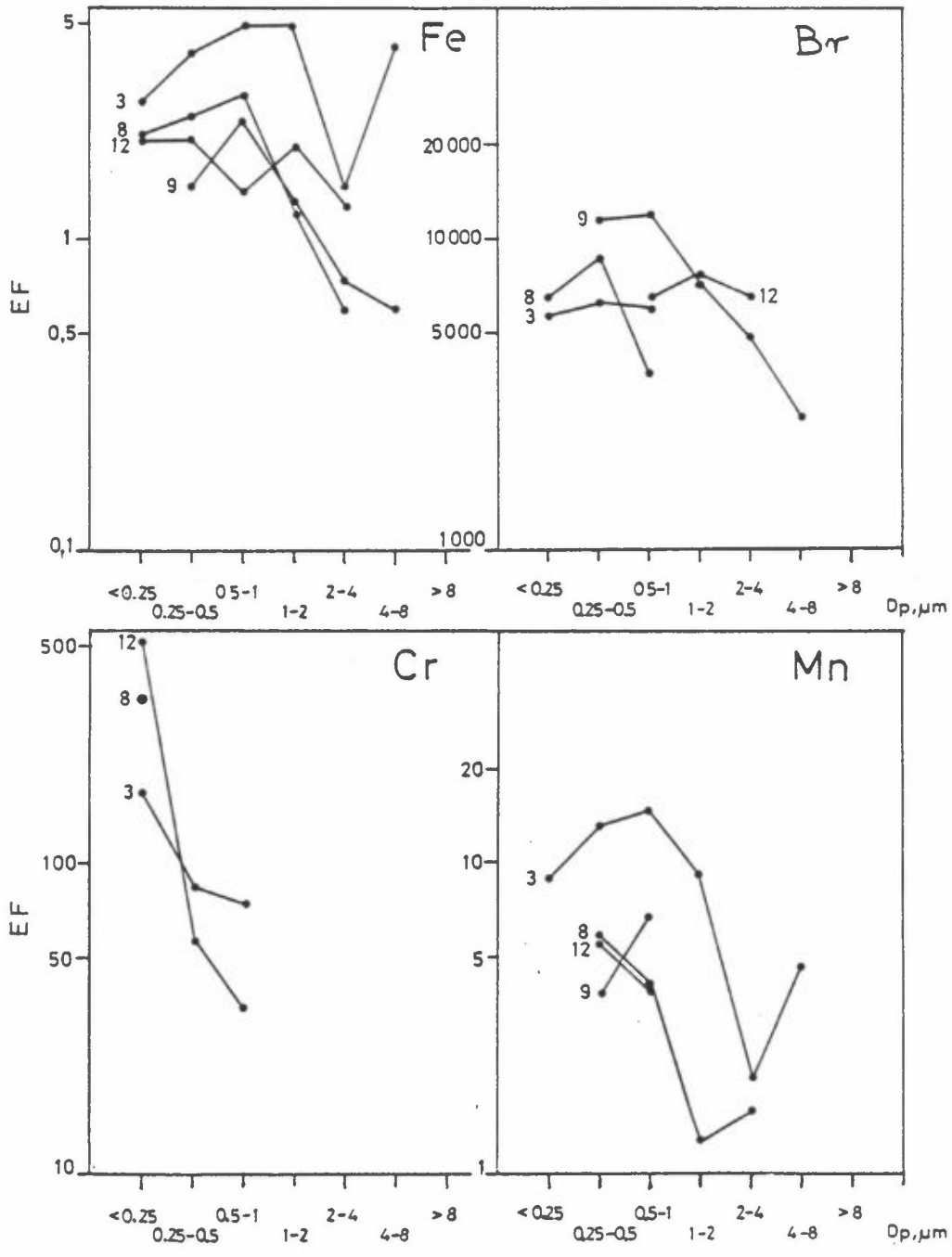

Figure 36: Cont.

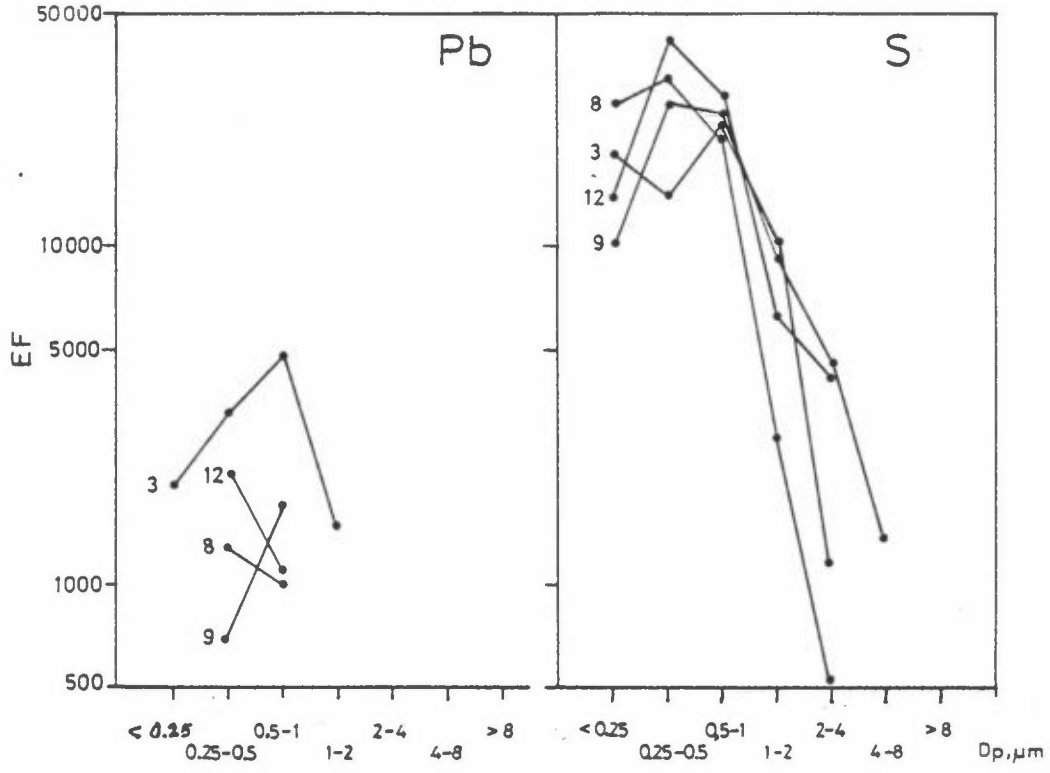

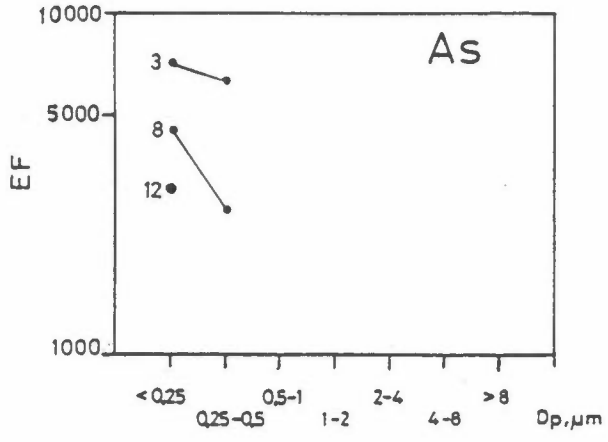

Figure 36: Cont.

Results from episodic periods in February/March/April 1984 only are considered in Figure 36. Generally, the enrichment factors of anthropogenic pollutants are slightly lower during episodes in 1984 than in 1983, reflecting the differences in particle trace element concentrations, discussed in Section 4.3.1. This is especially evident for the finest size fractions of anthropogenic elements (except Cr). On the other hand, the 1984 episodes added greatly to the 0.5 - 1.0 μm EAD fraction particles, perhaps as a result of differences in transformation and removel processes. The likely reasons have already been noted in Section 4.3.1.1.

4.3.2 The summer aerosol

4.3.2.1 Concentrations and size distributions

Eleven size-differentiated aerosol samples were collected with the BTL C.I. at NYA in August/September 1983, and nine in June/July 1984. Unfortunately, the first episode of possible long-range transport of air pollutants from the North American continent (see Pacyna et al., 1985a) during the period was apparently missed.

The results of BTL C.I. sampling during a transport episode between 1983-09-07 and 1983-09-09 are shown in Figure 28 (Samples 9 and 10), which also shows the mean concentrations in other samples, collected during non-episodic periods.

Two groups of trace elements are easily discerned for the episode in the figure. The first group includes the natural constituents Si, K, Cl, Fe, Al, and Ca, likely due to soil and rock erosion processes, reentrained dust, and airborne seasalt. The elements of crustal origin show a bimodal size distribution, with a minimum abundance on BTL C.I. Stage 3 (1-2 μm EAD). The concentration peaks of soil elements in the 0.5 - 1.0 μm EAD fraction suggest that the natural processes can generate not only coarse particles, but also contribute fine particles in remote areas (as noted earlier in Section 4.3.1). The group of naturally-derived elements appears to contain both crustal and marine components. During the summer/fall measurement campaigns the air masses were transported over open waters to Ny Ålesund. In Table 5, median ratios of K, S, and Ca to Cl under non-episodic conditions are given in the different BTL C.I. size fractions, and compared with the same elemental ratios in seawater (Riley and Chester, 1971). Based

on these results, seasalt seems to be the major source of K in the >1 μm EAD particles, and S and Ca in the >8 μm EAD particles. In the fine fraction particles, e.g., 0.5 - 1.0 μm EAD (Stage 4), only 50% of the K, 23% of the S, and 16% of the Ca appear to originate from seawater. The remainder may come from windblown dust. According to Gillette (1979), fine particles can be produced by the sandblasting effect of saltation, which dislodges fine particles from the surface of larger particles, and by "splashing" of the saltating particle into a reservoir of fine particles. Maenhaut et al. (1981) studied seawater and non-seawater aerosol components in the marine atmosphere of Samoa, and cautiously suggested that the non-seawater element group may, in fact, be surface-film-derived, since the sea surface can be a significant source of aerosols enriched in several elements.

Table 5: Median elemental ratios in aerosol at Ny Ålesund, summer 1983.

Elements	Ratios in seawater*	Ratio in particle size fraction					
		Stage 0 >8 μm	Stage 1 >4-8 μm	Stage 2 >2-4 μm	Stage 3 >1-2 μm	Stage 4 0.5-1 μm	Stage 5 0.25-0.5 μm
K/Cl	0.0209	0.025	0.028	0.030	0.017	0.042	0.067
S/Cl	0.0467	0.049	0.070	0.078	0.075	0.202	0.744
Ca/Cl	0.0212	0.025	0.046	0.046	-	0.131	0.523

* From Riley and Chester (1971).

It is recognised, however, that the BTL C.I. data represent a few samples only, and no definite conclusions can be drawn, other than that they agree with results from other studies of the composition of aerosols over the oceans (e.g., Maenhaut et al., 1979; Maenhaut et al., 1981).

The shapes of all distribution graphs for Cl in Figure 28 are very similar. However, the episodic Cl concentrations on all stages of the BTL. C.I., particularly for Sample 9 from 1983-09-07 to 1983-09-11, are lower than during non-episodic periods. During an episode (e.g., Okada et al., 1978; Larssen and Hanssen, 1980) aerosol Cl may be volatalised and driven off as hydrochloric acid by co-existing acidic constituents in the air, or in the collected samples.

The second group of elements in Figure 28 includes S, Pb, Cu, Ni, and Mn. With the exception of S, the concentrations of these elements were very low during the non-episodic period. Thus, the Pb, Cu, Ni, and Mn measured during the episode in September 1983 probably had an anthropogenic origin. An examination of weather maps and wind trajectories (see Pacyna et al., 1985a) implicates sources in central Europe. The mass-size distributions of the above elements (except S) show maximum abundance on Stage 4 (0.5 - 1.0 μm EAD). The concentrations were lower in the 0.25 - 0.5 μm EAD fraction, and sub-measurable in the <0.25 μm EAD fraction. Accelerated aerosol aging in summertime is the likely reason for a shift towards larger particles, since the high-temperature processes, which are the main emitters of Pb, Ni, and Cu, produce particles with diameters <0.5 μm EAD. In contrast, samples collected during episodic long-range transport of pollutants from sources in the USSR to the Arctic in March 1983 had Ni and Pb concentrated mostly in the <0.5 μm EAD fractions (see Section 4.3.1). The concentrations of the metal in the <0.25 μm EAD fraction were at that time several times higher than in the 0.5 - 1.0 μm EAD range (Stage 4).

No episodes of long-range transport of air pollutants were observed during the June/July 1984 BP Project campaign. The mean concentrations of the elements in the various size ranges are presented in Figure 29, and are very similar to the non-episodic concentrations in fall 1983, shown in Figure 28. Thus, the data from non-episodic periods in summertime may be representative of "background" concentrations of air pollutants in the Arctic during the summer half of the year.

4.3.2.2 Enrichment factors

The enrichment factors for S and Cl, calculated from the episodic and non-episodic data for August/September 1983, are shown together with the

episodic enrichment factors for Pb, Cu, Ni, V and Mn in Figure 37. These are compared in Table 6 with the enrichment factors for aerosols in other remote areas. All EFs were calculated with Al as reference element, and "crustal rock" as reference material.

Table 6 shows that the antarctic aerosol (Cunningham and Zoller, 1981) has the highest enrichment factors. Antarctica is much further away from industrialised regions than the Norwegian Arctic, and the emission sources contributing to the antarctic and arctic aerosols are for the most part different. Concerning the high enrichment factors of S and Cd, Cunningham and Zoller (1981) have suggested that most of the S comes from the upper troposphere (transport to the interior of Antarctica is usually through the mid- or upper-troposphere), while Cd is released during volcanic activity, which may also be an important source for Zn in antarctic aerosols.

The enrichment factors from measurements at Kap Harald Moltke in northern Greenland (Flyger and Heidam, 1978) seem to be quite similar to those for the non-episodic periods at NYA (see Table 6). A tentative conclusion is that the origins of the non-episodic aerosols measured in Greenland and at NYA were alike.Significant differences between non-episodic concentrations at NYA and Kap Harald Moltke are seen for Cl and Pb. Seasalt contribution of Cl seems to be much higher at NYA, while the extraction and processing of lead and zinc on Greenland likely affect the Pb concentrations.

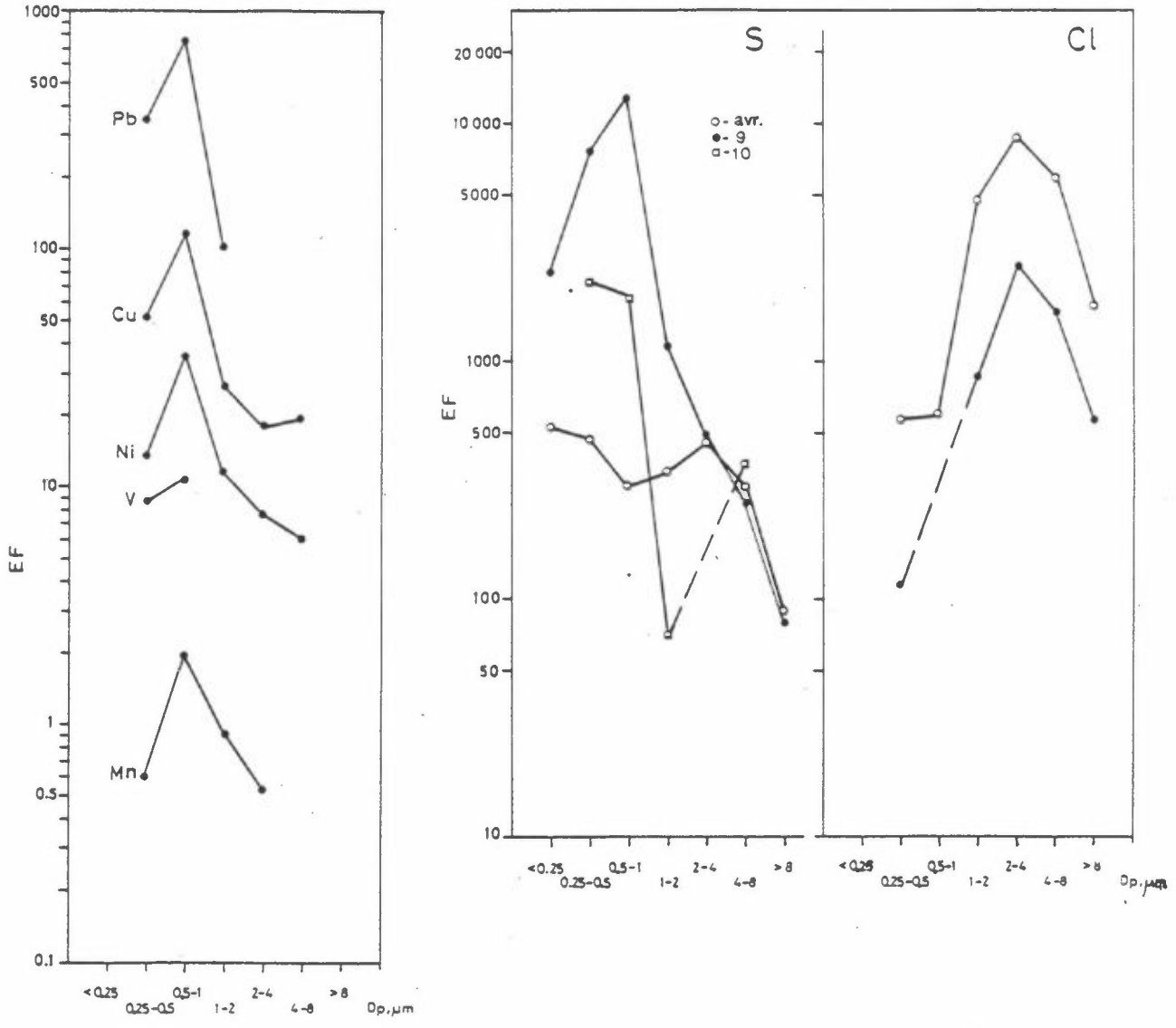

Figure 37: Enrichment factors of several trace elements in a given size fraction, in samples collected at Ny Ålesund in August/September 1983. The <0.25 µm EAD particles were collected on NP filter.

Table 6: Enrichment factors (reference: Al, crustal rock) of trace elements in fall 1983 at Ny Ålesund, and at other geographical locations.

Element	Ny Ålesund (this work)		Michigan, U.S.A. 1979 (Alkezweeny et al., 1982)	Antarctica 1971, 1975 1976, 1978 (Cunningham & Zoller, 1981)	Greenland 1974 (Flyger & Heidam, 1978)
	Episodic	Non-episodic			
S	1 900	370	710	30 000	610
Cl	1 140	3 480	-	5 500	450
K	0.8	0.7	1.3	2.9	1.1
Ti	0.8	0.6	0.5	2.0	0.9
V	2.0	-	1.8	1.2	5.2
Cr	11	9	2	13	5
Cd	2 910	110	3 700	24 000	-
Ni	1.3	-	3.8	-	6
Pb	83	18	270	-	94
Zn	55	16	30	50	15
Cu	11	8	23	110	-

5 CONCLUSIONS

Concurrent measurements with a condensation nuclei counter, an integrating nephelometer, and (to some extent) an optical particle counter help to distinguish between freshly-produced and aged aerosols in the Arctic. High CN concentrations in the absence of measureable particle light scattering suggest the presence of nucleation mode particles, perhaps from regional biogenic/photochemical production, and/or recirculation of local combustion aerosols.

The concentrations and enrichment factors of several trace elements, measured at Ny Ålesund during the BP Project campaigns, confirm that the size-differentiated chemical nature of particles is a very useful tool for assessing the origins of aerosols.

During long-range transport over ice-covered waters, the <0.5 µm EAD particles, emitted from various anthropogenic sources, are not appreciably altered "en route" by transformation and removal processes in wintertime (e.g., Heintzenberg and Larssen, 1983). High concentrationss of Ni, Cu, Mn, As, V, and Pb in the <0.5 µm EAD particle fractions were observed at NYA during episodes of long-range transport of air pollutants from industral regions in the USSR in March 1983. During transport of pollutants over open waters in summertime, there was a concentrations shift towards more aged

particles in the 0.5 - 1.0 μm EAD range.

Several anthropogenic trace elements had high concentrations and high enrichment factors in fine fractions of particles measured at NYA, which confirms that anthropogenic high-temperature processes are the main sources of long-range transported fine fraction aerosols reaching the Arctic.

The size distributions and enrichment of various elements from natural sources imply that some of them, e.g., Fe, K, Ca and Si, come, at least partially, from anthropogenic sources, such as windblown dust and airborne seasalt, and may occur not only as coarse particles, but also in the <1.0 μm EAD range.

Chemical interactions in the atmosphere between various air pollutants, such as seasalt Cl^- driven off by SO_4^{2-}, were evident during the episodic periods as well.

6 ACKNOWLEDGEMENTS

This work was funded by British Petroleum International Ltd.

The authors thank Drs. Hans Lannefors and Ann-Kristin Ekholm, Department of Nuclear Physics, Lund Institute of Technology, for BTL C.I./PIXE work; Dr. Jost Heintzenberg, Department of Meteorology, University of Stockholm, for helpful discussions, permission to use unpublished data, assistance in A-IN repairs, and loan of CNC and CNC sampling controller; Kari Arnesen, NILU, for providing the computer programming for OPC data reduction and processing; and Arne Semb, NILU, for comments.

7 REFERENCES

Agarwal, J.K. and Sem, G.J. (1980) Continuous flow, single-particle-counting condensation nucleus counter. J.Aerosol Sci., 11, 343-357.

Alkezweeny, A.J., Lanlainen, N.S., and Thorp, J.M. (1982). Physical, chemical and optical characteristics of a clean air mass over Northern Michigan. Atmos.Environ., 16, 2421-2430.

Andreae, M.O. and Raemdonck, H. (1983) Dimethyl Sulfide in the Surface Ocean and the Marine Atmosphere: A Global View. Science, 221, 744-747.

Bartz, H., Fissan, H. Helsper, C., Konsaka, Y., Okugama, K., Fukushima, N., Keady, P.B., Kerrigau, S., Fruin, S.A., McMurry, P.H., Pui, D.Y.H. and Stolzenburg, M.R. (1985) Response characteristics for four different condensation nucleus counters to particles in the 3-50 nm diameter range. J.Aerosol Sci., 16, 443-456.

Bowen, H.J.M. (1966). Trace Elements in Biochemistry. New York. Academic Press, 241 pp.

Carlsson, L.-E., Malmquist, K.G., Johansson, G.I. and Akselsson, K.R. (1981) PIXE analysis of samples of intermediate thickness. Nucl.Inst.Methods, 181, 179-183.

Cunningham, W.C. and Zoller, W.H. (1981). The chemical composition of remote area aerosols. J.Aerosol Sci., 12, 367-384.

Flyger, H. and Heidam, N.Z. (1978). Ground level measurements of the summer tropospheric aerosol in northern Greenland. J.Aerosol Sci., 9, 157-168.

Gillette, D.A. (1979). Environmental factors affecting dust emission by wind erosion. In: Saharan Dust. Ed. by C. Morales, New York, Wiley & Sons, SCOPE 14, pp. 71-91.

Hatakeyama, S., Izumi, K. and Akimoto, H. (1985) Yield of SO_2 and formation of aerosol in the photo-oxidation of DMS under atmospheric conditions. Atmos.Environ., 19, 135-141.

Heintzenberg, J., Hanssen, H.-C. and Lannefors, H. (1981). The chemical composition of Arctic haze at Ny Ålesund, Spitsbergen. Tellus, 33, 162-171.

Heintzenberg, J., Bäcklin, L. and Moberg, B. (1982) Direct recording of wind sector distribution in extreme environments with a wind vane. (University of Stockholm, Dept. of Meteorology, Stockholm, Report AP-20).

Heintzenberg, J. and Larssen, S. (1983) SO_2 and $SO_4^=$ in the Arctic: interpretation and observations at three Norwegian arctic-subarctic stations. Tellus, 35B, 255-297.

Heintzenberg, J. Bischof, W., Odh, S.-Å. and Moberg, B. (1983) An investigation of possible sites for a background monitoring station in the European Arctic. (University of Stockholm, Dept. of Meteorology, Stockholm, Report AP-20).

Heintzenberg, J. and Covert, D.S. (1984a) Size distribution of elemental carbon, sulphur and total mass in the range 10^{-6} to 10^{-4} cm. Sci.Total Environ., 36, 289-297.

Heintzenberg, J. and Covert, D.S. (1984b) The chemically resolved mass size distribution of the arctic haze aerosol (Extended Abstract). Paper presented at the Third Symposium on Arctic Air Chemistry, 7-9 May, 1984, Toronto, Canada.

Heller, F. and Liu, T.-S. (1982). Magnetostratigraphical dating of loess deposits in China. Nature, 300, 431-433.

Hoff, R.M. and Trivett, N.B.A. (1984) Ground-based measurements of arctic haze at Alert, N.W.T., Canada during the arctic gas and aerosol sampling project (AGASP). Geophys.Res.Lett., 11, 389-392.

Iversen, T. (1985). On air pollution transport to the Norwegian Arctic. Lillestrøm, Norwegian Institute for Air Research (NILU OR 59/85).

Jaenicke, R. and Schütz, L. (1982) Arctic aerosols in surface air. Idöjaras, 86, 235-241.

Joshi, P.V., Sawant, V.D. and Kelkar, D.N. (1984). Size distribution of microscopi size particles in Bombay atmosphere during a dust episode. Mausam, 35, 205-208.

Kienle, J., Roederer, J.G. and Shaw, G.E. (1983). Volcanic event in the Soviet Arctic?. EOS, 64, 377.

Kotra, J.P., Finnegan, D.L., Zoller, W.H., Hart, M.A., and Mayers, J.L. (1983). El Chichon: Composition of plume gases and particles. Science, 222, 1018-1021.

Lannefors, H., Heintzenberg, J. and Hansson, H.-C. (1983) A comprehensive study of physical and chemical parameters of the Arctic summer aerosol; results from the Swedish expedition Ymer-80. Tellus, 35B, 40-54.

Larssen, S. and Hanssen, J.H. (1980) Annual variations and origin of aerosol components in the Norwegian arctic-subarctic region. In: Special Environmental Report No. 14 (WMO No. 549), World Meteorological Organization, Geneva, Switzerland.

Lawson, D.R. and Winchester, J.W. (1979). A standard crustal aerosol as a reference for elemental enrichment factors. Atmos. Environ. 13, 925-930.

Lee, R.E. Jr., Crist, H.L., Riley, A.E. and MacLeod, K.E. (1975). Concentration and size of trace element emissions from a power plant, a steel plant, and a cotton gin. Environ. Sci. Technol. 9, 643-647.

Lee, R.E., Jr. and Goranson, S. (1976). National air surveillance cascade impactor network - III. Variations in size of airborne particulate matter over three-year period. Environ.Sci.Technol., 10, 1022-27.

Liu, B.Y,.H., Piu, D.Y.H. and Rubow, K.L. (1983) Characteristics of air sampling filter media. In: AEROSOLS in the Mining and Industrial Work Environments, Vol. 3, Instrumentation. Ed. by V.A. Marple and B.Y.H. Liu, Ann Arbor, MI., Ann Arbor Science,

Maenhaut, W., Zoller, W.H., Duce, R.A., and Hoffmann, G.E. (1979). Concentration and size distribution of particulate trace elements in the South Polar atmosphere. J.Geophys.Res., 84, 2421-2431.

Maenhaut, W., Darzi, M. and Winchester, J.W. (1981). Seawater and nonseawater aerosol components in the marine atmosphere of Samoa. J.Geophys.Res., 86, 3187-3193.

Mason, B.J. (1961). Clouds, Rain and Rainmaking. London. Cambridge University Press. p. 54.

Mason, B. and Moore, C.B. (1982) Principles of Geochemistry, 4th ed. New York, John Wiley & Sons. pp. 46-47.

Mitchell, R.J. and Pilcher, J.M. (1959) Improved cascade impactor for measuring aerosol particle sizes in air pollutants, commercial aerosols and cigarette smoke. Ind.Eng.Chem., 15, 1039-1042.

NILU (1984). Emission sources in the Soviet Union. Lillestrøm, Norwegian Institute for Air Research, NILU TR 4/84.

NRCC (1981). Effects of nickel in the Canadian environment, Ottawa, National Research Council of Canada, (NRCC/CNRC Report No. 18568).

Okada, K., Ishizaka, Y., Masuzawa, T. and Isono, K. (1978) Chloride deficiency in coastal aerosols. J.Meterol.Soc.Jpn., 56, 501-507.

Pacyna, J.M. (1980). Coal-fired power plants as a source of environmental contamination by trace metals and radionuclides. Habilitation thesis, Wroclaw, Technical University of Wroclaw.

Pacyna, J.M., Zwozdziak, A., Zwozdziak, J., Matyniak, Z., Kuklinski, A. and Kmiec, G. (1981). Air Pollution problems caused by the LGOM copper smelter complex - present situation and perspectives. Wroclaw, (Technical Rept. SPR 14-81, University of Wroclaw)

Pacyna, J.M., Semb, A. and Hanssen, J.E. (1984a). Emission and long-range transport of trace elements in Europe. Tellus, 36B, 163-178.

Pacyna, J.M., Vitols, V. and Hanssen, J.E. (1984b) Size-differentiated composition of arctic aerosol at Ny-Ålesund, Spitsbergen. Atmos.Environ. 18, 2447-2459.

Pacyna, J.M., Vitols, V. and Hanssen, J.E. (1985a) Chemical composition of aerosols at BP Project ground stations. Lillestrøm, Norwegian Institute for Air Research, (NILU OR 64/85).

Pacyna, J.M., Ottar, B. and Vitols, V. (1985b) The occurrence of air pollutants in the Arctic measured by aircraft. Lillestrøm, Norwegian Institute for Air Research, (NILU OR 66/85).

Pacyna, J.M., Ottar, B., Vitols, V. and Arnesen, K. (1985c). Aircraft measurements of air pollution in the Norwegian Arctic. Appendices A, B, C and D. Lillestrøm, Norwegian Institute for Air Research, (NILU OR 67/85).

Rahn, K.A., Borys, R.D. and Shaw, G.E. (1977) The Asian source of haze bands. Nature, 268, 713-715.

Riley, J.P. and Chester, R. (1971) Introduction to Marine Chemistry. New York. Academic Press, 465 pp.

Saltzman, E.S., Savoie, D.L., Zika, R.G. and Prospero, J.M. (1983) Methane sulfonic acid in the marine atmosphere. J.Geophsys.Res., 88, 10897-10902.

Schütz, L., and Rahn, K.A. (1982). Trace element concentrations in erodible soils. Atmos.Environ., 16, 171-176.

Shapiro, M.A., Schnell, R.C., Parungo, F.P., Oltmans, S.J. and Bodhaine, B.A. (1984). El Chichon volcanic debris in an Arctic tropopause fold. Geophys.Res.Lett., 11, 421-424.

Taylor, S.R. (1964). Abundance of chemical elements in the continental crust: a new table. Geochim.Cosmochim.Acta, 28, 1273-1285.

Tomza, U., Maenhaut, W. and Cafmeyer, J. (1982). Trace elements in atmospheric aerosols at Katowice, Poland. In: Trace Substances in Environmental Health - XVI, Ed. by D.D. Hemphill, Columbia, MO, Univ. Missouri.

Turekian, K.K., and Wedepohl, K.H. (1961) Distribution of the elements in some major units of the Earth's crust. Bull.Geol.Soc.Am., 72, 175-192.

Vitols, V. and Wasseng, J.H. (1985) BP Project ground station descriptions. Lillestrøm, Norwegian Institute for Air Research, (NILU OR 63/85).

Waggoner, A.P., Weiss, R.E. Ahlquist, N.C., Covert, D.S., Will, S. and Charlson, R.J. (1981) Optical characteristics of atmospheric aerosols. Atmos.Environ., 15, 1891-1909.

Whitby, K.T. (1978) Physical characteristics of sulfur aerosols. Atmos. Environ., 12, 135-159.

Winchester, J.W., Li, S.-M., Fan, S.-M., Schnell, R.C., Bodhaine, B.A. and Naegele, S.S. (1984). Coarse particle soil dust in arctic aerosols, spring 1983. Geophys.Res.Lett., 11, 995-998.

NORSK INSTITUTT FOR LUFTFORSKNING (NILU)
NORWEGIAN INSTITUTE FOR AIR RESEARCH

(NORGES TEKNISK-NATURVITENSKAPELIGE FORSKNINGSRÅD)

POSTBOKS 130, 2001 LILLESTRØM (ELVEGT. 52), NORGE

RAPPORTTYPE OPPDRAGSRAPPORT	RAPPORTNR. OR 65/85	ISBN-82-7247-636-3	
DATO DECEMBER 1985	ANSV. SIGN. T. Schjoldager	ANT. SIDER 104	PRIS kr.90,00
TITTEL Special measurements at Ny Ålesund: Physical and chemical properties of the arctic aerosol		PROSJEKTLEDER J.M. Pacyna	
		NILU PROSJEKT NR. O-8510	
FORFATTER(E) Val Vitols Jozef M. Pacyna		TILGJENGELIGHET A	
		OPPDRAGSGIVERS REF.	
OPPDRAGSGIVER (NAVN OG ADRESSE) BP International Ltd., ECC Britannia House, Moore Lane London, EC 24 9BU, England			
3 STIKKORD (à maks. 20 anslag) Arctic | Aerosol | Physical/chemical properties			
REFERAT (maks. 300 anslag, 7 linjer)			

TITLE
ABSTRACT (max. 300 characters, 7 lines) Physical and chemical properties of the arctic aerosol at Ny Ålesund, Spitsbergen, have been studied during the arctic winter and summer seasons. Size-differentiated chemical composition of aerosols has been used to assess the origin(s) of the winter and summer aerosol. Concurrently observed physical properties of the aerosol imply both natural production and long-range transport in summertime.

* Kategorier: Åpen - kan bestilles fra NILU A
Må bestilles gjennom oppdragsgiver B
Kan ikke utleveres C